Towards phototrophic tissue engineering: Optimization of a biotechnology platform for human recombinant protein in *Chlamydomonas reinhardtii*

Dissertation

zur Erlangung des akademischen Grades eines Doktors der Naturwissenschaften

an der Fakultät für Biologie

der Ludwig-Maximilians-Universität München

vorgelegt von

MONTSERRAT JARQUIN-CORDERO

München, Juli 2020

1. Gutachter: Prof. Dr. Jörg Nickelsen
2. Gutacher: Prof. Dr. Herwig Stibor

Tag der Abgabe: 20.10.2020

Tag der mündlichen Prüfung: 19.01.2021

Abstract

Chronic non-healing wounds represent not only a health problem but also a financial challenge for the global population. Appropriate oxygen supply is a fundamental issue in tissue engineering. The initial hypoxic condition triggers pro-regenerative cascade reactions, which promotes angiogenesis and extracellular matrix deposition, which are key for the generation of new tissue. Nevertheless, chronic hypoxia may cause apoptosis and, thus, wound healing impairment.

To target this unmet clinical need, our group developed a novel treatment that proposed the use of the photosynthetic organisms Chlamydomonas reinhardtii in biomedical applications. This approach, named HULK (from the German Hypoxie Unter Licht Konditionierung), aimed at providing a treatment option for several conditions related to acute and chronic tissue hypoxia, which directly affect the wound healing process. Moreover, we proposed the development of transgenic microalgae to produce recombinant human therapeutics proteins, given their many advantages compared to other less safe or less efficient organisms used as biotechnological platforms.

The first examples of transgenic Chlamydomonas strains were capable of simultaneous oxygen production through the local induction of photosynthesis and the constant release of human vascular endothelial growth factor A (hVEGF-165), human platelet-derived growth factor B (hPDGF-B) and stromal cell-derived factor 1 (hSDF-1). However, significant differences in the expression level of each recombinant protein evidenced the need to optimize the experimental design to obtain transgenic algae.

The main idea behind this doctoral thesis is to explore diverse strategies to improve and increase the potential of an established microalgae-based biotechnological platform, which may be used to expand the catalog of recombinant transgenic proteins expressed in *C. reinhardtii* and make them available for future biotechnological approaches. In the first stage of this work, new *C. reinhardtii* strains expressing hVEGF-165 were created. Two algae strains of different genetic backgrounds were transformed, two expression vectors using different promoters and secretion signal peptides, and purification tags to find an optimized strategy that would lead to the highest recombinant protein yield. In the second stage, the best conditions found to increase hVEGF-165 expression levels were evaluated for hPDGF-B, hSDF-1, and the human transforming growth factor β3 (hTGF-β3). Finally, the synergic effect of the pro-angiogenic recombinant proteins was assessed by addressing their capacity to stimulate blood-vessel tubes formation in an *in vitro* assay.

The results obtained in this study show how promoters, signal peptides, and purification tags directly affect recombinant protein yields, even if they have been reported to perform remarkably using other reporter genes. Besides, a significant advantage of a particular strain was found concerning

the expression yields and functionality of the recombinant proteins. Additionally, the multiplied biological effect found in the combination of transgenic strains expressing different human growth factors suggested the application of algal-derived biomolecule cocktails in biomedicine.

This thesis's findings have enabled the expansion of the catalog of human growth factors expressed by C. reinhardtii and demonstrated the synergic effect of secreted proteins produced by transgenic algae, thereby supporting the solidity of an algal-based biotechnological platform.

Zusammenfassung

Chronische nicht heilende Wunden sind nicht nur ein Gesundheitsproblem, sondern auch ein finanzielles Problem für die Weltbevölkerung.

Um diesen klinischen Bedarf zu decken, entwickelte unsere Gruppe eine neuartige Technologie, die die Verwendung von photosynthetischen *Chlamydomonas reinhardtii*-Algen in biomedizinischen Anwendungen vorschlug. Dieser Ansatz mit dem Namen HULK (von dem Deutschen "Hypoxie Unter Licht Konditionierung") zielte darauf ab, eine Behandlungsoption für akuter und chronischer Gewebehypoxie bereitzustellen. Darüber hinaus wurde die Entwicklung von transgenen Mikroalgen und deren Verwendung in Kombination mit dieser Photosynthesetechnologie als alternativer Ansatz zur Arzneimittelabgabe vorgeschlagen. Somit wurden photosynthetischen Organismen die Wunde mit Sauerstoff und rekombinanten bioaktiven Molekülen versorgen, die das Wundheilungsergebnis verbessern könnten. Die Anwendung von transgenen Mikroalgen ist vorteilhaft in Vergleich zu anderen weniger sicheren oder weniger effizienten Methoden für die Produktion und Verabreichung von menschelichen Therapeutika.

Viele wichtige Aspekte können jedoch die Expression von rekombinanten Proteine in *C. reinhardtii* beeinflussen, z. B. die Rolle von regulatorischen Elementen, die Wirksamkeit von Sekretionssignalen, der Einsatz von Affinitäts-Tags und den Einfluss des genetischen Hintergrunds des transgenen Stammes. Um die Relevanz dieser Parameter für die Ausbeute und Funktionalität der rekombinanten Proteinexpression zu verstehen, und die beste Kombination zu finden, die die Schaffung einer robusten Plattform für die Expression menschlichen Wachstumsfaktoren für biomedizinische Ansätze ermöglichen würde, wurde ein Optimierungsverfahren in Bezug auf die vielversprechendsten Algenstämme, Expressionsvektoren und Transgen-Designstrategien durchgeführt. Die Effizienz von zwei verschiedenen Expressionsvektoren in Kombination mit zwei verschiedenen *C. reinhardtii*-Stämme wurde in Bezug auf Transgenexpressionsraten, Proteinsynthese Ausbeute, Sekretionsraten und Biofunktionalität verglichen.

Basierend auf den erzielten Ergebnissen wurde der Katalog von transgenischen *C. reinhardtii* Stämme, die menschlichen Wachstumsfaktoren sekretieren können, erweitert, um die Solidität der Plattform, die sich als am effizientesten herausstellte, zu demonstrieren.

Table of content

Abbreviations

3T3	Murine fibroblast (embryo)
ATP	Adenosine triphosphate
ARS2	Arylsulfatase 2
BCA	Bicinchoninic acid assay
BSA	Bovine serum albumin
°C	Degree Celsius
C. reinhardtii	*Chlamydomonas reinhardtii*
cDNA	Complementary deoxyribonucleic acid
CO_2	Carbon dioxide
CXC4	C-X-C chemokine receptor 4
Da	Dalton
dH2O	Double distilled water
DNA	Deoxyribonucleic acid
DMEM	Dulbecco's modified eagle medium
E. coli	*Escherichia coli*
ECM	Extracellular matrix
EDTA	Ethylene diamin tetraacetic acid
ELISA	Enzyme-Linked ImmunoSorbent Assay
eNOS	endothelial nitric oxide synthase
Fig.	Figure
g	grams
GF	Growth Factors
GRAS	Generally Recognised as Safe
H_2O	Water
HIF-1α	Hypoxia-inducible factor-1α
hPDGF-B	Human Platelet-Derived Growth Factor B
hSDF-1	Human Stromal Derived Factor 1α
hTGF-β3	Human Transforming Growth Factor β3
HUVECs	Human umbilical vein endothelial cells
hVEGF-165	Human Vascular Endothelial Growth Factor
kb	Kilobase(s)
L	Liter
LHC	Light harvesting complex

LMW	Low molecular weight
mAb	Mononuclear antibody
M	Mole(s) per litre
min	Minute
mRNA	Messenger RNA
MSC	Mesenchymal stem cells
NADPH	Nicotinamide adenine dinucleotide phosphate
nt	Nucleotide(s)
(d)NTP	(Deoxy) nuclesidetriphosphate
OD	Optical Density
PAGE	Polyacrylamide gel electrophoresis
PBS	Phosphate buffered saline
PCR	Polymerase chain reaction
PDGF	Platelet-derived growth factor
PDGF-B	Platelet-derived growth factor- homodimer BB
PDGFR-β	Platelet-derived growth factor-β
pH	Negative decimal logarithm of proton activity
PQ	Plastoquinone
PSI	Photosystem I
PSII	Photosystem II
PVDF	Polyvinylidene difluoride
RIPA	Radio-Immunoprecipitation Assay
RNA	Ribonucleic acid
RNase	Ribonuclease
rpm	Revolutions per minute
RuBisCo	Ribulose-1,5-bisphosphate carboxylase/oxygenase
SDF-1	Stromal Derived Factor-1α
SDS	Sodium dodecyl sulphate
Smad2	Mothers Against Decantaplegic homolog 2
TβR	Transforming Growth factor receptor
TAPS	Tris Acetate Phosphate Sorbitol
TGF-β3	Transforming Growth Factor β3
Tris	Tris(hydroxymethyl)-aminomethane
U	Units
UTR	Untranslated region

UV	Ultraviolet
VEGF	Vascular endothelial growth factor
VEGFR-1	Vascular endothelial growth factor receptor-1
v/v	Volume per volume
w/v	Weight per volume
WT	wild type
µ	Micro

1. Introduction

1.1. Wound Healing

A wound is a break of an organ's epithelial integrity, which may be accompanied by disruption of the underlying tissue. Often, it can be a consequence of traumatic accidents, a result of surgical incisions, or may be associated with other pathologies as diabetes.

The treatment for skin injuries represents a high economic and social cost for many countries around the world. To give two examples, in the United States, Health Care spends around US$25 billion annually on chronic wound treatment (Sen, 2009). In the United Kingdom, the National Health Service estimated at £4.5-5.1 billion in 2012 for the treatment of wounds (Guest et al., 2017). Hence, it is remarkably essential to understand the wound healing process and contribute to new and effective therapies that support it.

1.1.1. Wound healing process

Wounds compromise tissue integrity and continuity. These have to be restored to re-establish the homeostatic mechanisms, prevent infection, and minimize fluid loss (Greaves et al., 2013). All these conditions should be achieved by a wound healing process, where multiple parallel and interrelated pathways are actively synchronized to induce wound repair (Werner & Grose, 2003).

The wound healing process is based on a complex signaling network that involves different types of cells, growth factors, cytokines, and chemokines. This process can be separated into four overlapping phases: hemostasis, inflammation, proliferation, and maturation or remodeling (Greaves et al., 2013) (Figure 1).

During the hemostasis phase, platelets and fibrin fibers promote blood coagulation by forming a clot to reduce blood loss. This fibrin matrix further allows the migration of the cells to the injury site and acts as a reservoir of growth factors (GFs). The platelets release the platelet-derived growth factor (PDGF) that stimulates the cellular activity to stop the bleeding (Guerra et al., 2018).

Then the inflammation phase starts. The neutrophils are the first cells to get to the wound to clean out particles, bacteria, and dead tissue. Then the monocytes are recruited to the wound site and maturate to macrophages to continue with the cleaning process. Macrophages release other GFs, among them the vascular endothelial growth factor (VEGF), to stimulate the transition from the inflammation to the proliferation phase, hence allowing the wound healing progress to proceed (Castaño et al., 2018; Sanon et al., 2016).

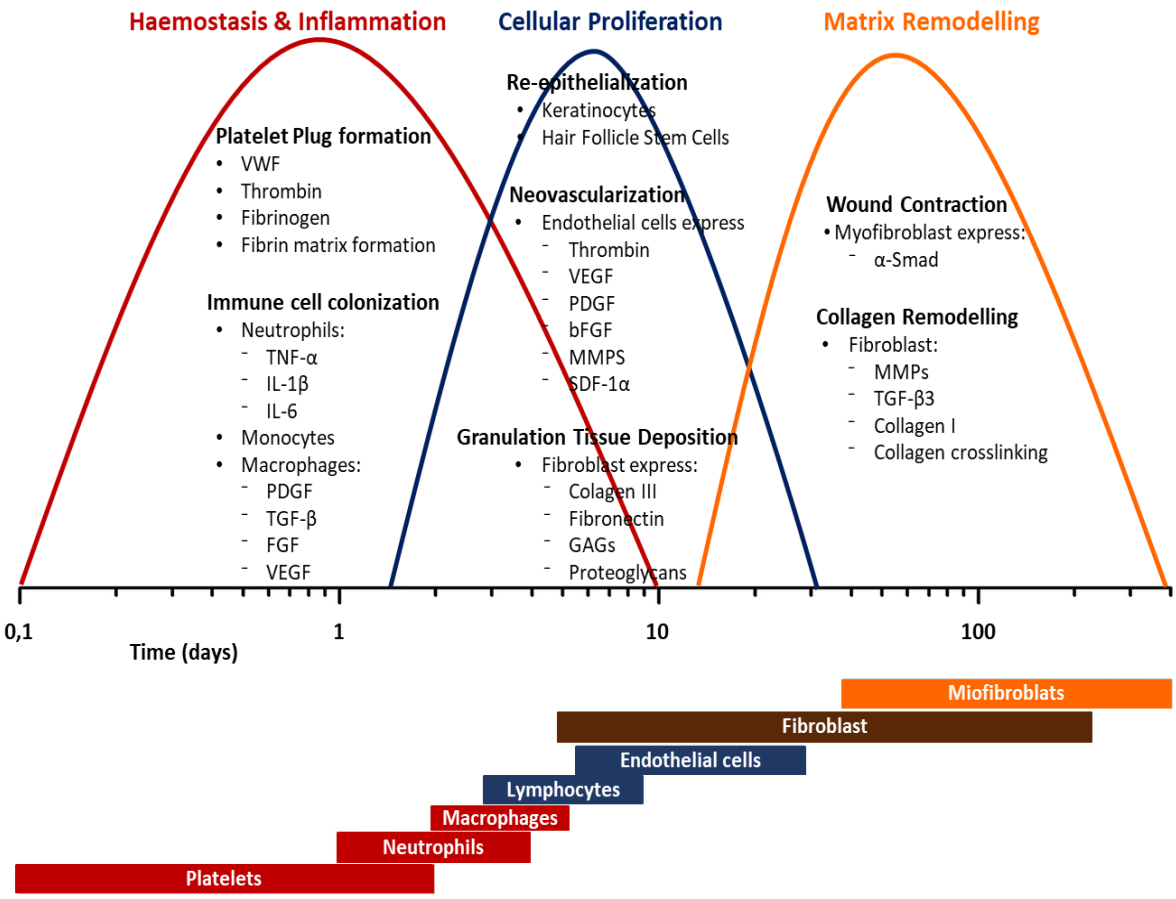

Figure. 1: Schematic representation of the overlapping wound healing process. The healing process is compounded by four phases (hemostasis, inflammation, proliferation, and remodeling), which overlaps in time, and different kind of cells take part. For more detailed information on the specific stages, see text . Modified from (Castaño et al., 2018).

The proliferation stage is characterized by reepithelization, neovascularization, and formation of granular tissue. This phase starts when fibroblasts reach the wound site and begin to proliferate and synthesize collagen, which is the main component of the extracellular matrix (ECM). For this, fibroblasts are stimulated by GFs, among them PDGF to begin to replace the provisional fibrin matrix in the wound bed for type III collagen and ECM molecules like fibronectin, glycosaminoglycans (GAGs) and proteoglycans (Greaves et al., 2013; Sanon et al., 2016; Werner and Grose 2003).

Also, during this phase, angiogenesis occurs in response to pro-angiogenic factors such as VEGF, PDGF, and the stromal-derived growth factor (SDF-1). Angiogenesis is the process of the new vascular network formation from already existing blood vessels. It is essential for wound healing and occurs in response to pro-angiogenic factors, including vascular endothelial growth factor (VEGF), fibroblast growth factor (FGF), angiogenin, angiotropin, and angiopoietin-1 (ang-1). From this GFs, VEGF-A and its receptor VEGFR-2 are the best-studied due to their crucial role in the formation and

maintenance of the new blood vessels (Greaves et al., 2013; Shibuya 2011). Angiogenesis restores tissue perfusion, re-establishes the microcirculation, and increases oxygen in the wound site (Barrientos et al., 2008; Greaves et al., 2013).

The final phase is maturation or remodeling; this phase is characterized by the contraction and remodeling of granulation tissue and restructuration into a mature scar. Fibroblasts differentiate into myofibroblasts mediated by the presence of PDGF and transforming growth factor (TGF-β); also, the type III collagen is gradually changed to type I collagen, which increases the tensile strength of the skin. The interaction of the myofibroblast with the ECM consequently reduces the size of the wound (Greaves et al., 2013; Guerra et al., 2018; Sanon et al., 2016).

Wounds can be categorized according to the healing time into acute and chronic (Dreifke et al., 2015). Those that can recover the epidermal integrity relatively quickly are referred to as acute wounds, and those who take more than 12 weeks in the initial phase are chronic wounds (Singh et al., 2017).

1.1.2. Growth factors related to the Wound healing process

As mentioned before, wound healing comprehends a cascade of events regulated by multiple growth factors and cytokines, and it depends on their interaction and timely regulation if the wound healing process is successful (Werner and Grose 2003). VEGF, PDGF, SDF-1, and TGFB are four GFs that have been thoroughly studied because of their essential role in the wound healing process. In particular, these GF are required to achieve the re-vascularisation and restoration of the tissue defect via stimulation of angiogenesis and cell- recruitment and proliferation (Barrientos et al., 2008; Castaño et al., 2018; Sanon et al., 2016; Werner and Grose 2003).

1.1.2.1. Vascular Endothelial Growth Factor

VEGF is part of the VEGF family, which includes seven cytokine members (VEGF-A, VEGF-B, VEGF-C, VEGF-D, VEGF-E and placenta growth factor (PLGF) that bind to at least one receptor of the VEGF-receptor (VEGFR) family, which is constituted by three or four members depending on the vertebrate species (Shibuya 2011; Werner and Grose 2003).

VEGF-A binds to two related receptors tyrosine kinases (RTKs) on the cell surface of vascular endothelial cells (ECs), VEGFR-1 (Flt-1) and VEGFR-2 (KDR). Both have seven immunoglobulin-like domains in the extracellular domain, a single transmembrane region, and a consensus tyrosine kinase sequence that is interrupted by a kinase-insert domain, which is activated by ligand triggered dimerization. Although VEGF shows a high affinity to VEGFR-1, VEGFR-2 is phosphorylated much more efficiently upon ligand binding. Therefore, this is the main receptor responsible for controlling the cell functions and is an essential mediator of chemotaxis and proliferation of ECs and its differentiation. A

third receptor, the neuropilin-1 (NRP1), has been proposed to act as a co-receptor for VEGFA-165, enhancing VEGF binding-affinity to VEGFR-2, (Barrientos et al., 2008; Ferrara et al., 2003; Pan et al., 2007).

VEGF-A is a 34 to 42 kDa dimeric, disulfide glycoprotein, which has been identified as the primary mediator of angiogenesis. Its messenger RNA (mRNA) undergoes alternative splicing to give at least six isoforms containing 121, 145, 165, 183, 189, and 206 amino acids, respectively. All isoforms are secreted as covalently linked homodimers and differ in their ability to bind to the cell surfaces and ECM-components (Ferrara 2001; Pan et al., 2007). Among these isoforms, VEGF-A_{165} has been reported to be essential and sufficient for angiogenesis (Maes et al., 2002).

VEGF-A_{165} stimulates angiogenesis by promoting endothelial migration and proliferation (Castaño et al., 2018; Sanon et al., 2016). It is expressed by ECs, keratinocytes, fibroblasts, platelets, neutrophils, and macrophages upon injury, where the primary stimulus for VEGF-release is the onset of hypoxia in the acute wound due to the disrupted vasculature. Pro-angiogenic hypoxic effects are mediated through hypoxia-inducible factor-1α (HIF-1α) (Sanon et al., 2016). This growth factor upregulates VEGF, which stimulates endothelial nitric oxide synthase (eNOS) and, in turn, eNOS-derived nitric oxide. Then, the VEGF gradient within the wound, along with the hypoxia gradient, stimulates ECs migration towards central hypoxic regions. This step is essential since it is required to restore the provision of nutrients and oxygen to the new tissue. In normal conditions, the serum VEGF concentration is 0.4 ± 0.2 ng/ml, yet in post-surgery patients, this concentration can reach 6.9 ± 1.3 ng/ml on the 7^{th} postoperative day (Nissen et al., 1998).

In clinical applications, tissue ischemia due to poor oxygenation is one of the principal pathologies and is the most frequent cause of strokes and heart failure. The attempts of reconstructing the microvasculature with gene therapy were the first treatments in humans for peripheral- and coronary-artery disease, and have focused on the different application ways of angiogenic molecules, including VEGF-A (reviewed by Gupta et al., 2009). Furthermore, the field of tissue engineering has developed many strategies to directly deliver VEGF-A or stimulate its local synthesis in the wound due to its role as the initiator of angiogenesis and other several stages of the repair process (Johnson and Wilgus 2014). For instance, biomaterials have been used to support its administration into wounds by establishing the GF and control its secretion (Aguirre et al., 2012; Castaño et al., 2018; Sanon et al., 2016). Some examples of this are the use of Poly (N-isopropilaclylamideco-acrylic acid) gels, for direct administration of VEGF which enhanced scarless wound healing (Hughes et al., 2004) or the use of an electrospun scaffold with collagen, hyaluronic acid, and gelatin with pro-angiogenic GFs (among them VEGF), showed excellent results concerning wound closure and the maturation of new blood vessels formed (Lai et al., 2014).

1.1.2.2. Platelet-Derived Growth Factor

The PDGF family consists of five members of homo- and heterodimers, including PDGF-AA, PDGF-AB, PDGF-BB, PDGF-CC, and PDGF-DD. Their respective receptors consist of the tyrosine kinase receptor units PDGFR-α and PDGFR-β, which contain a transmembrane domain and an intracellular kinase domain. These two receptors isoform units dimerize upon ligand binding and lead to the possible receptor combinations -αα, -αβ or -ββ. This dimerization results in the autophosphorylation of tyrosine residues in the intracellular domain and triggers several different pathways. Only the ~30 kDa glycosylate dimer PDGF-BB binds to all the isoforms (Folestad et al., 2018). Moreover, the patterns of ligand binding and receptor expression suggest a paracrine mechanism of action, as PDGF-B is expressed in the epidermis, while its receptors are found in the dermis or granulation tissue (Ataliotis and Mercola 1997).

PDGF-B takes part in every phase of the wound healing process. After an injury, platelets release PDFG-B to stimulate the mitogenesis and chemotaxis of neutrophils, macrophages, and fibroblasts to the wound site (Werner and Grose 2003). It also stimulates macrophages to produce and secrete other growth factors such as TGF-β or VEGF-A (Barrientos et al., 2008). PDGF-B stimulates cell growth through the expansion of the oligodendrocyte compartment and chemotaxis, which is necessary to prevent the apoptosis (Heldin and Westermark 1999).

During re-epithelization, PDGF-B upregulates the production of insulin-like growth factor 1 (IGF-1) and thrombospondin 1. Additionally, PDGF-B helps to enhance fibroblast proliferation and ECM-production during the proliferative phase, as well as wound contraction in the remodeling phase by stimulating the fibroblast to contract collagen matrices and inducing the myofibroblast phenotype in these cells. Furthermore, it helps to break down old collagen by upregulating matrix metalloproteinases (Barrientos et al., 2008; Castaño et al., 2018).

PDGF-B works synergistically with hypoxia to increase VEGF-A expression and is essential for blood vessel maturation. It had been shown the action of PDGF-B, together with VEGF-A increases not only pericyte- but also smooth muscle cell-recruitment, further enhancing the integrity of the capillaries (Barrientos et al., 2008).

Different studies have demonstrated the therapeutic potency of PDGF-B in the wound healing process. It has been found that the expression of PDGF-B and their receptor was reduced in wounds of genetically healing-impaired diabetic mice and glucocorticoid-treated mice, pointing out that the expression of PDGF-B and its receptor is essential for normal healing. In normal conditions, PDGF-B concentration is 1.7 ng/ml in serum, but after exercise, the levels of this growth factor can rise to 4.64 ng/ml in a healthy person (Czarkowska-Paczek et al., 2006).

Recombinant human PDGF-B was the first and only treatment for diabetic foot ulcer (DFU) approved by the Food and Drug Administration (FDA) under commercial name Becaplermin in 1997.

This drug was shown to accelerate wound closure, thereby increasing the healing rates by 32%. However, in 2008, the FDA warned about the cancer risk associated with Becaplermin (reviewed by Barrientos et al., 2014), which pointed out the need for more precise GFs administration methods. Recent studies have engineered new delivery forms for growth factors, including PDGF-BB, and related gene therapies for skin wound healing. For instance, Jiang and collaborators developed some microspheres of Poly(lactic-co-glycolic acid) (PLGA) loaded with PDGF-B and chlorhexidine, which showed to decrease the rate of infection and enhance wound healing (Jiang et al., 2013).

1.1.2.3. Stromal Cell-Derived Factor

The SDF-1 or CXCL12 is a member of the CXC chemokine family of pro-inflammatory mediators and an effective chemoattractant for a variety of cells. Its biological activity is related to its oligomeric states; nevertheless, in natural conditions, SDF-1 exists as dimer and monomer. The monomer is approximately 10kDa in size, and its main receptor is CXCR4, which is a G protein-linked transmembrane chemokine receptor, selectively found on the surface of the endothelial cells (Chang et al., 2017; Ding et al., 2011; Zhang et al., 2017; Ziegler et al., 2016).

SDF-1 is secreted by many cells, among them: monocytes, macrophages, endothelial cells, astrocytes, mesenchymal stem cells, which act as chemoattractants to promote the migration and proliferation of epidermal cells, particularly keratinocytes (Ding et al., 2011; Guo et al., 2015; Salcedo and Oppenheim 2003).

This chemokine is a crucial factor in angiogenesis because it promotes ECs migration and tube formation. It also influences physiological processes such as inflammation, wound healing, and embryonic development (Cheng et al., 2014). Some researchers have reported the role of SDF-1 in the recruitment of bone marrow-derived hematopoietic stem cells and mesenchymal stem cells, which should aid the regeneration of blood vessels, bones, cartilage and skeletal muscle (Zhao et al., 2017). Additionally, several studies have reported that bone marrow mesenchymal stem cells (BMSCs) utilize the SDF-1/CXCR4 axis to migrate to damaged tissues in varied pathological conditions as myocardial ischemia, wound area, bone fracture and cerebral ischemia (reviewed by Gong et al., 2014). In normal circumstances, the SDF-1 levels in serum are around 0.3 ± 0.2 ng/ml in healthy patients; in tuberculosis active patients, these are higher and can reach 1.3 ± 0.5 ng/ml (Mizuno et al., 2005).

Most of the efforts to test the angiogenic potential of SDF-1 have been demonstrated in different types of cells, such as epidermal stem cells (Guo et al., 2015) or bone marrow-derived endothelial cells (Velazquez 2007). Yeboah and co-workers recently developed an SDF-1 derivate that induces cell migration and revascularization in full-thickness skin wounds in diabetic mice (Yeboah et al., 2017). Other approaches have intended to load SDF-1 in biomaterials such as gelatin hydrogels,

degradable hydrogels, commercial collagen, or PLGA to improve the regeneration of blood vessels, myocardium, cartilage, and bone (reviewed by Zhao et al., 2017).

1.1.2.4. Transforming Growth Factor

The Transforming Growth Factor (TFG) family includes three isoforms of TGF-β (TGF-β1, TGF-β2, TGF-β3) all of them secreted as inactive latent peptides that require activation through a multistage process before binding to the TGF-β receptors. The TGF's polypeptides are initially synthesized as pre-pro-TGF-β, which is a monomer of approximately 55 kDa and contains the called latency associated peptide (LAP). The next step involves proteolysis and dimerization, creating the small latent TGF-β complex (SCL), which is the connection between two LAP chains by disulfide bonds established between the cysteine residues of the latent TGF-β binding protein (LTBP). Then the large latent TGF-β complex (LLC) is formed and secreted from the cell to interact with ECM components, including integrins. Bonding with these molecules allows the activation of the mature form of TGF-β (Barrientos et al., 2008; Poniatowski et al., 2015; Rybska et al., 2018).

Once the TGF-β active form is released, they can bind to the cell surface complex of two pairs of the transforming β receptor-I and II (TβRI and TβRII, respectively). The TβRII is constitutively phosphorylated, then the next step is the phosphorylation of TβRI; thus, the resulting heterotetramer can transmit the signal into the cell.

The functional activation of the receptors is regulated through posttranslational modifications, spatial regulation at the cellular level, and the availability of the receptors in the cell surface. This mechanism is due to the cells that can mobilize the TGF-β receptors from the intracellular compartment to the plasma membrane, increasing its abundance and make it available to the binding. Structurally, the receptors contain a domain that shows serine/ threonine kinase activity, a transmembrane region, and the ligand-binding domain (Duan and Derynck 2019; Poniatowski et al., 2015; Rybska et al., 2018). This receptor complex phosphorylation activates the SMAD-intracellular signaling pathway through the Smad-receptors (Smad2 and Smad3), which interacts with DNA binding transcription factors and cofactors to amplify or repress gene expression (Penn et al., 2012; Poniatowski et al., 2015). There is evidence that the TβRII receptor specifically binds to the TGF-β3, acting as traffic control because of the differential responses of keratinocytes migration to human serum or plasma (Bandyopadhyay et al., 2006).

The transforming growth factor family is involved in all phases of the wound healing process, and different kinds of cells produce its members during this process, such as platelets, keratinocytes, macrophages, and fibroblasts. More specifically, TGF- β1 is expressed in dendritic cells, leukocytes, and epithelial cells; meanwhile, TGF-β2 is present in epithelial and nerve cells and TGF- β3 in fibroblasts (Barrientos et al., 2008; Rybska et al., 2018).

The TGF-β family has a chemoattractant effect for neutrophils, macrophages, and fibroblasts. Also, it stimulates the proliferation and differentiation of mesenchymal stem cells (MSCs) and the synthesis and deposition of collagen fibers, as well as ECM-remodeling (Penn et al., 2012; Poniatowski et al., 2015; Werner and Grose 2003). The TGF-β family is also related to scarring, where sequestration of TGF-β by the glycoprotein decorin inhibits their activity, thus inducing hypertrophic scars (Penn et al., 2012). In normal conditions, human plasma serum levels of TFG-β3 are 1-2 ng/mL (Bandyopadhyay et al., 2006).

The therapeutic application of TGF-β3 was tested by direct delivery of recombinant hTGF-β3 (Avotermin); this drug showed a significant reduction of scarring in clinical trials phase I/II (Occleston et al., 2011), but failed in phase III (Yamakawa and Hayashida 2019). In biomedicine, TGF-β3 has been reported as a reducer of hypertrophic scars (Bandyopadhyay et al., 2006) and as an aid in bone fracture healing, among other clinical uses (Poniatowski et al., 2015).

1.1.3. Oxygen in wound healing and regeneration

Oxygen is an essential molecule for life. Besides, oxygen is particularly necessary for wound healing, where oxygen is involved in four main healing mechanisms: the oxidative killing of bacteria, re-epithelialization, angiogenesis, and collagen synthesis (Knighton et al., 1983).

Oxygen concentration in the human body is expressed in terms of oxygen partial pressure (pO_2). In normal conditions, oxygen is provided by the circulatory system, where the pO_2 in the arterial blood is approximately 100 mm Hg (Gordillo and Sen 2003). However, when a disruption of vasculature occurs due to a wound, the central area of the dermal injury is hypoxic (pO_2 values between 0 – 10 mm Hg), the periphery of the wound is normoxic (pO_2 60 mm Hg).

Hypoxia is defined as a lower tissue pO_2 compared to the pO_2 under healthy conditions *in vivo*. Hypoxia leads to anaerobic metabolism, where the acid environment and the inadequate ATP production make it impossible to maintain normal cellular function (Rodriguez et al., 2008). The three main factors that contribute to wound tissue hypoxia are peripheral vascular diseases (PVDs) impeding O_2 supply, an increase of O_2 demand of the healing tissue and generation of reactive oxygen species (ROS) by way of respiratory burst and for redox signaling (G Rodriguez et al., 2008; Sen 2009).

It is known, ROS has an essential role in the oxidative killing of bacteria acting as a first defense against infections. Low levels of reactive oxygen species (ROS) and the elevated lactic acid acts as cellular messengers to stimulate the critical process associated to wound healing, as cell motility, cytokine action, angiogenesis, and ECM formation (G Rodriguez et al., 2008; Gordillo and Sen 2003; Singer and Clark 1999). However, if the ROS levels are extremely low, the cell cycle can get cytostasis, then the cell growth and proliferation is inhibited. Moreover, if there is an excess of ROS, no oxygen is available in the wound, then, the perfusion decrease causing ischemia, resulting in cell death, also the

availability of the growth factors are reduced, as well as the nutrient supply (Dunnill et al., 2017; Gordillo and Sen 2003; Sen 2009).

Oxygen is required for the adenosine triphosphate (ATP) synthesis in the mitochondria and is, therefore, crucial to maintaining adequate energy levels in the cells involved in the formation of the newly growing tissue. Additionally, the ATP released from the damaged epithelial cells can activate purigenic or adenosine receptors, influencing the immune response, inflammation, vasculogenesis, and endothelial cell proliferation. Besides, extracellular ATP turns on NADPH oxidases. This activation is critically required to produce the redox signals needed for wound healing, increasing vascularity and inducing the molecular markers of angiogenesis, specifically VEGF (Roy et al., 2006; Sen 2009).

As it has been established, oxygen concentration has a crucial role during the whole wound healing process. The initial hypoxic condition in wounds leads to the hypoxia-inducible transcription factor 1α (HIF-1) expression, which is the start point for the cascade reaction of the cytokines related to the healing process, among them PDGF, VEGF, SDF-1 and TGF-β (G Rodriguez et al., 2008; Gordillo and Sen 2003; Tandara and Mustoe 2004). Additionally, the low O_2 concentration stimulates neutrophils to provide immunity and prevent infections through NADPH-oxygenase, which produces superoxide able to kill bacteria in the environment. Nevertheless, if the hypoxic conditions became chronic, all this process can not be sustained, compromising tissue survival (Hopf and Rollins 2007).

Although hypoxia is known for its role in the early phase of neovascularisation, only acute hypoxia has this angiogenic effect, whereas severe or chronic hypoxia inhibits new blood vessel-formation (Sen 2009; Tandara and Mustoe 2004). Moreover, acute hypoxia (0-72hrs) enhances fibroblast migration, proliferation, and production of the collagen matrix, whereas under chronic hypoxic conditions, this activity decreases (Siddiqui et al., 1996). Furthermore, oxygen delivery to chronic hypoxic wounds restores mitochondrial respiration, ATP synthesis and enables ROS production, which in turn is the primary stimulus for VEGF synthesis to promote angiogenesis (Howard et al., 2013).

On the other hand, a temporary lack of oxygen in a wound tissue is also required to induce the wound healing process (Ong and Dilley 2018). For example, keratinocytes move faster under this condition, and the same situation happens with human dermal fibroblasts (Menon et al., 2012).

Collagen deposition and proteoglycan constitute the main components of the ECM, which is required to provide support to new blood vessels, otherwise, new capillary tubes assembly poorly and remain fragile (Eisenbud 2012; Sen 2009). Furthermore, the ECM deposition is entirely dependent on oxygen, since collagen production and remodeling are two processes that depend on oxygen. The hydroxylation of proline and lysine in procollagen is required for the maturation of the collagen, since this procollagen hydroxylation is entirely oxygen-dependent, even an oxygenation increase, rise the collagen deposition and tensile strength (Tandara and Mustoe 2004). In chronic wounds, excessive

degradation of extracorporeal membrane oxygenation by metalloproteinases occurs, then the ECM can not be formed, thus there is the only procollagen, which does not have the functional properties of collagen (Eisenbud 2012).

1.2. Oxygenic photosynthesis

In 1772 Joseph Priestly demonstrated that oxygen (O_2) was an indispensable molecule for life when he showed that a mouse could live in a closed compartment when a plant is also inside, thereby concluding that the plants cover the breathing needs of the mouse (West 2013).

Photosynthesis is the main process that provides oxygen and energy as biomass for heterotrophic living organisms in the earth. During 1950 and 1960, Danial I. Arnon and colleagues reported that photosynthesis involves two phases: the so-called light-dependent reactions, where O_2, adenosine triphosphate (ATP), and nicotinamide adenine dinucleotide phosphate (NADPH) are produced; the second phase, known as the light-independent reactions (Calvin-Benson cycle), which reduce CO_2 to carbohydrate and consume ATP and NADPH in the light-dependent reactions (Buchanan et al., 2000).

This process takes place in the chloroplasts of plants, algae, and some cyanobacteria (Rumpho et al., 2011), which was demonstrated by showing that the chloroplast thylakoid membranes oxidize water molecules and result in the reduction of $NADP^+$ and synthesis of ATP and oxygen release (Nelson and Yocum 2006).

The photosynthesis reactions are catalyzed by four large protein complexes (Figure 2.): photosystem I (PSI) and photosystem II (PSII), an ATP synthase (F-ATPase) and the cytochrome b_6f complex (Cyt b_6f). PSI and PSII are supported by peripheral light-harvesting complexes (LHCs) that work together in the linear electron transport (Dekker and Boekema 2005). A serial of biochemical reactions must take place to complete this cooperative action of photosynthesis between pigments and protein complexes.

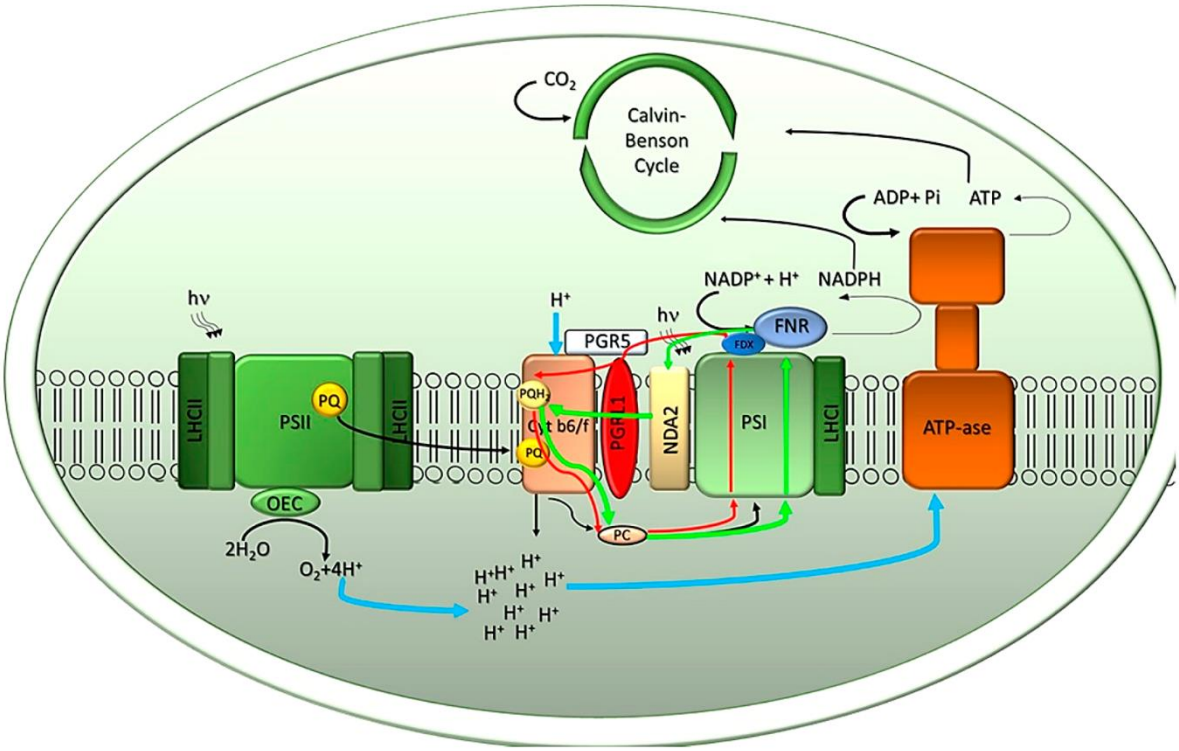

Figure. 2: Schematic representation of electron transport trough the photosynthetic complexes in the thylakoid membrane. Arrangement of PSI, PSII, Cyt b_6f and ATP synthase complexes within the thylakoid membranes is shown. The light-driven water splitting reaction leads to O_2 evolution and originates linear electron transport, indicated with black arrows, from water to $NADP^+$, which is coupled to proton translocation from stroma into the luminal side of thylakoids during the light phase. The electrochemical gradient formed is used by the ATP synthase to produce ATP from Adenosine diphosphate (ADP) and Pi in the stroma. The NADPH and ATP formed during the light phase drive the Calvin–Benson–Bassham cycle reactions in the stroma. Two pathways of cyclic electron transport around PSI are indicated with red (Ferredoxin-dependent pathway) and green (NDA2-dependent pathway) arrows. Taken from (Vecchi et al., 2020).

First, sunlight is harvested by the light-harvesting complexes (LHCII), the photon-excited chlorophyll pigments, which transfer energy to the reaction centers (PSI and PSII). Here start a series of electron transfer steps from a donor to an acceptor electron carrier molecule, which is driven by the proximity of the electronic charge through the photosynthesis complexes (Vecchi et al., 2020).

In the PSII, the energy harvested protons are used to excite the reaction chlorophyll center (P680) and used to split H_2O into oxygen, protons, and electrons and to reduce the plastoquinone (PQ) Q_A, to another PQ molecule Q_B. This reaction involves four consecutive turnovers of the reaction center P680 and requires two H_2O molecules to release one O_2 molecule (Minagawa and Takahashi 2004). When Q_B is double reduced, it binds to protons from the stroma and is converted to plastoquinol

(PQH_2), which moves inside the thylakoid membrane to the specific binding site on the Cyt b_6f complex where it is oxidized.

The Cytb_6f complex receives electrons from the PSII by PQH_2 and passes to the PSI by reducing plastocyanin (PC) or cytochrome c_6, both in plants and algae or cyanobacteria (Hippler 2017). This electron transfer is guided by the translocation of protons across the membrane, from the stroma to lumen, and creates a proton electrochemical gradient across the membrane via the Q-cycle for ATP synthesis (Dekker and Boekema 2005).

In the PSI, its primary donor P700 (chlorophyll dimer), is excited. This P700* transfers an electron to chlorophyll A_0 ($ChlA_0$), then the PSI catalyzes the oxidation of PC and the reduction of ferredoxin (Fd) via FeS-cluster (Buchanan et al., 2000). After passing through PSI, electrons are transferred from Fd to $NADP^+$ and form NADPH, due to the ferredoxin-NADP oxidoreductase (FNR), which catalyzes this reaction (Eberhard et al., 2008).

Finally, the two photosynthetic products, ATP and NADPH, which are high-energy compounds of intermediate stability, are used in the Calvin-Benson cycle to fix CO_2 and convert it into sugar. This process is completed through three different phases. First, during the carboxylation phase, one CO_2 molecule is added to the 5-carbon sugar ribulose biphosphate (RuBP) by the Ribulose bisphosphate carboxylase/oxygenase (Rubisco) enzyme, to form two molecules of 3-phosphoglyceric acid (PGA). Then, in the reduction phase, the NADPH and some ATP are consumed to reduce the PGA to triose phosphate (Triose-P). During the last phase, called regeneration, the initial RuBP is restored from the Triose-P through several reactions and involves eight different enzymes, which has a crucial role in the carbon fixation due to the carboxylation (Blankenship 2014; Vecchi et al., 2020).

1.3. *Chlamydomonas reinhardtii*

1.3.1. General considerations

The unicellular green alga *Chlamydomonas reinhardtii* is worldwide distributed in soil and freshwater (Figure 3). It has about 10 micrometers in diameter and has an oval shape, which is enclosed by a multilayered cell wall made of hydroxyproline-rich glycoproteins and non-cellulosic polysaccharides. *C. reinhardtii* has a prominent nucleus that harbors the nucleolus, and the nucleus is surrounded by a membrane that is continuous with the endoplasmic reticulum and Golgi bodies. Characteristic organelles of this alga are two flagella of 10-12 micrometers in length used for motility and matting, contractile vacuoles, a single cup-shaped chloroplast that occupies a large proportion of the cell (40%), cytosol-dispersed mitochondria, a large pyrenoid within the chloroplast, which is responsible for carbon fixation and near to the cell equator is the eyespot of high condensed

carotenoid pigments that works as a directional antenna that helps it moves toward or away to the light (Harris et al., 2009).

As mentioned before, *C. reinhardtii* cells are enclosed by a multilayered cell wall, which consists of an insoluble hydroxyproline-rich glycoprotein innermost layer and three layers of chaotrope-soluble glycoproteins forming the central triplet, which is an amorphous outer layer of branching glycoprotein fibers. The widely used cw-15 wall-less laboratory strain has a rudimentary cell wall with a reduced amount of cell wall components because it fails to assemble layers of the central triplet. Instead, it creates branches of cell-wall fibers that resemble the outer layer of the wild type cells (Harris et al., 2009). Nevertheless, cell-wall deficient mutants are extensively used for transformation due to its high efficiency in incorporating exogenous DNA (Harris 2001).

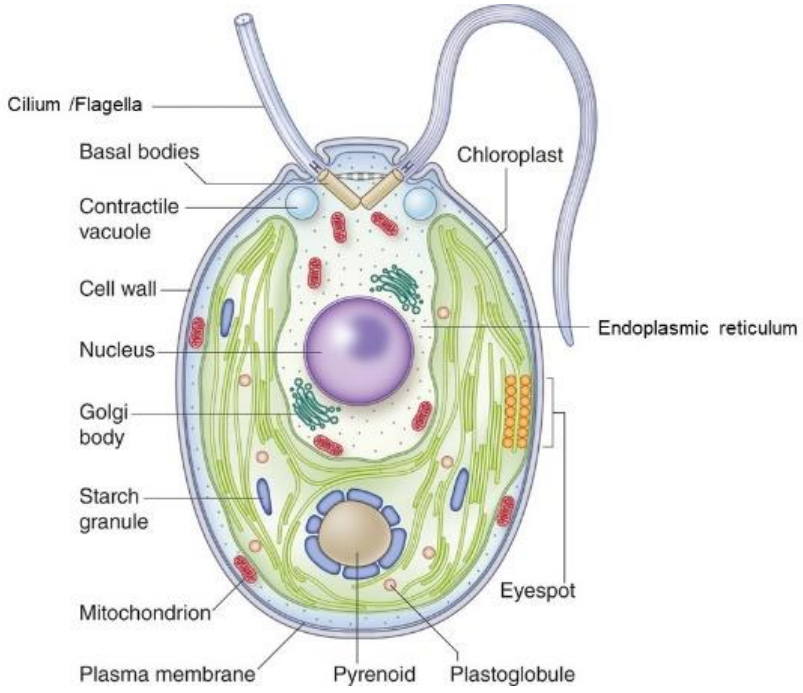

Figure. 3: Cell structure of *C. reinhardtii*. Showing the nucleus, endoplasmic reticulum with the Golgi bodies, the cup-shape chloroplast with the eyespot and the pyrenoid, starch granule and plastoglobules, also the mitochondrion, the contractile vacuoles and the two flagella. Adapted from (Sasso et al., 2018).

Chlamydomonas reinhardtii, have been used as a model organism to study photosynthesis, due to its closely related photosynthetic apparatus to the vascular plants. Also, its ability to grow heterotrophically using acetate as a carbon source allows the isolation of mutants that can synthetize chlorophyll and assemble a complete photosynthetic apparat in the dark (Dent et al., 2001). *C. reinhardtii* has a maximal photosynthetic activity of 7.584 ± 0.416µg O_2 (237 ± 13 nmol O_2) per $1{\cdot}10^6$ cells in one hour under continuous illumination (Janssen et al., 2000).

1.3.2. *C. reinhardtii* as a model organism for protein expression

Over decades *C. reinhardtii* has been a model organism to study photosynthesis due to its numerous advantages. This unicellular haploid alga can be grown easily in the laboratory conditions, it reproduces sexually or asexually and can grow under three different conditions: photoautotrophic which means using light and CO_2 as a carbon source, mixotrophic, which means under illumination, but in this case, the acetate-containing medium provides the carbon, or heterotrophic conditions (without light), where it can still synthesize and assemble a fully functional photosynthetic apparatus, which is similar to the photosynthetic reactions centers to those of higher plants (Dent et al., 2005; Harris et al., 2009).

In the laboratory, the optimal conditions for growing are long-established. For a wild-type strain, optimal cultivation conditions include temperature around 20-25 °C in minimal liquid or agar medium and illumination at around 200-400 µE (photosynthetically active radiation), which allow a population doubling time of 6 or 8 hours (Harris 2001). *C. reinhardtii* nuclear genome is about 111 Mb, organized in seventeen chromosomes, a 15.8 kb mitochondrial genome, and 50-80 identical copies of a 205 kb chloroplast genome (Gallaher et al., 2018). All three genomes are fully sequenced (Merchant et al., 2007) and amenable for genetic modification.

Another advantage of *C. reinhardtii* as a model organism is that this green alga is considered a "Generally Recognized as Safe" (GRAS) organism, which means that it does not have any pathogens that can cause damage to humans, which makes it an attractive cell factory for recombinant proteins for biomedical purposes. For instance, they can be used as topical application of biopharmaceuticals such as anti-microbial proteins in crude cell lysates or even use the whole algae for oral delivery of vaccines, anti-microbials or hormones (Taunt et al., 2018). As a result, *C. reinhardtii* has become an attractive a model organism in other research areas, such as biotechnology, where recent research has been devoted to developing strategies to efficiently express heterologous proteins including antibodies or therapeutic molecules using *C. reinhardtii* (Leon-Banares et al., 2004), as introduced in the next section.

1.3.3. Recombinant protein expression in *C. reinhardtii*.

C. reinhardtii has a high potential as a bio-factory, as it has many features that are desirable in a commercial platform for recombinant protein production such as high growth rate and easy cultivation, ability to synchronize cultures, the capacity for classical genetic crosses, existing tools for genetic manipulation, efficient long-term cryo-conservation protocols and the ability to perform post-transcriptional and post-translational modifications (Potvin and Zhang 2010b).

More recently, transgenic microalgae emerged as an alternative to produce therapeutic molecules instead of bacteria, yeast, or mammalian cell lines, which had been the most used organisms by the pharmaceutic industry as an expression platform to produce recombinant proteins. Table 1 summarizes the advantages and disadvantages of each system (Yan et al., 2016).

Table 1. Rough comparison among different expression platforms to produce pharmaceuticals. (Adapted from Yan et al., 2016).

	BACTERIA	YEASTS	MAMMALIAN CELLS	ANIMALS	PLANTS	MICROALGAE
PROTEIN FOLDING ACCURACY	Low	Medium	High	High	High	High
GLYCOSYLATION	None	Incorrect	Correct	Correct	Minor Differences	Minor Differences
PRODUCT QUALITY	Low	Medium	High	High	High	High
PROTEIN YIELD	Medium	High	High	High	High	High
PRODUCTION SCALE	Limited	Limited	Limited	Limited	Worldwide	High
PRODUCTION TIME	Short	Medium	Long	Long	Long	Short
SCALE-UP COST	High	High	High	High	Medium	Low
OVERALL COST	Moderate	Moderate	Expensive	Expensive	Inexpensive	Low
CONTAMINATION RISK	Endotoxins	Low	High	High	Low	Low
SAFETY	Low	Unknown	High	High	High	High
STORAGE COST	Moderate	Moderate	Expensive	Expensive	Inexpensive	Low
DISTRIBUTION	Medium	Medium	Difficult	Difficult	Easy	Very easy
REPRODUCTION	Easy	Easy	Difficult	Medium	Easy	Very easy

Interestedly, in microalgae, it is possible to express recombinant proteins either from the nucleus in a eukaryotic environment or the chloroplast for prokaryotic conditions. Nowadays, the number of recombinant proteins successfully expressed in by *C. reinhardtii* is increasing and includes antibodies, vaccines, therapeutic proteins, feed supplements, bioremediation, and environmental control proteins. The increasing interest in *C. reinhardtii* as a biomanufacturing platform of recombinant protein led to the production of many different compounds such as antibodies and immunotoxins, hormones, industrial enzymes, and orally-active colostral protein and subunit vaccines, which are summarized in Table 2 (Rasala and Mayfield 2015).

Table 2. Overview of *C. reinhardtii* produced therapeutics, feed supplements and another recombinant protein (Adapted from Hempel and Maier 2016)

Recombinant protein	Expression site	Expression level	Genome promoter	Reference
Human IgG αPA83	Intracellular (chloroplast)	100 µg/g dw	Chloroplast, *psbA*	(Tran et al., 2009)
Immunotoxin αCD22-PE40	Intracellular (chloroplast)	0.2–0.4 % TSP	Chloroplast, *psbA*	(Tran et al., 2013b)
Immunotoxins αCD22-Gelonin	Intracellular (chloroplast)	0.1–0.7 % TSP	Chloroplast, *psbA*	(Tran et al., 2013a)
lsc αHSV glycoprotein D	Intracellular (chloroplast)	n.s.	Chloroplast, *atpA*, *rbcL*	(Mayfield et al., 2003)
Nanobodies αBoNT/A	Intracellular (chloroplast)	5 % TSP	Chloroplast, *psbA*	(Barrera et al., 2015)
D2-CTB	Intracellular (chloroplast)	0.7 % TSP 1.6 mg/g dw	Chloroplast, *rbcL*	(Dreesen et al., 2010)
AMA1- and MSP1-GBSS	Intracellular (chloroplast)	0.2–1 µg/ mg starch	Nucleus, *HSP70A - RBCS2*	(Dauvillée et al., 2010)
Pfs25, Pfs28	Intracellular (chloroplast)	0.5 %, 0.2 % TSP	Chloroplast, *psbA*	(Gregory et al., 2012)
Psf25-CTB	Intracellular (chloroplast)	0.09 % TSP	Chloroplast, *psbA*	(Gregory et al., 2013)
Pfs48/45 C-term	Intracellular (chloroplast)	n.s.	Chloroplast, *psbA*, *psbD*	(Jones et al., 2013)
HIV antigen P24	Cytosol	0.25% TCP	Nucleus, *PsaD*	(Barahimipour et al., 2016a)
E7 HPV-16	Intracellular (chloroplast)	0.12 % TSP	Chloroplast, *psbD*	(Demurtas et al., 2013)
VP1 (FMDV)-CTB	Intracellular (chloroplast)	3 % TSP	Chloroplast, *chlL*	(Sun et al., 2003)
VP28 (WSSV)	Intracellular (chloroplast)	0.2–21 % TCP	Chloroplast, *psbA*, *atpA*	(Surzycki et al., 2009)
E2 (CSFV)	Intracellular (chloroplast)	1.5–2 % TSP	Chloroplast, *rbcL*	(He et al., 2007)
Angiotensin II-HBcAg	Intracellular (n.s.)	0.05 % TSP	Nucleus, CaMV 35S	(Soria-Guerra et al., 2014)
M-SAA	Intracellular (chloroplast)	5 % TSP	Chloroplast, *psbD*, *psbA*	(Manuell et al., 2007)
Human Epo	Secreted	~100 µg/L	Nucleus, *HSP70A - RBCS2*	(Eichler-Stahlberg et al., 2009)

Table 2: Overview of *C. reinhardtii* produced therapeutics, feed supplements and another recombinant protein (continued)

Recombinant protein	Expression site	Expression level	Genome promoter	Reference
Epo, interferon-ß, proinsulin, VEGF, HMGB1, 10FN3, 14FN3	Intracellular (chloroplast)	Up to 3 % TSP	Chloroplast, *psbA*, *atpA*	(Rasala et al., 2010)
Human TRAIL	Intracellular (chloroplast)	0.43–0.67 % TSP	Chloroplast, *atpA*	(Yang et al., 2006)
hGAD65	Intracellular (chloroplast)	0.25–0.3% TSP	Chloroplast, *rbcL*	(Wang et al., 2008)
apcA + apcB	Intracellular (chloroplast)	2–3 % TSP	Chloroplast, *psbA*	(Su et al., 2005)
PDGF, SDF-1	Secreted	1.25 ng/mL and 0.326 ng/mL	Nucleus, *PsaD*	(Centeno-Cerdas et al., 2018)
Phytase AppA	Intracellular (chloroplast)	n.s.	Chloroplast, *atpA*	(Yoon et al., 2011)
Endo-β-1,4-xylanase	Intracellular (cytosol) Secreted	0.25 % TSP n.s.	Nucleus, *AR4*	(Rasala et al., 2012)
hu Sep15	Intracellular (n.s.)	n.s.	Nucleus, *hsp70 - RBCS2*	(Hou et al., 2013)
Metallothioneinlike protein (*F. rubra)*	Intracellular (chloroplast)	n.s.	Chloroplast, *atpA*	(Han et al., 2008)
hMT-2	Intracellular (chloroplast)	n.s.	Chloroplast, *psbA*	(Zhang et al., 2006)

CTB cholera toxin subunit B, *dw* dry weight, *n.s.* not specified, *TCP* total chloroplast protein, *TSP* total soluble protein

There are different methods to transform microalgae; all of them are based on the temporal permeability of the cell membrane, enabling the DNA to get into the cell (León and Fernández 2007). A simple and efficient method for cell-wall deficient strains is to vortex the cells in the presence of DNA, glass beads, and polyethylene glycol (PEG) (Kindle et al., 1989). Another possibility for whole cell-wall strains is to use this agitation method, but instead of glass beads, silicon carbide whiskers can be used (G Dunahay 1993). Electroporation is another technique successfully employed to achieve stable transformants in *C. reinhardtii* (Shimogawara et al., 1998). In this method, transient holes in the cell membrane are formed when electric pulses are applied; the temperature, osmolality, electric conditions, field strength ($kVcm^{-1}$), time of discharge, and DNA concentration should be optimized to get high transformation efficiencies. In the biolistic or microparticle bombardment, small gold or tungsten particles are covered with DNA, and those are shoot into the host cell with a gene gun (León and Fernández 2007). *Agrobacterium tumefaciens* transformation is another way to insert trans-genes

into the algae; in this method, the delivery of genetic material is mediated by the stimulation of cell division by-products encoded by T-DNA from Agrobacterium to the host cell (Potvin and Zhang 2010b).

Most of the efforts to express recombinant proteins in *C. reinhardtii* have focused on the chloroplast, The chloroplast of this algae represents the 40% of the cellular volume, which provides a favorable environment, and it prevents the proteolysis of the proteins, thereby allowing high accumulation yields (Hippler 2017). However, the chloroplast is not the best platform to produce biopharmaceutical products, because it does not allow for eukaryotic post-translational modifications, which are remarkably crucial to the stability and the biological activity of the proteins (Walsh and Jefferis 2006).

Nuclear expression, on the other hand, permits correct disulfide bond bridge formation, glycosylation, and phosphorylation of recombinant proteins, and hence the efficient production of biopharmaceuticals. Moreover, the nuclear expression of transgenes also allows secreting the proteins outside the cell, which is an advantage in the downstream process, simplifying it and reducing the production costs (Hempel and Maier 2016).

When designing an expression strategy for a specific recombinant protein, one should consider the following elements. First, effective transformation requires selection markers that allow identifying the successful transformants. Most commonly, co-transformation with a transgene that confers resistance against antibiotics such as spectinomycin (*aadA*) and paromomycin (*aphVIII*) (Potvin and Zhang 2010b) is used. Second, promotor choice is an essential feature for efficient protein expression. For recombinant protein expression from the nuclear genome of *C. reinhardtii,* the 5' UTR of *RBCS2*, *PsaD*, *HSP70A*, (Berthold et al., 2002; Fischer and Rochaix 2001; Schroda et al., 2002) or the fusion of *HSP70A-RBCS2* (Eichler-Stahlberg et al., 2009; Lauersen et al., 2015b; Schroda et al., 2000) have been used successfully in the past.

Also, non-coding regulatory elements have been used to enhance nuclear expression of recombinant proteins, this includes introns like the Rubisco Small Subunit 2 first intron (*RBCS2i*) (Eichler-Stahlberg et al., 2009; Lauersen et al., 2013a; Lumbreras et al., 1998), and thiamine pyrophosphate riboswitches (*THI4*) (Croft et al., 2007; Moulin et al., 2013) reviewed by (Scaife et al., 2015).

Moreover, functional peptides are another element that can be used to express recombinant proteins, so that the proteins can be directed or secreted to different subcellular locations by employing characterized targeting peptides, such as Arylsulfatase 2 (*ARS2*) (Centeno-Cerdas et al., 2018; Chavez et al., 2016; Eichler-Stahlberg et al., 2009) and Carbonic anhydrase 1 (*cCA1*) (Lauersen et al., 2015b) signal peptides for secretion. Besides, tag-sequences may be used for downstream immunodetection or purification, such as the sequences coding for His-tag, Strep-tag, or hydrophobin (HFBI) (Barahimipour, 2016; Baier, 2018; Lauersen, 2015).

While selecting an appropriated reporter gene is also necessary for the development of an efficient transformation system, these reporters can help for the detection of the transgene. Several different reporter genes are available GFP, mVENUS, mCHERRY, EYFP, tdTOMATO (Rasala et al., 2013). As well these fluorophores, other genes have been used as reporters for *C. reinhardtii* transformation, such as the antibiotic-resistant gene *aadA*, endogenous chloroplast genes as *chlB*, *chlL,* and *chlN*, where a single change of color phenotype can be used as a reporter. Additionally, the *E. coli* gene *uidA* encodes β-glucuronidase (GUS) widely used in plants and algae, has also been described as a reporter in *Chlamydomonas* to test promoters and 5' UTR from different chloroplast genes (Esland et al., 2018).

Finally, for *C. reinhardtii* microalgae, the adaptation of the foreign gene sequence to the host-specific codon-usage is critical, because of its unique genomic high GC content of ~65% (Merchant et al., 2007). Otherwise, the transgenes might be susceptible to silencing effects and translational stalling, premature translational termination, translational frame shifting, and amino acid misincorporation (Heitzer et al., 2007).

1.3.4. Optimization strategies of *C. reinhardtii* nuclear recombinant protein expression

As mentioned before, achieving a high rate of recombinant proteins expressed in the nucleus of *C. reinhardtii* is a challenge. First, nuclear transformations occur by random insertion (Zhang et al., 2014), which entails the risk of introducing detrimental mutations into the genome. It has also been demonstrated that both epigenetic transcriptional inactivation of a transgene and the genomic region where the gene of interest was inserted influence in the transgene expression (Cerutti et al., 1997; Jinkerson and Jonikas 2015).

During the last years, there has been a research interest to increase the protein expression rates in *C. reinhardtii* by developing several different approaches. Some of them include high-frequency transformation protocols (Kindle et al., 1989), mutant strains with improved nuclear expression potential (Neupert et al., 2009), nuclear transgene expression vectors (Lauersen et al., 2013a; Neupert et al., 2009), secretory signals (Molino et al., 2018) and reporters (Rasala et al., 2013).

To circumvent this problem, Neupert *et al*. 2009 developed the strains UVM4 and UVM11, which showed uniformly high accumulation levels of recombinant protein in all their transgenic clones. For the creation of these strains, they assumed that the reason behind the low efficiency of transgene expression in *C. reinhardtii* was related to the presence of non-conventional epigenetic suppression activities and a compact chromatin structure that does not allow the transgene transcription. Therefore, they isolated mutants in which this suppression-mechanism was defective. First, they performed a co-transformation of cw15 strain with CRY1-1 gen and selected through a low concentration of emetine resistance. Then they mutated the selected strains by UV-light, after a second resistance selection, the five strains that showed the highest tolerance to emetine were chosen

for transformation with a green fluorescent protein (GFP) and yellow fluorescent protein (YFP) for further analysis (Neupert et al., 2009). The strains UVM4 and UVM11 showed an accumulation of the recombinant fluorescent reporter proteins that reached 0.2% of the total soluble protein. These strains became an essential part of the available toolbox for genetic engineering using *C. reinhardtii*, and they have been used in many different approaches and working groups (*e.g.*(Barahimipour et al., 2016b; Bohne et al., 2013; Chavez et al., 2016; Lauersen et al., 2015b).

On the other hand, researchers have been working on the development of vector systems that increase the expression rates of recombinant proteins. Fischer and Rochaix made the first approach about vector systems; they generated a vector (pBC1) for high-level expression of endogenous and exogenous genes. They identified the nuclear gene coding for the *C. reinhardtii* photosystem I reaction center subunit II (*PsaD*) as one whose regulatory elements are restricted to the flanking promoter and 3' untranslated regions (Fischer and Rochaix 2001). Using the *PsaD* genomic sequence, they developed a vector that allowed the efficient generation of transgenic strains as well as the subcellular targeting of recombinant proteins, when a peptide signal is included in the construct.

Finally, Lauersen and colleagues developed a vector system, which promised recombinant proteins yields up to 10 mg/ml. It was later optimized by the same group to become a modular vector (pOpt) that allows the rapid cloning of genes of interest in *C. reinhardtii*. The expression cassette in this construct uses the Heat Shock 70A (*HSP70A*)-Rubisco small subunit 2 (*RBSC*2) fusion promoter, along with the Rubisco small subunit intron 1 (*HSP70A-RBCS2*-i1) and *RBCS2* 3' untranslated region as regulatory elements. Furthermore, in order to target the reporter proteins into the supernatant, the 21 aa carbonic anhydrase-1 secretion signal (Menon et al., 2012) was fused to the transgene. Both constructs, pBC1 and pOpt, contain the APHVIII gene as a selectable marker that conferred resistance to paromomycin under the same hybrid promoter consisting of the *HSP70A* and *RBCS2*-i1 elements (Lauersen et al., 2013b; Lauersen et al., 2015a).

1.4. HULK project

Given the inherent hypoxia that comes with its application, tissue engineering has focused its efforts on finding out the appropriate oxygen supply for cell proliferation, collagen production, re-epithelization, and antibacterial activity (Tandara and Mustoe 2004). Moreover, every year, the treatment cost of non-wound healing patients increases, mostly due to pathological diseases as diabetes and obesity. Additionally, hypertrophic scarring represents another problem because it is challenging to treat and impossible to prevent (Sen et al., 2009).

As an alternative to blood-vessel mediated oxygen perfusion, our group has developed the concept of HULK (from the German abbreviation of *Hyperoxie Unter Licht Konditionierung*). The main

idea behind this project is to deliver oxygen *in situ* by inducing localized photosynthesis through the co-culture of *C. reinhardtii* into the Integra matrix scaffold.

It has previously been shown that the photosynthetic microalgae *C. reinhardtii* may be co-cultured with murine fibroblast and incorporated into the Integra matrix bilayer skin as a scaffold. Then, the oxygen concentrations in normoxic and hypoxic conditions were measured in the photosynthetic scaffold. This first study was demonstrated that the algae and human cells could proliferate together, and the constant delivery of oxygen in response to light is possible (Hopfner et al., 2014).

The second step was the evaluation of this photosynthetic scaffold for *in vivo* transplantations in mice. In order to do that, the scaffolds containing *C. reinhardtii* was prepared to be implanted in a full-skin defected model. This experiment has demonstrated that the chimeric tissues (mammalian and photosynthetic cells) survived for at least five days, the algae keep its photosynthetic activity, and the vascularization was possible in the presence of the microalgae; also the algae do not have any effect in the immune system of the mice or zebrafish (Schenck et al., 2015) as well in a fully immunocompetent mouse skin defect (Chavez et al., 2016).

In a third study, our group aimed at engineering transgenic *C. reinhardtii* microalgae, which would be capable of secreting angiogenic growth factors besides oxygen. For that reason, the codon-optimized sequences for VEGF, PDGF, and SDF-1 were incorporated into the nuclear genome of this microalgae. The transgenic algae strains were able to secrete the human growth factors, and these angiogenic proteins were biologically active. Furthermore, the transgenic strains could be seeded, not only in dermal scaffolds but also in surgical sutures (Centeno-Cerdas et al., 2018; Chavez et al., 2016).

Despite these excellent results, the recombinant growth factors yields varied among the transgenic strains. Notably, the low concentrations of hPDGF and hSDF-1 in the algae supernatant prevented any further bio-functional analysis (Centeno-Cerdas et al., 2018). Thus, the standardization and optimization of the expression platform in *C. reinhardtii* are crucial; this platform will allow us to create a catalog of transgenic strains that express and secretes different growth factors that are essential for the wound healing process.

Also, the cumulative effect of the angiogenic proteins and its role during the wound healing process makes a significant important attempt to increase the expression and secretion yields of the recombinant human growth factors from *C. reinhardtii*. In this way, the possibilities for wound treatment can be improving and increasing.

2. Aims of this work

The present work aims to explore the possibility of increasing the biotechnological platform to improve and expands the catalog of recombinant strains that could be used to supply oxygen and therapeutic molecules *in situ*. To make them available for future biotechnological applications. It is hypothesized that by standardizing the microalgae-based platform to express recombinant proteins from the *C. reinhardtii* nucleus, will be guaranteed the expression and the efficient secretion of pro-angiogenic proteins; thus, the possibilities for wound treatment will improve.

One specific goal was to perform an exhaustive screening of expression vectors in combination with mutant strains was analyzed to determine the best platform to express and secrets hVEGF-165 from *C. reinhardtii*, which allows achieving high yields of this recombinant growth factor. Molecular characterization of the transgene integration and transcription of the protein in the nuclear genome of the microalga should be assessed, as well as protein expression and secretion rates for each transgenic strain.

The promising results for the optimized platform expressing hVEGF-165 were used to develop a new transgenic strain to express hTGF-β3 and to optimize the existing hPDGF-B and hSDF-1 strains, then, the current strain catalog will be improved. For each transgenic strain, the best expressing and secreting clone should be identified by biochemistry characterization, and secretion yields of the growth factors must be estimated.

As previously mentioned, the recombinant proteins bio-functionality is remarkably crucial to therapeutic applications. Thus, the biological activity of the growth factors secreted by the transgenic strains was evaluated through the *in vitro* detection and quantification of the respective phosphorylated receptors and by the synergy effect of the growth factors assessing a tube formation assay.

3. Material and Methods

3.1. Materials

This section provides an overview of the main materials used in this study. A summary of the material suppliers is presented in Table 3.

Table 3. List of all suppliers for chemicals, enzymes and laboratory equipment

Supplier	Address
AppliChem	AppliChem GmbH, Darmstadt, Germany
ATCC	ATCC, Manassas, VA, USA
Berthold Technologies	Berthold Technologies GmbH & Co. KG, Bad Wildbad, Germany
BD Biosciences	Becton, Dickinson and Company, Franklin Lakes, NJ, USA
Biozym	Biozym Diagnostik GmbH, Hameln, Germany
BioRad	BioRad Laboratories, München, Germany
Clear Line	Kisker Biotech GmbH & Co. KG, Steinfurt, Germany
Cell Signaling	Cell Signaling Technology, Inc., Danvers, MA, USA
Dianova	Dianova GmbH, Hamburg, Germany
Ibidi	Ibidi GmbH, Martinsried, Germany
IDT	Integrated DNA Technologies, Inc., Coralville, IA, USA
Lonza	Lonza Group, Basel, Switzerland
MACS Miltenyl Biotec	Miltenyi Biotec GmbH, Bergisch Gladbach, Germany
Metabion	Metabion international AG, Martinsried, Germany
Millipore	Millipore Corp., Bedford, USA
Miltenyi Biotec	Miltenyi Biotec GmbH, Bergisch Gladbach, Germany
MERCK	Merck & Co., Kenilworth, NJ, USA
NIPPON Genetics	NIPPON Genetics EUROPE GmbH, Dueren, Alemania
Pierce	Pierce, Rockford, USA
Promocell	Promocell, Heidelberg, Germany
R&D Systems	R&D Systems, Minnesota, USA
Roche	Roche, Basel, Switzerland
ROTH	C. Roth GmbH & Co, Karlsruhe, Germany
Serva	Serva Feinbiochemika, Heidelberg, Germany
Sigma	Sigma Chemical Company, St. Louis, USA
Thermo Scientific	Thermo Scientific, Rockfold, USA
Whatman	Whatman Paper, Maidstone, England
Zeiss	Carl Zeiss MicroImaging GmbH, Göttingen, Germany

3.1.1. Enzymes

The enzymes were used with specific buffer systems supplied by the corresponding companies. Restriction enzymes were bought from Thermo Scientific, Protease Inhibitor cocktail (Leduc et al., 2016) from BD Biosciences.

3.1.2. Oligonucleotides

All oligonucleotides were ordered from Metabion or Sigma. Lyophilized oligonucleotides were resuspended in sterile ddH_2O to a final concentration of 100 µM and stored at -20°C. Sequences of used oligonucleotides are denoted in respective chapters in Methods.

3.1.3. DNA-Vectors

DNA-vectors used in this work are listed in Table 4

Table 4. List of DNA-vectors used

Plasmid	Description	Reference
pJET1.2/blunt	Cloning vector; confers ampicillin resistance in *E. coli*	Thermo Scientific
pBC1-VEGF	pBC1 expression vector containing the *C. reinhardtii* codon adapted VEGF coding sequence (pBC1_V) under control of the *PsaD* 5' and 3' UTRs; confers paromomycin resistance in *C. reinhardtii* by expression of the APHVIII gene and ampicillin resistance in *E. coli*	(Chavez et al., 2016)
pBC1-PDGF and pBC1-SDF	pBC1 expression vector containing the *C. reinhardtii* codon adapted PDGF and SDF coding sequence (pBC1_P and pBC1_S) under control of the *PsaD* 5' and 3' UTRs; confers paromomycin resistance in *C. reinhardtii* by expression of the APHVIII gene and ampicillin resistance in *E. coli*	(Centeno-Cerdas et al., 2018)
pOpt-mVenus	pOpt expression vector containing the *C. reinhardtii* codon adapted VEGF, and TGF coding sequence (pOpt_V and pOpt_T) under control of the (*HSP70A*)-(RBSC2) fusion promoter, along with the Rubisco small subunit intron 1 (*HSP70A-RBCS2*-i1) and *RBCS2* 3' untranslated region; confers paromomycin resistance in *C. reinhardtii* by expression of the APHVIII gene and ampicillin resistance in *E. coli*	(Lauersen et al., 2015)

3.1.4. Reaction systems (Kits)

The following kits were used in this study, according to the manufacturer's protocols:

- CloneJET PCR Cloning Kit (Fermentas).
- TriReagent (Sigma)
- Human VEGF DuoSet ELISA kit, Human PDGF-BB DuoSet ELISA kit, Human CXCL12/SDF-1 DuoSet ELISA kit, Human TGF-beta 3 DuoSet ELISA kit, Human Phospho-VEGF R2/KDR DuoSet IC ELISA kit, and Human Phospho-PDGFR-β, DuoSet IC ELISA kit (R&D Systems)
- Phospho-CXCR4 (Ser339) Colorimetric Cell-Based ELISA Kit and Smad2 (Phospho-Ser467) Colorimetric Cell-Based ELISA Kit (Assay Biotech)

3.1.5. Membranes

Nitrocellulose membranes were obtained from AppliChem, PVDF-membranes from BioRad, and positively charged Nylon membranes from Roth.

3.1.6. Antibodies

The antibodies list used in this work is listed in Table 5.

Table 5. List of antibodies and respective titers used in this research work

Antibody	Dilution	Origin	Catalogue No.	Company
Primary antibodies				
α-VEGF	1:1000	Rabbit	ab52917	Abcam
α-VEGFR	1:1000	Rabbit	2479S	Cell signaling
α-pVEGFR	1:1000	Rabbit	2478S	Cell signaling
Secondary antibodies				
α-rabbit IgG HRP	1:5000	Goat	111-030-003	Dianova

3.1.7. Bacterial strains

Recombinant plasmids were propagated in *Escherichia coli* (*E. coli*) strain XL1-Blue [endA1 gyrA96 hsdR17 lac recA1 relA1 supE44 thi-1F´proAB lacIq Z_M15 Tn10(Tetr)] (Stratagene) or DH5α.

3.1.8. *C. reinhardtii* strains

The ultraviolet mutagenized (UVM) strains, cell-wall deficient cw15-30-derived UVM4, and UVM11 (Neupert et al., 2009) were used in the present work.

3.1.9. Cell lines

The cell lines used in this work are listed in Table 6

Table 6. List of cell lines

Cell line	Description	Catalogue No	Company
HUVECs	Human umbilical vein endothelial cells	C-12203	Promocell
hASCs	Human adipose-derived stem cells	PT-5006	Lonza
NIH-3T3	Murine fibroblast (embryo)	CRL-1658™	ATCC

3.2. Methods

3.2.1. *C. reinhardtii* cell culture

The cell-wall deficient, arginine phototropic, cw15-30-derived UVM4 or UVM11 *C. reinhardtii* strains (Neupert et al., 2009) and derived transgenic strains were grown mixotrophically at 23˚C on either solid Tris Acetate Phosphate (TAP) medium or in liquid TAPS-medium supplemented with 1% (w/v) sorbitol (Harris et al., 2009) under standard culture conditions (23˚C, constant illumination at 30 $\mu E \cdot m^{-2} \cdot s^{-1}$ and agitation at 120 rpm). Plate cultures were refreshed once a month, or according to the experimental needs in order to maintain the optimal metabolic state of the microalgae.

3.2.2. Bacteria cell culture

Recombinant plasmids were propagated in *Escherichia coli* (*E. coli*) strain XL1-Blue or DH5α. Bacteria were grown in LB liquid medium (1% peptone, 1% NaCl, 0.5% yeast extract, pH 7.0) or 1.5% agar LB-plates under standard conditions (37˚C, 150 rpm). For selection media, proper amounts of antibiotics were added under sterile conditions after the media was cooled down to approximately 60°C after autoclaving.

3.2.3 Construction of transformation vectors

3.2.3.1 pBC1 vector derivatives

The pBC1-CrGFP (pJR38, Neupert et al., 2009)-derived vectors pBC1_VEGF-165, pBC1_PDGF-B and pBC1_SDF-1, which were described previously (Chavez et al., 2016; Centeno-Cerdas et al., 2018) and have been used to create *C. reinhardtii* UVM4 transgenic strains secreting the human growth factors hVEGF-165 (pBC1_V-4), hPDGF-B (pBC1_P-4) and hSDF-1 (pBC1_S-4), respectively, were transformed into the UVM11 strain (pBC1_V-11, pBC1_P-11, pBC1_S-11). Briefly, the synthetic human genes with sequences adapted to the codon usage of *C. reinhardtii* (GenBank Accession No.: MN496135, MN496136, MN496137) were cloned into the pBC1-CrGFP vector backbone via its *Nde*I and *EcoR*I restriction sites, thereby replacing the CrGFP cassette between the endogenous *PsaD* 5' and 3' UTRs (Fig. 1). The coding sequence for the synthesis of hTGF-β3 was amplified by PCR from the construct pOpt_TGF-11, using synthetic primers to add a stop codon and the restriction sites *Nde*I and *EcoR*I, enabling the insertion into the pBC1-CrGFP (pJR38, Neupert et al., 2009). The PCR product was inserted into the backbone of the pBC1 vector under the same regulatory elements as the human growth factors that we previously reported (Chavez et al., 2016; Centeno-Cerdas et al., 2018). For secretion of the recombinant proteins, the sequence encoding the 21-amino-acid leader peptide of

the *C. reinhardtii* extracellular enzyme arylsulfatase (*ARS2*, Cre16.g671350, Phytozome, release C. reinhardtii v5.5) was inserted upstream of the protein-coding sequence. The vectors also carried the *APH*VIII resistance gene, providing for selection on paromomycin.

3.2.3.2. pOpt vector derivatives

The coding sequence for the synthesis of hVEGF-165 (GenBank Accession No. NP_001165097) was amplified by PCR from the construct pBC1_VEGF-165, using synthetic primers to add a stop codon and restriction sites for *Bgl*II and *EcoR*I to enable their insertion into the basis vector pOpt_mVenus_Paro (Lauersen et al. 2015). The PCR product was then inserted into the pOpt expression cassette between the *HSP70A-RBCS2*-i1 promoter and the *RBCS*2 3' UTR, and downstream of the sequence encoding the 23-amino-acid leader peptide of *C. reinhardtii* periplasmic enzyme carbonic anhydrase 1 (cCA1, Cre04.g223100, Phytozome, release *C. reinhardtii* v5.5) that enables the proteins to be secreted into the culture medium. The resulting construct was named pOpt_VEGF-165. To create the construct pOpt_VEGF-165-strep (pOpt_VEGF-165-s), the hVEGF-165 coding sequence was amplified using PCR primers that added the same restriction sites but obliterated the stop codon sequence, thus allowing for translation of the sequence encoding the C-terminal Strep-tag (amino acid sequence: WSHPQFEK). The sequences of the primers used for cloning experiments were VEGF-*Bgl*II-fw; VEGF-*EcoR*I-rev; VEGF-*EcoR*I-rev2. The synthetic human gene for hTGF-β3 with sequence adapted to the codon usage of *C. reinhardtii* (GenBank Accession No.: P_10600) was cloned into pOp_mVenus_Paro backbone via its *Bgl*II and *EcoR*I restriction sites, in the same cloning site as hVEGF-165 to create the construct pOpt_TGF-β3 (pOpt_T-11). All constructs were verified by sequencing before *C. reinhardtii* transformation. Table 7 summarizes the primer-sequences used in this section.

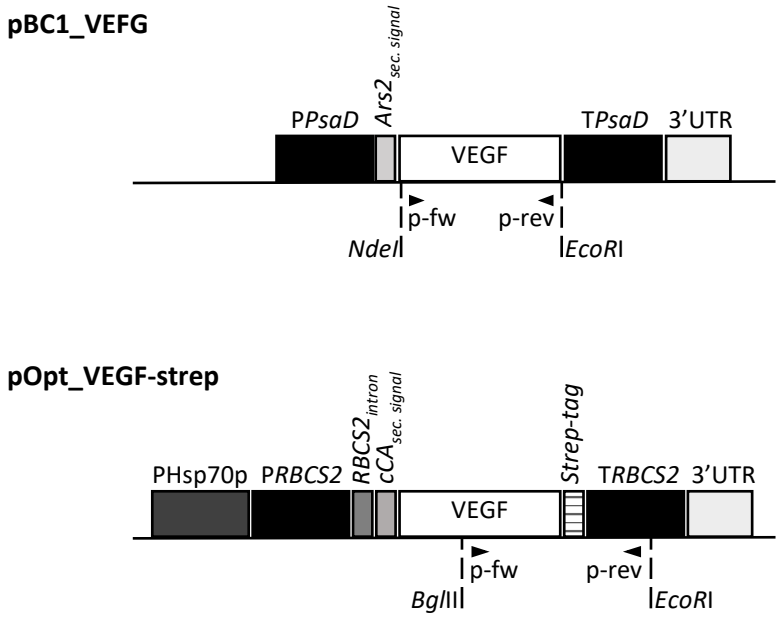

Figure. 4: Transgenic constructs to generate hVEGF-165-expressing *C. reinhardtii* strains. Schematic representation of vectors coding for hVEGF-165 used to generate the transgenic algal strains. The correct insertion of the codon-adapted human VEGF into the *C.*reinhardtii-genome was verified by PCR using specific primers for the transgene. *RBCS2*: *CAH*1, *ARS2*, *PsaD*, P: promoter, p-fwd: forward primer, p-rev: reverse primer.

Table 7. Sequences of the oligonucleotides-primers used for cloning experiments

Primer name	Primer sequence (5′- 3′)
VEGF-BglII-fw	AGATCTGCCCCCATGGCCGAGGGC
VEGF-EcoRI-rev	GAATTCTTAGCGGCGGGGCTTGTCG
VEGF-EcoRI-rev2	GAATTCTAAGCGGCGGGGCTTGTCG
TGFb3 BglIIfw	AGATCTGCGCTGGACACCAACTACT
TGFb3 EcoRIrev	GAATTCTAAGCTGCACTTGCAGCTC
ARS2_TGFb3fw	CATATGGGTGCCCTCGCGGTGTTCGCCGTCGCTTGCCTCGCGGCAGTGGCGTCGGTTG CGCATGCGGCCGACAGATCTGCGCTGGACACCAACTACT

3.2.4. Transformation of *C. reinhardtii*

C. reinhardtii UVM4 or UVM11 cultures were grown to mid-log phase under standard conditions. Then, $1 \cdot 10^7$ cells were suspended in a volume of 1 ml and vortexed with glass beads (diam. 0.5 mm) for 20 s in the presence of 5 µg plasmid DNA. The following incubation overnight under low light levels, the cells were grown under standard levels of illumination on TAP-Agar plates containing paromomycin (10 mg·ml^{-1}) to select for transgenic clones.

3.2.5. PCR-assay

Genomic DNA from 50 ml of *C. reinhardtii* cells was extracted using phenol/chloroform/isoamyl alcohol (25:24:1) (Carl Roth GmbH, Mannheim, Germany) and chloroform/isoamyl alcohol (24:1). DNA was then precipitated with ice-cold isopropanol and washed twice with ethanol 70%. Pellets were air-dried for 5 minutes and re-suspended in 50 µL H_2O. Integration of the recombinant gene was confirmed by polymerase chain reaction (PCR) using gene-specific primers pairs (Metabion GmbH, Planegg, Germany): 5'-GAAGTTCATGGACGTGTACC-3' and 5'-TTGTTGTGCTGCAGGAAG-3', for hVEGF-165 (258-bp product); 5'-AACGCCAACTTCCTGGTG-3'and 5'-GTGGCCTTCTTGAAGATGGG-3', for hPDGF-B (164-bp product); 5'- CGTGAAGCACCTGAAGATCC-3' and 5'- CTTCAGCTTGGGGTCGATG-3', for hSDF-1 (103-bp product), 5'-AGATCTGCGCTGGACACCAACTACT-3' and 5'- GAATTCTTAGCTGCACTTGCAGCTC-3', for hTGF-β3 (321-bp product). The primer sequences for the amplification of the *psbD* sequence (Sigma-Aldrich, Taulfkirchen Germany) were 5'-CCGTCACCGTCTTCGAATAAT-3' and 5'-GCTAACAGTATGGCTCACTCTC-3' for a (440-bp product).

3.2.6. Southern blot

Genomic DNA from *C. reinhardtii* cells was extracted from 150-ml cultures of each strain using CTAB buffer (2% cetyltrimethylammonium bromide, 100mM Tris-HCl, pH 8,) and phenol/chloroform/isoamylacohol (25:24:1) (Carl Roth GmbH, Mannheim, Germany). Aliquots (30 µg) of DNA were then digested with *Xho*I or *BamH*I at 37 ˚C for 48 h. Samples were analyzed as described before (Chavez et al. 2016), using gene-specific digoxigenin-nucleotide-labelled DNA probes (Digoxigenin-11-dUTP alkali-labile, Roche, Basel, Switzerland) obtained using the same primer pairs and conditions as for the PCR. Signals were detected using an alkaline-phosphatase-conjugated anti-DIG antibody (Roche, Basel, Switzerland) and CDP* (Roche) as a reaction substrate.

3.2.7. Northern blot

To analyze transcript accumulation in the different strains expressing hVEGF-165, 50-ml samples of C. reinhardtii cells were harvested at mid-log phase (~3×10^6 cells$\cdot$$ml^{-1}$) by centrifugation (4000 g, 15 min, 4°C) and total cellular RNA was extracted using Tri-Reagent® (Sigma Aldrich, Darmstadt, Germany). Aliquots (40 µg) of total RNA were electrophoretically fractionated on denaturing agarose gels, blotted onto positively charged nylon membranes (Roti®-Nylon plus, pore size 0.45 µm; Carl Roth GmbH, Karlsruhe, Germany), hybridized to gene-specific digoxigenin-nucleotide labeled DNA probes and visualized as described above.

3.2.8. Protein isolation and western blot of recombinant proteins

To quantify the expression level of the hVEGF-165 protein, *C. reinhardtii* cells were inoculated in triplicate into 100 ml of TAPS and incubated under standard conditions for approximately 4 to 5 days or until they reached a density of 10^7 cells·ml^{-1}. Supernatants were collected and passed through a 0.22-µm filter (ClearLine®, Kisker Biotech GmbH & Co. KG, Steinfurt, Germany), and then centrifuged (3000 g, 40 min) through Amicon®Ultra-15 30K filter units (Merck Millipore Ltd., Carrigtwohill, Ireland) to concentrate the recombinant protein to a final volume of 250 µl. Protein amounts were determined with the Bradford assay (Roti®-Quant, Carl Roth GmbH) according to the manufacturer's instructions. Then, 15-µg aliquots of protein were denatured at 95 ˚C for 5 min in the presence of reducing loading buffer Roti®Load-1 (Roth GmbH), fractionated by SDS-PAGE (12 % acrylamide), and transferred to nitrocellulose membranes (0.45 µm, AppliChem GmbH, Darmstadt, Germany). Commercially available recombinant hVEGF-165 was loaded in parallel as a positive control (Peprotech, Rocky Hill, NJ, USA). Protein detection was performed using a monoclonal rabbit anti-VEGF primary antibody (1:1000 dilution, ab52917, Abcam plc, Cambridge, UK) and a goat anti-rabbit HRP secondary antibody (1:5000, Dianova GmbH, Hamburg, Germany), using the SuperSignal West Pico detection system (Pierce-Thermo Fisher Scientific Inc., Rockford, IL, USA).

3.2.9. Enzyme-linked immunosorbent assay (ELISA) for the detection of recombinant growth factors

C. reinhardtii cells were inoculated in triplicate into 25 ml TAPS-liquid cultures and incubated under standard conditions for approximately 4 to 5 days or until they reached a cell density of 10^7 cells·ml^{-1}. Culture supernatants were collected by centrifugation (5 min, 10,000 g) and stored at -80 °C before analysis. The pelleted cells were then resuspended to a density of 107 cells in 200 µl of lysis buffer (100 mM Tris-HCl, 10 mM EDTA, 0.5 % Triton-X-100, 25 mg·ml^{-1} pepstatin, 25 mg·ml^{-1} leupeptin, 25 mg·ml^{-1} aprotinin) and disrupted by vortexing with glass beads (diam.: 0.5 mm). The protein concentration in the supernatant was determined by the Bradford assay (Roti®Quant, Carl Roth GmbH), and with the PierceTM BCA Protein assay (Thermo Scientific) in the protein lysates, both according to the manufacturer's instructions. For recombinant protein quantification in the medium samples (supernatant) and lysates (cells), the human VEGF DuoSet ELISA kit, human PDGF-BB DuoSet ELISA kit, human CXCL12/SDF-1 DuoSet ELISA kit and human TGF-beta 3 DuoSet ELISA kit (R&D Systems, Minneapolis, MN, USA) were used according to the manufacturer's instructions. The secretion and retention ratios were calculated from the normalized growth factor concentrations determined in the supernatant and the cell lysate, respectively (total concentration of growth factor (100%) = growth factor concentration in cell culture supernatant pro µg total protein + growth factor concentration in cell lysate pro µg total protein).

3.2.10. Bioactivity of the recombinant protein

3.2.10.1. Recovery of the recombinant protein from the culture supernatant

Triplicate samples of *C. reinhardtii* were cultured under standard conditions in 150 ml TAPS-liquid cultures until they reached a density of $1 \cdot 10^7$ cells·ml^{-1}. In order to obtain concentrates with comparable amount of different growth factors, based on previous experience, different volumes of culture-supernatant were filtered and concentrated (30mL pBC1_V-4 and pBC1_v-11, 60mL pOpt_V-4 and pOpt_V-11, 150mL pOpt_Vs-4 and pOpt_Vs-11, 60mL pBC1_P-4 and pBC1_P-11, 150mL pBC1_S-4 and pBC1_S-11 and 150mL pBC1_T-11 and pOpt_T-11). Filtration units capable of retaining peptides above 30kD, Amicon®Ultra15 30K (Merck Millipore Ltd., Carrigtwohill, Ireland) were used to recover hVEGF-165 and hPDGF-B, while the Amicon®Ultra-15 10K (Merck Millipore Ltd.) was used to recover hSDF-1 and hTGF-β3. Then, in a final filtration step, the diluent was changed to cell starvation medium (AIM-V serum-free media with stable glutamine, streptomycin sulfate (50 µg/ml) and gentamycin sulfate (10µg/mL) (Life Technologies, New York, USA) for HUVECs, or RPMI 1640 (with stable glutamine and 2.0 g/L $NaHCO_3$, Biochrom, Berlin, Germany) supplemented with 1% fetal calf serum (heat-inactivated FCS, Biochrom GmbH, Berlin, Germany) for hASC. The total protein content of this conditioned medium was assessed by Bradford quantification (Roti®Quant, Carl Roth GmbH), whereas the amount of recombinant protein (hVEGF-165, hPDGF-B, hSDF-1, and hTGF-β3) was quantified by ELISA.

3.2.10.2. Cell culture of human endothelial progenitor cells

Human umbilical vein endothelial cells (HUVECs) were purchased (Promocell, Heidelberg, Germany) and maintained in supplemented Endothelial Cell Growth Medium 2 (Promocell, Heidelberg, Germany) with 1% penicillin/streptomycin (Biochrom, Berlin, Germany) under standard cell culture conditions (37 °C, 5% CO_2). For all experimental settings, cells from passages 2-5 were used.

3.2.10.3. Cell culture of mesenchymal stem cells

Human Adipose-derived Stem Cells (hASCs) were purchased (PT-5006, Lonza, Basel, Switzerland), and maintained in StemMACS™ MSC Expansion Media (Miltenyi Biotec GmbH, Bergisch Gladbach, Germany) supplemented with 1% antibiotic/antimycotic (100x ab/am; Capricorn Scientific, Ebsdorfergrund, Germany). For all experimental settings, cells from passages 2-5 were used.

3.2.10.4. Cell culture of 3T3 murine fibroblast

Murine fibroblast NIH/3T3 (3T3) were purchased (ATCC® CLR-1685™, ATCC, Manassas, VA, USA) and kept in Dulbecco's modified Eagle medium (DMEM; Biochrom) supplemented with 20% fetal calf serum (FCS; PAA, Pasching, Austria). For all experimental settings, cells from passages 20-23 were used.

3.2.10.5 Receptor phosphorylation assay

To evaluate the biological activity of hVEGF-165, a receptor phosphorylation assay was performed. For this purpose, $1 \cdot 10^5$ HUVECs per well were cultured for 24 h in 12 well plates and then starved for 16 h before activation. Cells were then stimulated for 5 min, with either 50 $ng \cdot ml^{-1}$ recombinant hVEGF-165 (Preprotech, NJ, USA) or concentrated protein supernatants of the genetically modified or wild-type strains cultures with either the same amount of total protein or the same amount of recombinant hVEGF-165. The same procedure was performed to evaluate the biological activity of hSDF-1, but the cells were stimulated for 10 min, with $2ng \cdot ml^{-1}$ recombinant hSDF-1 (Prepotech). To evaluate the biological activity of hPDGF-B $1 \cdot 10^5$ hASCs per well were cultured for 24 h, starved for 16 h before activation by cultivation in RPMI medium, then the cells were stimulated for 5 minutes with 20 $ng \cdot ml^{-1}$ recombinant hPDGF-B (Prepotech). Finally, for the assessment of the biological activity of hTGF-β3 $1 \cdot 10^5$ 3T3's per well were cultured for 24h in 96 well plates, starved for 16h before activation by cultivation in RPMI medium, then stimulated for 19 minutes with $10ng \cdot ml^{-1}$ recombinant hTGF-β3 (Prepotech).

Cells were then snap-frozen by submerging the plate in liquid nitrogen and lysed in RIPA-buffer with phosphatase inhibitors (Phosphatase Inhibitor Mini Tablets; Pierce-Thermo Fisher Scientific Inc, IL, USA) and proteinase inhibitors (PIC, BD Pharmingen, NJ, USA; Pefabloc SC-Protease Inhibitor, Carl-Roth, Karlsruhe, Germany; cOmplete, Roche, Basel, Switzerland; and PMSF, SigmaAldrich, MO, USA). Cells were scratched from the well-floor, and lysates were homogenized by pipetting up and down and stored at −80 °C for further analysis.

3.2.10.5.1. Western blot for receptor phosphorylation assay

For western blot analysis, equal protein amounts were loaded in 7.5% acrylamide gels (Mini-PROTEAN®TGX Stain-Free™ Precast Gels, Bio-Rad Laboratories, California, USA) and separated by gel-electrophoresis under reducing conditions and then blotted to PVDF-membranes (Immun-Blot®PVDF Membrane, Bio-Rad Laboratories, California, USA). The primary mononuclear antibodies rabbit mAb anti-VEGFR-2 (55B11) (Cell-Signalling MA, USA) and rabbit mAb anti-phospho-VEGFR-2 (Tyr1175) (Cell-Signalling MA, USA) and rabbit mAb anti-PDGFR-β (C82A3) (Cell-Signaling) and rabbit mAb anti-

phospho-PDGFR-β (Tyr751) (Cell-Signaling), and the secondary goat-anti-rabbit (1:5000, Dianova GmbH, Hamburg, Germany) were used for the detection of the phosphorylated and non-phosphorylated receptor epitope, respectively, with overnight incubation periods. Clarity™ Western ECL Substrate (Bio-Rad Laboratories, California, USA) was used as a detection system. Pixel intensity quantification was performed with the Image Lab software (Bio-Rad Laboratories, California, USA).

3.2.10.5.2. ELISA receptor phosphorylation assay

Detection of receptor and phospho-receptor was performed in a semi-quantitative way by using a Human Phospho-VEGF R2/KDR DuoSet IC ELISA kit and Human Phospho-PDGFR-β, DuoSet IC ELISA kit (DYC1767-2 and DYC1766-2, R&D Systems, Minneapolis, MN, USA) according to the manufacturer's instructions. For hSDF-1, Phospho-CXCR4 (Ser339) Colorimetric Cell-Based ELISA Kit and for hTGF-β3, Smad2 (Phospho-Ser467) Colorimetric Cell-Based ELISA Kit (CBP1352 and CBP1029, Assay Biotech, San Diego, CA, USA) were used according to manufacturer's instructions. HUVECs were used to test the recombinant hVEGF-165 and hSDF-1 bio-functionality, whereas hASCs were used for the hPDGF-B experiments, and 3T3s were used for the hTGF-β3. As positive controls, cells were then stimulated with either 50 $ng \cdot ml^{-1}$ recombinant hVEGF-165 for 5 min (Preprotech, NJ, USA), 20 $ng \cdot ml^{-1}$ recombinant hPDGF-B for 5 min (Prepotech, NJ, USA), 2$ng \cdot ml^{-1}$ recombinant hSDF-1 (Preprotech, NJ, USA), and 10$ng \cdot ml^{-1}$ recombinant hTGF-β3 (Preprotech, NJ, USA), for 10 min. Concentrated protein supernatants of the genetically modified or wild-type strains cultures had either the same amount of total protein or the same amount of recombinant protein according to the experiment.

3.2.11. Angiogenesis assay

3.2.11.1. Preparation of the conditioned mediums

For the preparation of conditioned medium for the angiogenesis tube formation assay, the recipient (UVM4 and UVM11) and transgenic *C. reinhardtii* cells were cultured (alone or in co-cultivation) in volumes that were adjusted to maintain the same cell density in all experimental samples (e.g., double volume when co-culturing two strains). Supernatants were collected from the cultures at a cell density of $1 \cdot 10^7$ $cells \cdot ml^{-1}$ and mixed in a 1:1 ratio with AIM-V medium (Life Technologies, NY, USA). Commercially available recombinant growth factors were used as positive controls at the following concentrations: hVEGF-165, 30 $ng \cdot ml^{-1}$; hPDGB-B, 20 $ng \cdot ml^{-1}$ and hSDF-1, 10 $ng \cdot ml^{-1}$. Besides, AIM-V medium was used as a negative control to normalize the results from each independent experiment.

3.2.11.2. Tube formation assay

Confluent HUVECs were starved (AIM-V medium, Life Technologies) 24h before the experiment. Matrigel (Corning®Matrigel® Growth factor reduced, Tewksbury, MA, USA) was thawed on ice overnight, used to coat µ-Slide Angiogenesis (Ibidi, Martiensried, Germany) and allowed to polymerize for 1h at 37 °C. Then, 10µL aliquots of HUVECs ($1 \cdot 10^6$ cells·ml^{-1}) were seeded on the Matrigel-coated slide, and 40µL of conditioned mediums or controls were plated onto the Matrigel layer and incubated for 4 to 6 h (37 °C, 5% CO_2). Finally, viable cells were distinguished from dead cells by staining with Calcein AM/Propidium iodide live/dead-staining (1.6µM Calcein, 3µM Propidium iodide), which was directly added to each well and incubated for 5min at 37°C before imaging the cells on a fluorescence contrast microscope (Axiovert 25, Carl Zeiss AG, Oberkochen, Germany). Loop-formation was quantitatively determined by computer-assisted image analysis using ImageJ software (Schneider et al., 2012).

3.2.12. Statistical analysis

All results presented were obtained from at least three independent experiments and are expressed as means ± standard deviation. To determine the statistical significance of differences between groups, one-way ANOVA tests were performed using the GraphPad Prism 8.0 software (San Diego, CA, USA). Differences between means were considered significant when $p \leq 0.05$.

4. Results

4.1. Transformation of *C. reinhardtii* to express hVEGF-165

4.1.1. Using different expression vectors

Our group previously demonstrated the use of transgenic photosynthetic microalgae to deliver bioactive molecules and oxygen to wounds, when they are combined into biomaterials (Centeno-Cerdas et al., 2018; Chavez et al., 2016). The focus of the work pretended here is to evaluate different strategies that could help to engineer efficient genetically modified microalgae, capable of high transgene expression and high recombinant pro-angiogenic growth factors yields.

hVEGF-165 plays a central role in the angiogenic process, and in our previous study, this growth factor led to the best results regarding expression and bio-functionality. For those reasons, hVEGF-165 was selected as a target gene to evaluate six vector-strain combinations available for the production of human recombinant proteins in *C. reinhardtii*. Thus, the mutants strain UVM4 and UVM11, which improved the nuclear transformation efficiency, and the expression vectors pBC1 and pOpt were tested (see section methods 3.1.3 and 3.1.8, for details).

To compare the efficiency of the vectors pBC1 and pOpt, regarding transgene expression and recombinant protein yield, the vectors pBC1_V and pOpt_V were created to generate *C. reinhardtii* strains expressing hVEGF-165. The cDNA sequence of the growth factor was codon-optimized and amplified with specific primers (Table 7., section methods 3.2.3.2.) that allowed its insertion into the respective expression cassettes, thereby maintaining the regulatory elements provided by each construct. Besides, a variation of hVEGF-165 was designed to include a short-affinity tag (Strep-tag) and cloned into the pOpt-construct (pOpt_Vs) to generate a version of the growth factor that would be easy to purify later on. Moreover, to assess if there was a significant advantage using one mutant strain or other, both strains UVM4 and UVM11, were used to create hVEGF-165 strains. Also, the previously generated pBC1_V UVM4-derived strain was used as a reference for the findings in this work, except for the transformation efficiency experiments. Thus, a total of six different construct-strains combinations were compared pOpt_Vs-4, pOpt_Vs-11, pOpt_V-4, pOpt_V-11, pBC1_V-4, and pBC1_V-11.

Table 8. Summary of the hVEGF-165 *C. reinhardtii* transgenic strains generation efficiency obtained with each plasmid.

	pOpt_Vs-4	pOpt_Vs-11	pOpt_V-4	pOpt_V-11	pBC1_V-11
Transformants	220	250	220	213	253
Transgenic	112(51%)	210 (84%)	147 (67%)	114 (54%)	171 (68%)
Secreting	35 (31%)	99 (47%)	39 (27%)	28 (25%)	147 (86%)

Regarding the transformation efficiency for each construct or strain, it was possible to get at least 200 clones from each combination, where the maximum number of clones was pOpt_Vs-11 (250 clones), and the minimum was pOpt_V-11 (213 clones) (Table 8.). However, after screening by PCR, remarkable differences were observed in the number of transformants that integrated the hVEGF-165 sequence. The results showed that the construct-strain combination pOpt_Vs-11 reached the highest integration rates (84%); meanwhile, the lowest value corresponded to the pOpt_Vs-4 (51%). The other combinations pOpt_V-4, pOpt_V-11 and pBC1_V-11 showed intermediate values of 67%, 54% and 68%, respectively.

Next, the secretion of the recombinant proteins into the medium was analyzed by ELISA (Table 8.). Here, the results showed higher differences in the secretion efficiency between each construct-strain combination, where the most efficient combination was the pBC1_V-11 since 86% of its transformants were able to secrete VEGF-165 in detectable levels into the medium, followed by pOpt_Vs-11 with 47% and pOpt_Vs-4 with 31%. The lowest rates were achieved by pOpt_V-4 and pOpt_V-11, with 27% and 25%, respectively.

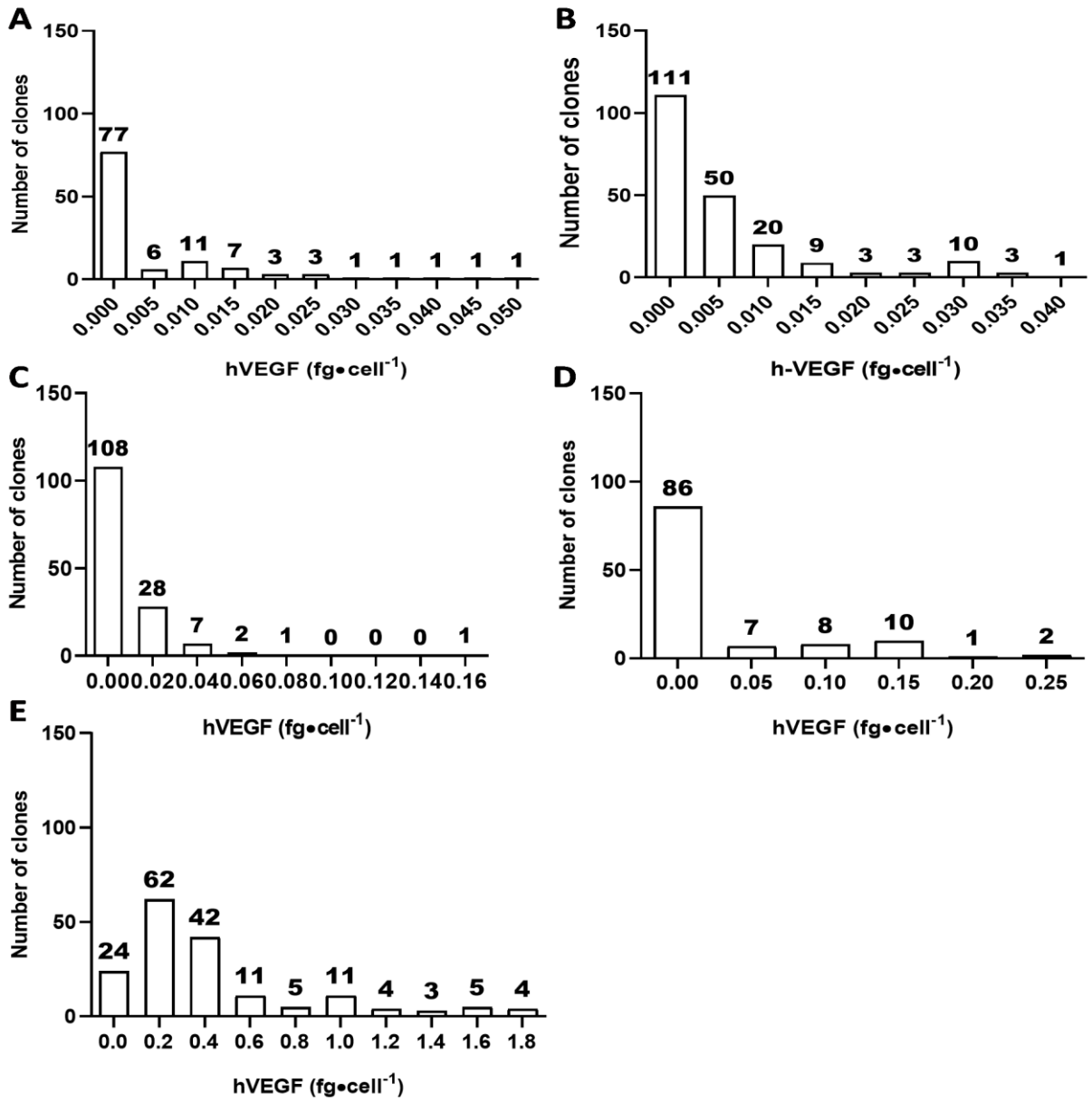

Figure. 5: Histogram representation of the transgenic clones generated with each construct. Culture supernatants from the hVEGF-165 transgenic clones generated using the pOpt_Vs-4 **(A),** pOpt_Vs-11 **(B)**, pOpt V-4 **(C),** pOpt_V-11 **(D)** and pBC1_V-11 **(E)** were analyzed by ELISA to quantify the concentration of the recombinant growth factors. Data were then ordered to represent the distribution of the clones according to the amount of secreted hVEGF-165.

Furthermore, to analyze these differences in the secretion yields, the dispersion of the data was assessed according to each construct-strain combination (Fig. 5).

According to these results, only a few clones of each combination reached suited secretion levels of the recombinant protein hVEGF-165, for further applications. For the pBC1_V-11 combination only 2.72% were in the upper 25% percentile (Fig. 5E), for pOpt_V-11 only 1.75% reached the highest yields (Fig. 5D), for the combinations pOpt_V-4, pOpt_Vs-4 and pOpt_Vs-11 this values were even lower (Fig. 5 A-C) with only 0.7%, 0.9% and 0.5%, respectively. From each construct-strain combination,

the clone that secreted the highest amount of growth factor in this initial ELISA screening was selected for all the further experiments.

4.2. Molecular characterization of hVEGF-165 *C. reinhardtii* transgenic clones

4.2.1. Integration of the hVEGF-165 gene in *C. reinhardtii*

The correct insertion of the transgenes into the genome of the strains was evaluated first by PCR using transgene targeted primer-pairs (Fig. 6A), and the *psb*D gene was used as a control (used primers are described in section 3.2.4). Since the copy number of the inserted genes is essential information for further molecular evaluation, Southern blot analysis was performed to determine this. Then, a specific hybridization probe was used to detect the hVEGF-165 gene in the different strains (Fig. 6B).

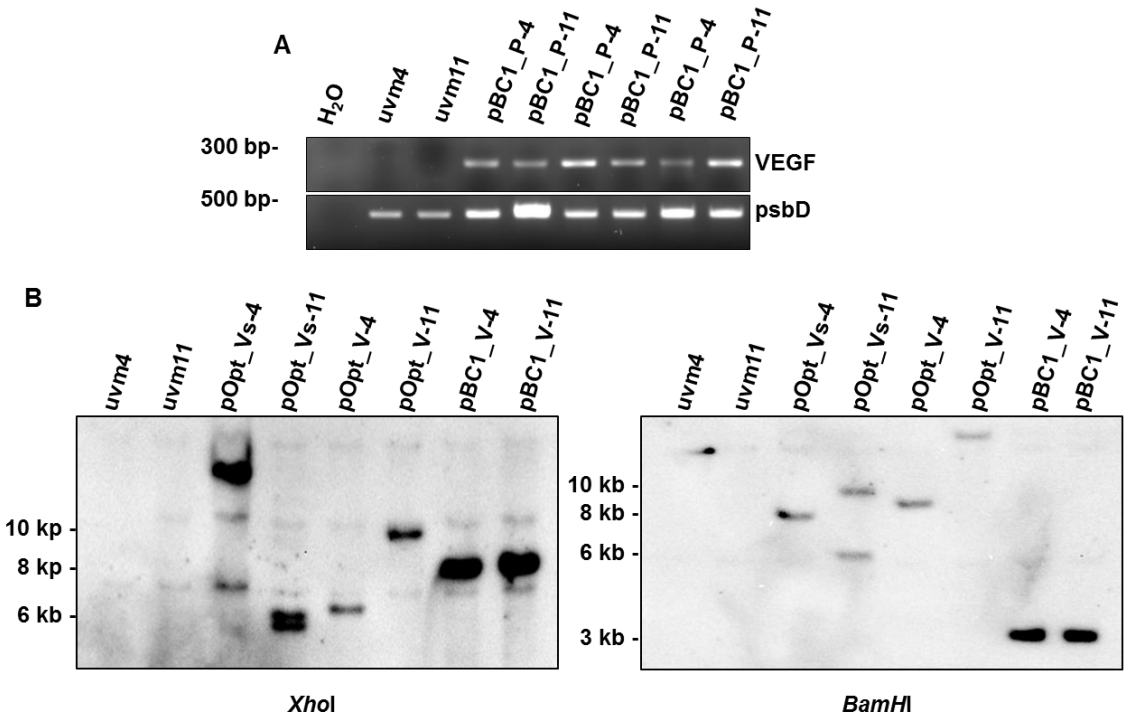

Figure. 6: hVEGF-165 transgene integration in *C. reinhardtii*. The DNA coding sequence for hVEGF-165 was inserted into the nuclear genome of *C. reinhardtii*. **(A)** The correct size of the codon adapted human VEGF was verified by PCR using specific primers for the transgene. Non-transformed wild type alga was used as a negative control and the algae psbD-gene as a positive control of the reaction. **(B)** The number of integrated copies of the hVEGF-165-coding transgene was verified by Southern blot. Total DNA was digested with the restriction enzymes *Xho*I and *BamH*I and separated by agarose gel electrophoresis. Wild type strains (UVM 4 and 11) were included as negative controls to test the specificity of the hVEGF-165-labelling probe. All the transformants but pOpt_Vs_11, have a single copy of the VEGF transgene. A representative image of three independent experiments is shown.

The PCR results showed that all the mutants integrated the hVEGF-165 gene into their genome. The expected size of the transgenic sequences in each construct did not vary much (pBC1-V: 567 bp; pOpt-V: 564 bp; pOpt-Vs: 594 bp, 23.1 kD) (Fig. 6A) since the difference between the sequences was just given by the different secretion signals and the tag-sequence (Fig. 4). However, when transformants were generated, the gene is randomly integrated into the algae genome, which can lead to mutants with multiple insertions. The southern blot results showed that in almost all the construct-strain combinations, only a single copy of the gene was integrated into the *C. reinhardtii* genome, with the only exception being pOpt_Vs-11, where two copies of the hVEGF-165 were detected in both digestion assays (Fig. 6B). Therefore, it can be concluded that this particular strain will show different results from the other strains that will be analyzed in the next sections.

4.2.2. Accumulation of hVEGF-165 transcripts in *C reinhardtii*

Northern blot was performed to elucidate the correlation between transcript abundance and secreted recombinant protein levels achieved by each construct-strain combination (Fig. 7), using a specific probe for hVEGF-165 coding sequence.

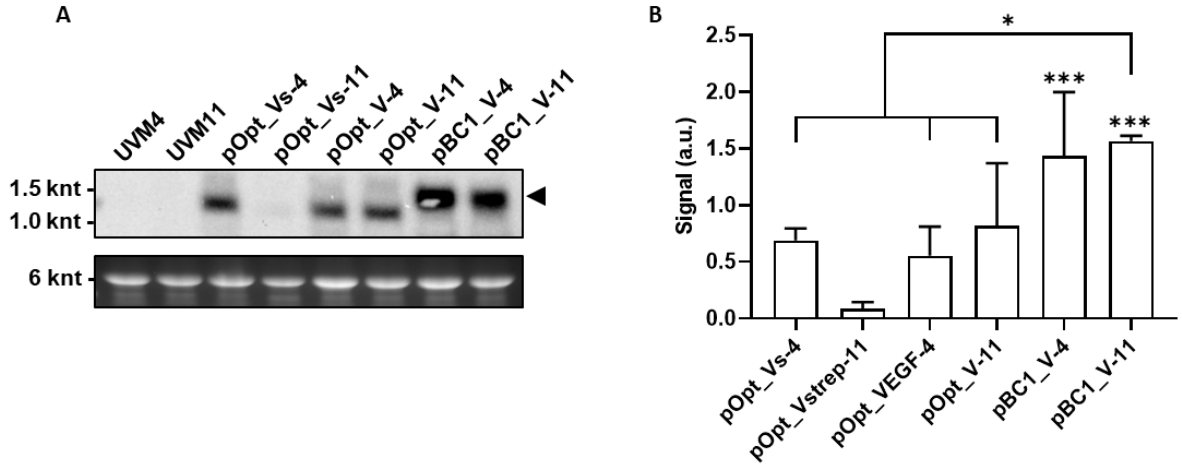

Figure. 7: Transcript abundance of hVEGF-165 in *C. reinhardtii*. (A) Transgene transcription was verified by Northern blot. RNA samples extracted from wt-strains (UVM4, UVM11) were used as negative controls to test the specificity of the hVEGF-165 mRNA labelling probe, rRNA was used as a loading control. **(B)** Chemiluminescence signals were digitally quantified, normalized to a loading control (6000 bp band from total RNA gel electrophoresis, lower panel (A)) and averaged from three independent experiments. A representative image of three independent experiments is shown. *p≤0.05, **p≤0.005, ***p≤0.001.

Both pBC1 derived clones showed the highest levels of mRNA transcription rates, where the pBC1_V-11 expression levels were significantly the highest. In contrast, all pOpt-derived clones performed poorly, in particular, pOpt_Vs-11, where almost no hVEGF-165 mRNA was detected, which can be related to the two copies of the gene detected in the southern blot.

4.2.3. Characterization of recombinant hVEGF-165 expression in *C. reinhardtii*

In order to evaluate the protein secretion level of the new strains, the supernatant was collected and analyzed by Western blot using the anti-VEGF specific monoclonal antibody to detect the recombinant proteins. Also, an ELISA was performed to quantify the secreted proteins and the relationship between the protein accumulation and the protein secretion by *C. reinhardtii*.

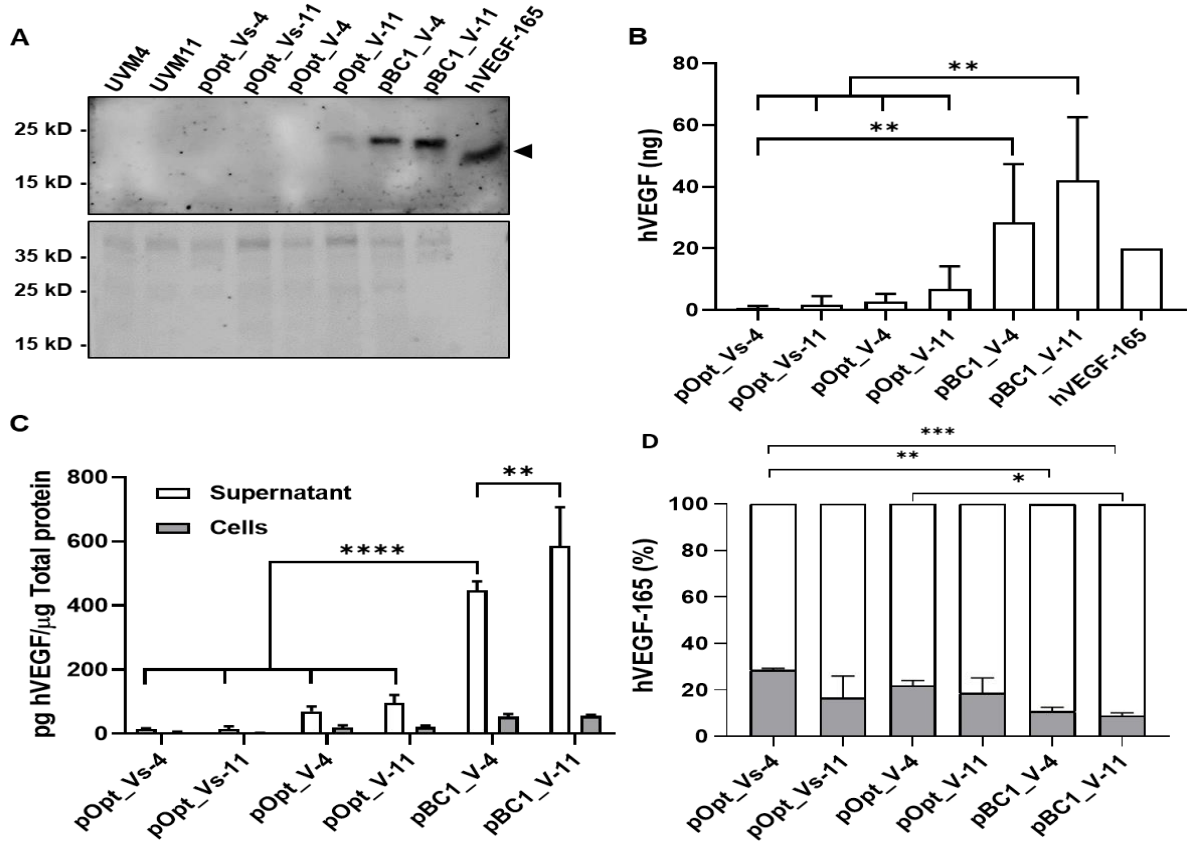

Figure. 8: Protein expression of hVEGF-165 from *C. reinhardtii*. (A) Western blot analysis of hVEGF-165 secreted by each *C. reinhardtii* strain. Equal protein amounts of concentrated culture-supernatant samples were separated through SDS-PAGE under reducing conditions. **(B)** Quantification of secretion of hVEGF-165 by each strain. Equal amounts of concentrated culture supernatant samples were blotted in a PVDF membrane. The amount of hVEGF-165 in the sample was normalized in reference to a commercially available *E.coli*-expressed recombinant hVEGF-165. **(C)** Recombinant hVEGF-165 concentrations in the cell lysates (cells) and algae culture medium (supernatant) were measured by ELISA. Results were normalized to the total protein concentration in the samples. The pBC1-clones showed significantly higher secreted protein yields compared to all others. **(D)** Secretion yields were calculated from the protein concentrations obtained by ELISA (cells: grey; supernatant: white) and proved to be significantly higher for the pBC1-derived clones compared to the worst-performing clone (pOpt_Vs-4).*p≤0.05 **p≤0.005, ***p≤0.001, ****p≤0.0001.

Relate with the observed at the transcript level, in the Western blot analysis of supernatants showed that the secreted recombinant protein was only detectable in the pBC1-derived clones, where the anti-VEGF specific monoclonal antibody detected a single band around 22,1 kD corresponding to

the hVEGF-165 monomer. Compared to the commercially available hVEGF-165, the growth factor expressed by *C. reinhardtii* showed a higher molecular weight (Fig. 8A. 22,1 kD versus 19,2kD). These differences in size could be explained by the secretion signal tagged to the 5' coding sequence of the gene, the 21 amino acid export sequence of *ARS*2 (1,97 kD), and also by the post-translational modifications of the protein. For an estimation of the amount of recombinant protein in the concentrated supernatant, the protein signal was quantified by pixel intensity and normalized to the sample of commercially available hVEGF-165 (Fig. 8B). The calculation led to an estimate of 28.5 ± 18.9 and 42.0 ± 20.5 ng hVEGF-165 for the pBC1-derived UVM4 and UVM11 strains, respectively.

The culture supernatants and cell lysates were analyzed by ELISA to quantitatively determine the amount of recombinant protein expressed and secreted by each clone (Fig. 8C). These results showed that the two pBC1-derived clones achieved higher yields of recombinant protein. Remarkably, the pBC1_V-11 clone produced superior yields compared to the other clones, including the previously characterized pBC1_V-4, where a small but significant increase of 1.3 fold in the secretion yields of hVEGF-165 was achieved. However, the pOpt-derived clones were only capable of producing low growth factor yields. The secretion and retention ratios calculated from the ELISA results, where the supernatants denote the secretion efficiency (white bars) and the retention were given by the cells (gray bar) (Fig. 8D). This particular analysis showed that both pBC1-transformants had a more efficient secretion ratio compared to the worst secreting clones (pOpt_Vs-4 and pOpt_Vs-11). However, only pBC1_V-11 was statistically better regarding the secreting efficiency compared to a non-tagged protein (pOpt_V-4 and pOpt_V-11), which is in agreement with the observed in the ELISA results.

The biological functionality of the recombinant hVEGF-165 secreted by each strain was evaluated to identify the capacity of the produced growth factor to bind and phosphorylate the receptor VEGFR-2 in the human cells. The binding of the recombinant growth factor to the receptor VEGFR-2 induces its auto-phosphorylation. This phosphorylation can be assessed via Western Blot and ELISA- semi-quantitative analyses. Then, human endothelial cells (HUVECs) were stimulated with the concentrated supernatant of each transgenic algal strain. This stimulation was normalized either by the total amount of protein (Fig. 9A, B) or the same amount of recombinant growth factor (Fig. 9C, D).

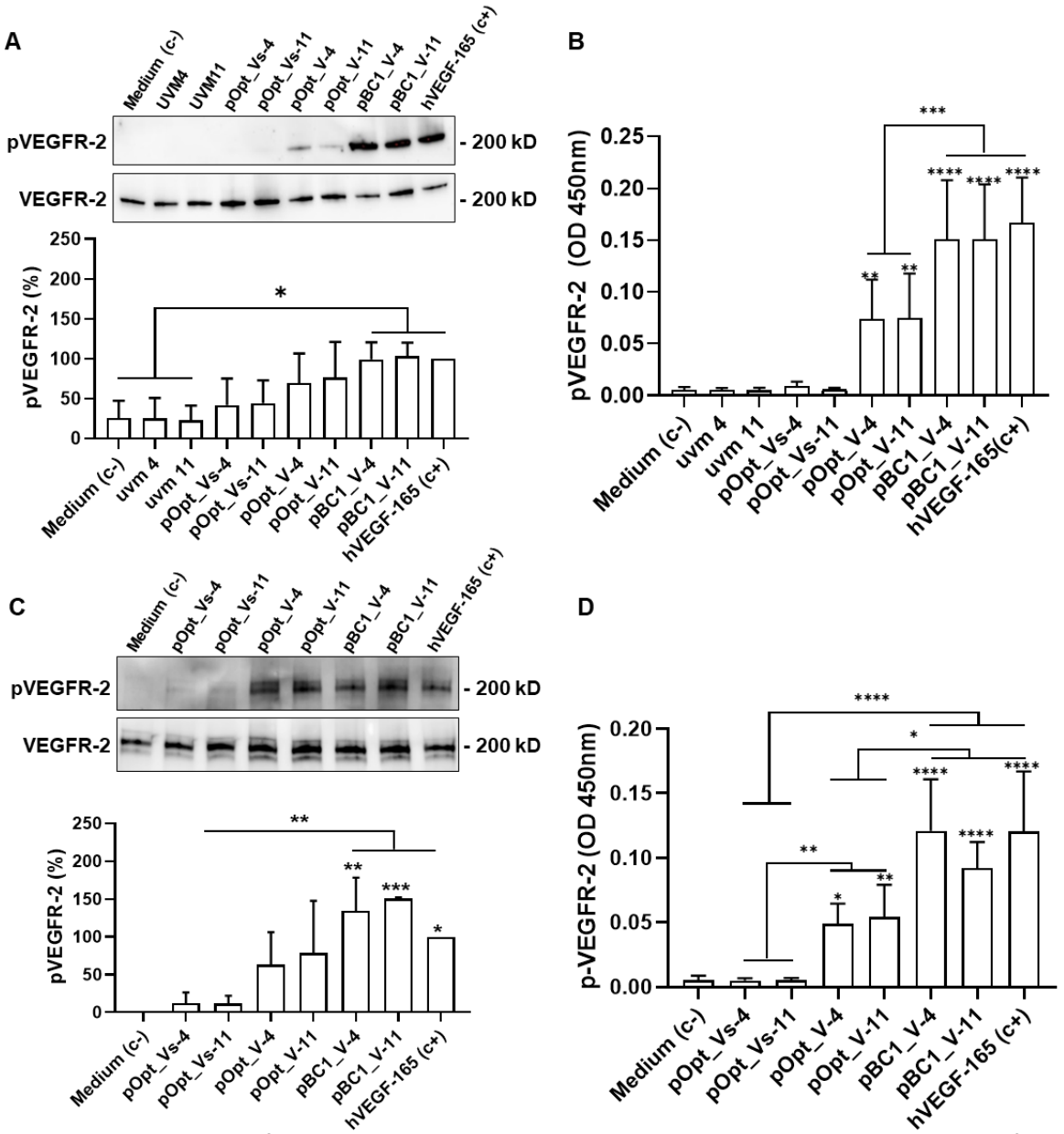

Figure. 9: Bioactivity of hVEGF-165 expressed by *C. reinhardtii*. The biological activity of the secreted recombinant protein was evaluated for each transgenic strain based on the detection and quantification of the phosphorylated activated VEGFR-2 via Western Blot analysis **(A, C)** and ELISA **(B, D)**. For this, HUVECs were stimulated with volumes of concentrated algae culture supernatant that corresponded to either equal amount of total protein **(A, B)** or equal amount of recombinant hVEGF-165 **(C, D)**. Statistical analysis was performed in regard to the negative control (starvation AIM-V medium) and to determine differences among the different strains. A commercially available recombinant hVEGF-165 was used as a positive control (c+, 50 ng/ml). *p≤0.05, **p≤0.005, ***p≤0.001, ****p≤0.0001.

The results showed that the growth-factor produced by the pOpt-strep clones were not able to activate the receptor at all, as the ratio of receptor phosphorylation was similar to the negative controls (Fig. 9).

Interestingly, even though the Western Blot results did not reveal any statistical difference between the pOpt-encoded and the pBC1-encoded hVEGF-165 (Fig. 9A, B), these differences were found significant when the samples were analyzed by ELISA (Fig. 9C, D). On the other hand, the hVEGF-165 expressed by the pBC1-derived clones showed the highest phosphorylation activity. Moreover, it was comparable to the commercially available (Fig. 9B, D), as no statistical differences were found among the treatments when equal amounts of commercial or algal-derived hVEGF-165 were used (pBC1_V-4, pBC1_V-11, and c+). Altogether, the results obtained showed that the pBC1-vector and the UVM11 strain are the most suitable combination for the production of hVEGF-165 in *C. reinhardtii*.

4.3. Genetic modification of *C. reinhardtii* to express hTGF-β3

To expand our protein catalog of growth factors available for the wound healing treatment, both vectors (pBC1 and pOpt), in combination with the UVM11 strain, were tested to assess the feasibility of producing hTGF-β3 in *C. reinhardtii*.

Table 9. Summary of the transgenic strain generation efficiency obtained with each plasmid.

	pBC1_T-11	**pOpt_T-11**
Transformants	285	207
Transgenic	191(67%)	176(85%)
Protein secreting	3(1.6%)	1(0.6%)

Unfortunately, even though the transgene integration ratio were high (pOpt_T-11 67% and pBC1T-11 85%, Table.9), the number of clones showing high transgene expression was extremely low (1.6% of pBC1_T-11 and 0.6% of pOpt_T-11, Table. 9)

Considering that only a few clones were able to secret hTGF-β3, the dispersion of the data was analyzed for both constructs (Fig. 10).

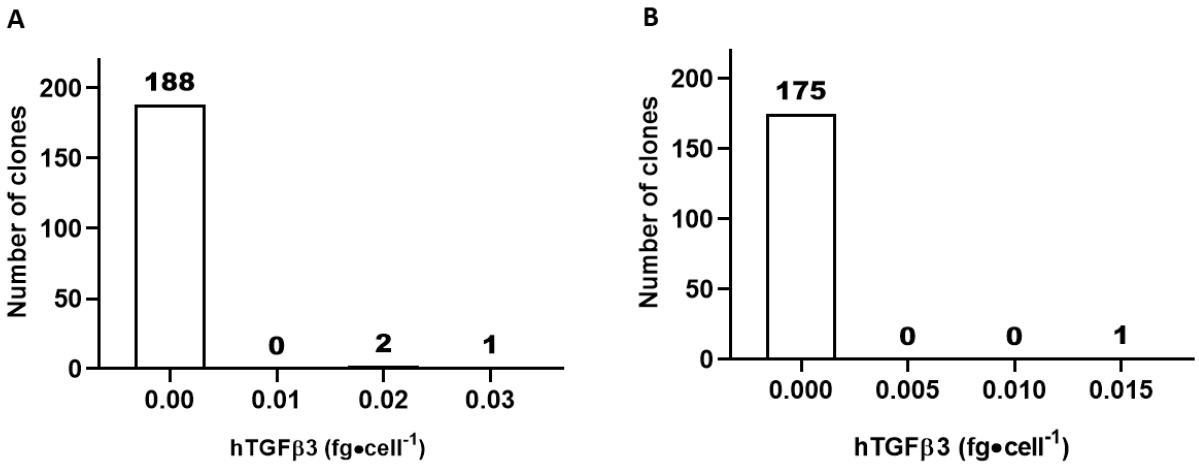

Figure. 10: Histogram representation of the transgenic clones generated for each recombinant growth factor. Culture supernatants from the pBC1_T-11 **(A)** and pOpt_T-11 **(B)** transgenic clones were analyzed by ELISA to quantify the concentration of the recombinant growth factors. Data were then ordered to represent the distribution of the clones according to the amount of secreted each recombinant protein.

Also, a wide dispersion in the secretion yield-data was observed for the pBC1_T-11- and pOpt_T-11-derived clones, where only 0.5% and 0.6% of the clones reached the upper percentile, respectively (Fig. 10 A, B). Here, too, the clone which expressed the highest amount of growth factor in this initial ELISA screening was selected for further analysis.

4.3.1. Characterization of hTGF-β3 in *C. reinhardtii*

The correct insertion of the transgenes into the genome of these strains was evaluated by PCR using transgene targeted specific primer-pairs (Fig. 11). The results showed that the generated strains integrated the respective hTGF-β3 transgene. For this experiment, the *psbD* gene was also used as a control.

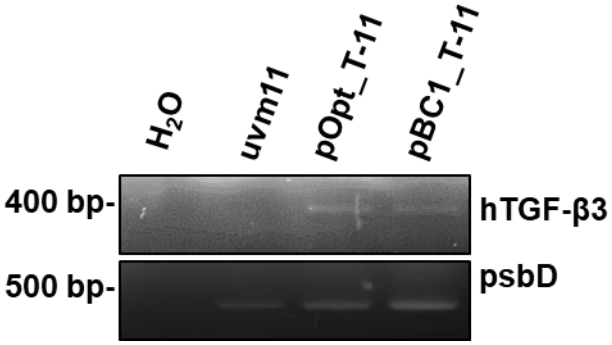

Figure. 11: Integration of transgenes coding for human growth factors in *C. reinhardtii*. The DNA coding sequence for hTGF-β3 were inserted into the nuclear genome of *C. reinhardtii*. The correct insertion of the codon adapted human genes was verified by PCR using specific primers for the transgene. A non-transformed wild type algae was amplified as a negative control and algae psbD was amplified as a positive control of the reaction.

4.3.2. Characterization of hTGF-β3 synthesis in *C. reinhardtii*

The achieved hTGF-β3 yields were evaluated for each vector system via ELISA in supernatant and Chlamydomonas cells.

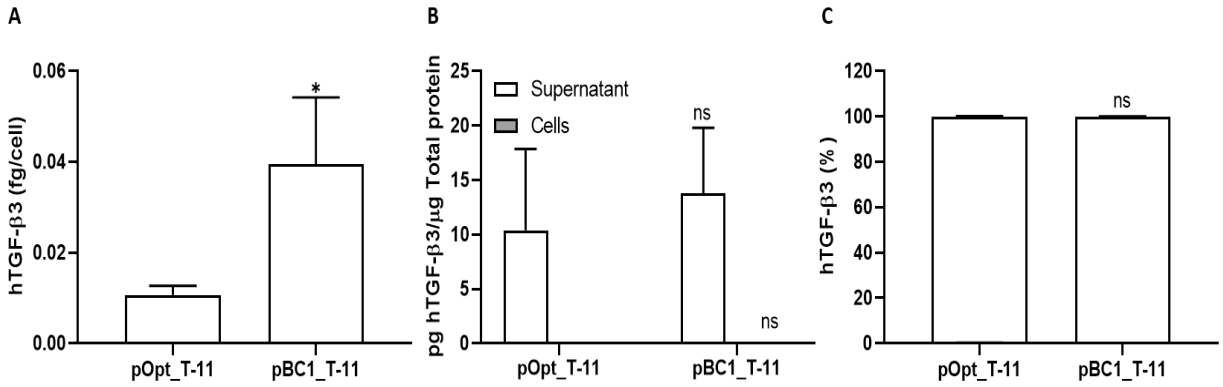

Figure. 12: Recombinant hTGF-β3- expression in *C. reinhardtii*. The concentration of hTGF-β3 by nuclear transformed *C. reinhardtii* clones was measured by ELISA, in both, cell lysates and culture medium samples. Results are normalized to the cell-density **(A)** and to the total protein in the samples **(B)**. Secretion rates were calculated based on the results obtained **(C)**. *p≤0.05, **p≤0.005, ***p≤0.001, ****p≤0.0001.

The results showed that the pBC1-derived clone was only able to secrete 2.4 fold more protein compared to the pOpt derived clone (Fig. 12A; pOpt-T-11: 0.0107± 0.0021 fg hTGF-β3, pBC1_T-11: 0.0395± 0.0147 fg hTGF-β3). However, when the secretion was analyzed, the pBC1_T-11-clone secreted 1.3-times more hTGF-β3 compared to the pOpt_T-11-derived clone (Fig. 12B). Remarkably, the secretion efficiency ratios for hTGF-β3 were quite similar to the pBC1_V-11 clone, since the pOpt_T-11- and pBC1_T-11-clones secreted 99.8± 0.14% and 99.8± 0.07% of the total protein, respectively (Fig. 12.C).

To evaluate the biological activity of recombinant hTGF-β3 algae-derived clones, the capacity of the produced protein to bind to its receptors pSmad2 was tested. 3T3-Fibroblast were stimulated with the same amount (2 $ng \cdot ml^{-1}$) of hTGF-β3 from the concentrated culture supernatants or commercially available hTGF-β3.

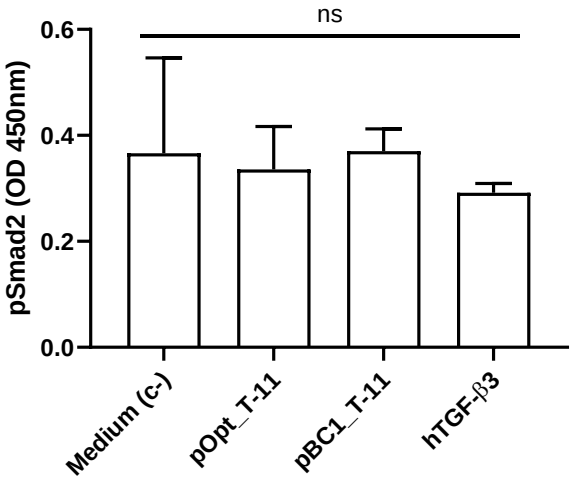

Figure. 13: Biofunctionality of hTGF-β3 expressed by *C. reinhardtii*. Biofunctionality of the recombinant growth factor was measured by ELISA by stimulating cells 3T3 fibroblast with 2ng·mL^{-1} *C. reinhardtii* secreted or commercially available recombinant growth factor. *p≤0.05, **p≤0.005, ***p≤0.001, ****p≤0.0001.

In this preliminary data, the bioactivity for the hTGF-β3 expressing clones could not be demonstrated, as no statistical differences between the samples (c-, pOpt-, pBC1- derived clones or c+) were observed through the ELISA-base semi-quantitative analyses (Fig.13). Then, repeat and optimize this experiment is essential for the research.

4.4. Genetic modification of *C. reinhardtii* to express hPDGF and hSDF-1

To improve the yields of previously reported growth factors expressed by UVM4-derived *C. reinhardtii* (Centeno-Cerdas et al., 2018) and increase the availability of proteins that can be used for wound healing therapeutic applications, the UVM11 strain was used to create new clones expressing hPDGF-B and hSDF-1.

Table 10. Summary of the transgenic strain generation efficiency obtained with each plasmid.

	pBC1_P-11	pBC1_S-11
Transformants	218	259
Transgenic	158 (72%)	200(77%)
Protein secreting	34(22%)	47(24%)

Interestingly, although the integration rates were quite similar compared to the pBC1_V-11 (68% Table. 8; pBC1_P 72%, pBC1_S 77%, Table. 10), the fraction of the transgenic clones that secreted the recombinant proteins was remarkably low compared to hVEGF-165 clones is higher related to hTGF-β3 expressing clones. While with the pBC1_V-11 construct, 58% of the clones secreted the protein, only 22% of pBC1_P-11 and 24% of pBC1_S-11-derived clones did (Table 10).

Additionally, to analyze the expression yields differences, the dispersion of the data was also assessed for these clones (Fig. 14).

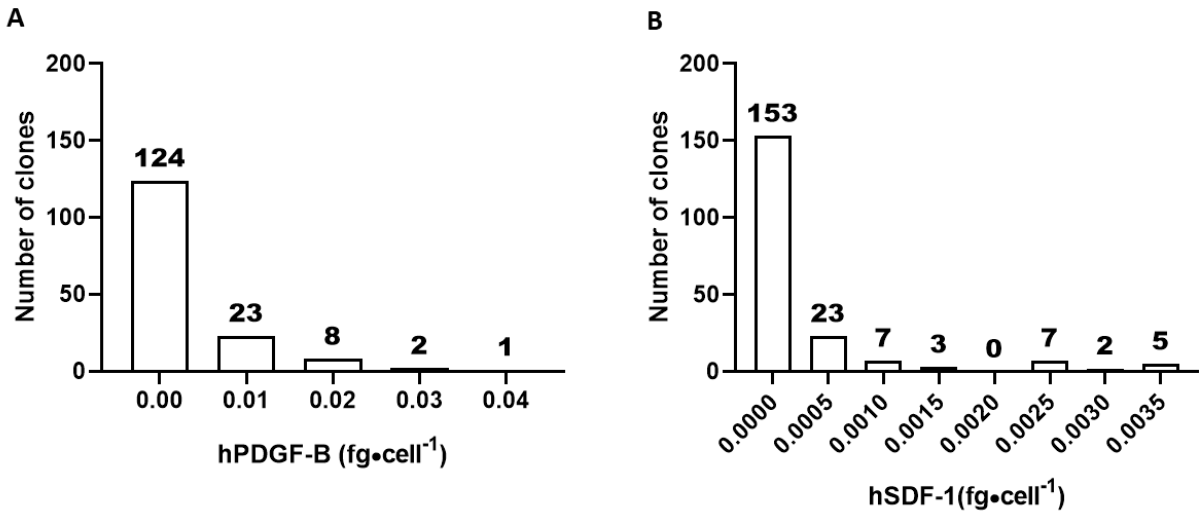

Figure. 14: Histogram representation of the transgenic clones generated for each recombinant growth factor. Culture supernatants from the pBC1-derived hPDGF-B **(A)** and hSDF-1 **(B)** transgenic clones were analyzed by ELISA to quantify the concentration of the recombinant growth factors. Data were then ordered to represent the distribution of the clones according to the amount of secreted each recombinant protein.

A wide dispersion regarding secretion yields was observed for these new clones, where just a few clones reached the highest secretion yields for each recombinant protein. For instance, with the pBC1_P-11-construct, only 0.6% of the clones reached the upper 25% percentile (Fig. 14A), whereas with pBC1_S-11 (Fig. 14B) 2.5% of the clones secreted the highest yields. For each construct, the clone which expressed the highest amount of growth factor in this initial ELISA screening was selected for further analysis.

4.4.1. Characterization of hPDGF-B and hSDF-1 in *C. reinhardtii*

The correct insertion of the transgenes into the genome of these strains was evaluated by PCR using transgene targeted specific primer-pairs (Fig. 15). The results showed that the generated strains integrated the respective hPDGF-B and hSDF-1 transgene. For this experiment, the *psbD* gene was used as a control.

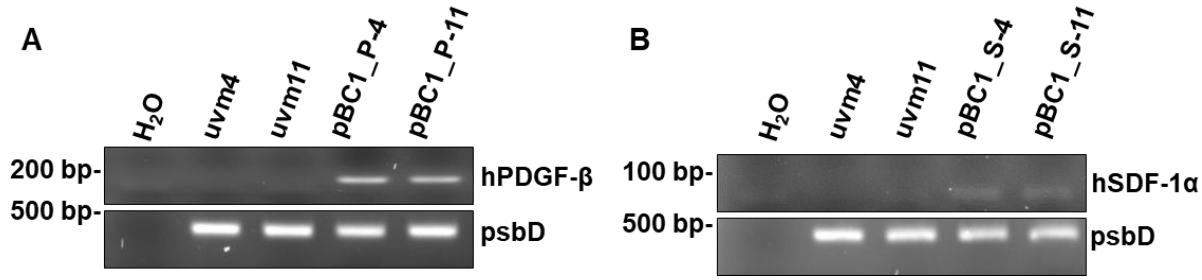

Figure. 15: Integration of transgenes coding for human growth factors in *C. reinhardtii*. The DNA coding sequence for hPDGF-B and hSDF-1 were inserted into the nuclear genome of *C. reinhardtii*. **(A, B)** The correct insertion of the codon adapted human genes was verified by PCR using specific primers for the transgene. A non-transformed wild type algae was amplified as a negative control and algae psbD was amplified as a positive control of the reaction.

4.4.2. Characterization of the recombinant growth factors expression in *C. reinhardtii*

The supernatants and algae cells were collected and quantified by ELISA to evaluate the protein accumulation and calculate the secretion ratios in order to analyze the newly generated clones' protein secretion.

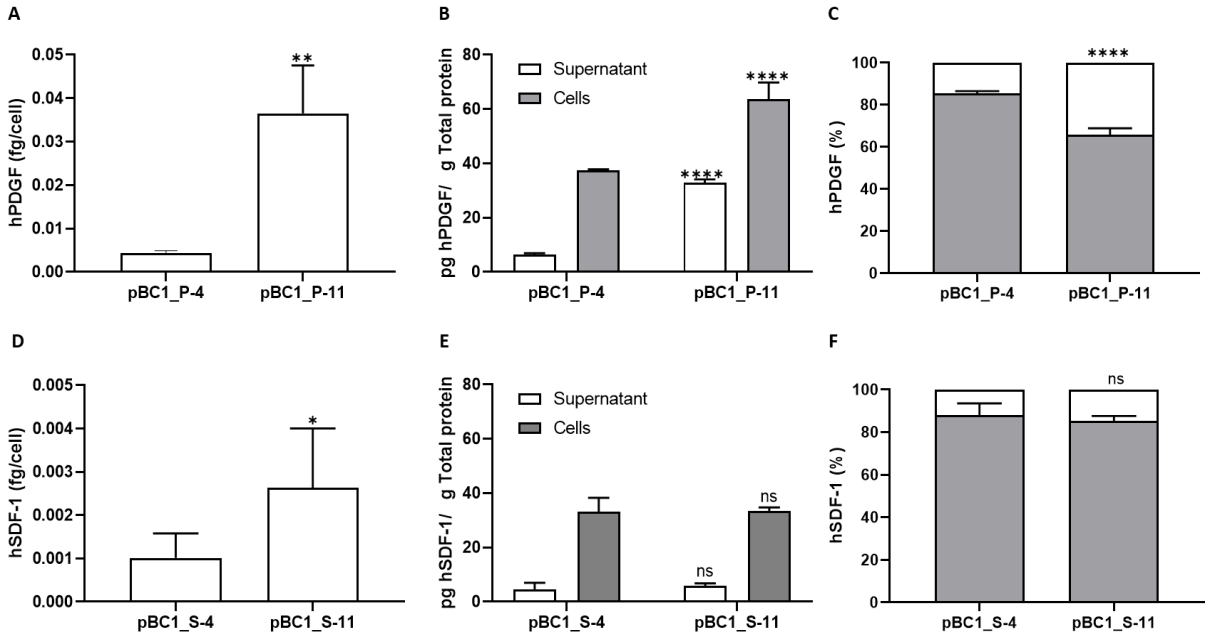

Figure. 16: Recombinant human growth factors expression in *C. reinhardtii*. The concentration of hPDGF-B and hSDF-1 synthetized by nuclear transformed *C. reinhardtii* clones was measured by ELISA, in both, cell lysates and culture medium samples. Results are normalized to the cell-density **(A, D)** and to the total protein in the samples (B, E). Secretion rates were calculated based on the results obtained **(C, F)**. *p≤0.05, **p≤0.005, ***p≤0.001, ****p≤0.0001.

Despite the low number of clones which were capable to express the recombinant proteins hPDGF-B and hSDF-1, the new clones UVM11-derived clones (pBC1_P-11 and pBC1_S-11) were able to

synthetize and secrete 8.4 and 2.6-times more fg growth factors per cells, respectively, compared to the previously obtained transgenic clones (Fig. 16A,D; pBC1-P-4: 0.0043± 0.0005 fg hPDGF-B, pBC1-P-11: 0.0363 ± 0.0114 fg hPDGF-B, pBC1-S-4: 0.001 ± 0.0006 fg hSDF-1, pBC1-S-11: 0.0026 ± 0.0014 fg hSDF-1).

Furthermore, when comparing the secretion yields of the newly obtained UVM11-derived clones with the previous UVM4-clones, the results showed that the UM11-derived clones had a better performance. For instance, the pBC1_P-11-clone secreted 5.1-times more than the pBC1_P-4-clone, whereas the pBC1_S-11-clone performance was 1.3-fold higher compared to the pBC1_S-4 clone (Fig. 16 B, E; pBC1-P-4: 6.4 ± 0.5 pg hPDGF-B, pBC1-P-11: 32.9 ± 1.2 pg hPDGF-B; pBC1-S-4: 4.6 ± 2 pg hSDF-1, pBC1-S-11: 5.78 ± 1.0 pg hSDF-1).

In contrast, when the secretion-rates of the growth factors were compared to the UVM4-strains, UVM11-derived clones, the hPDGF-B showed the best performance, but for hSDF-1 the secretion-rates were more or less similar in both clones (Fig. 16 C, F: pBC1_P-11: 34.2 ± 3 %, pBC1_P-4: 14.6 ± 1.2%, pBC1_S-11: 14.8 ± 2.4%, pBC1_S-4: 12 ± 5%). Hence, neither of these two transformants reached the secretion-rates of pBC1_V-11 (Fig. 8D, 91.2 ± 1.3%) or the hTGF-β3 expressing clones (Fig.12C, 99.8 ± 0.14% and 99.8 ± 0.07%), which means the pBC1-P and pBC1-S clones are the fewer efficiencies secreting clones from our catalogue.

The bioactivity of hPDGF-B and hSDF-1 pBC1-derived clones was also evaluated, analyzing their capacity to induce the auto-phosphorylation of their respective receptors. First, hASCs were stimulated with the same amount of hPDGF-B (15 $ng \cdot ml^{-1}$) from concentrated culture supernatants or commercially available protein. In order to evaluate the bioactivity of hSDF-1, HUVECs were stimulated with the same amount of hSDF-1 (2 $ng \cdot ml^{-1}$) from the concentrated culture medium or commercially available protein (Fig. 17).

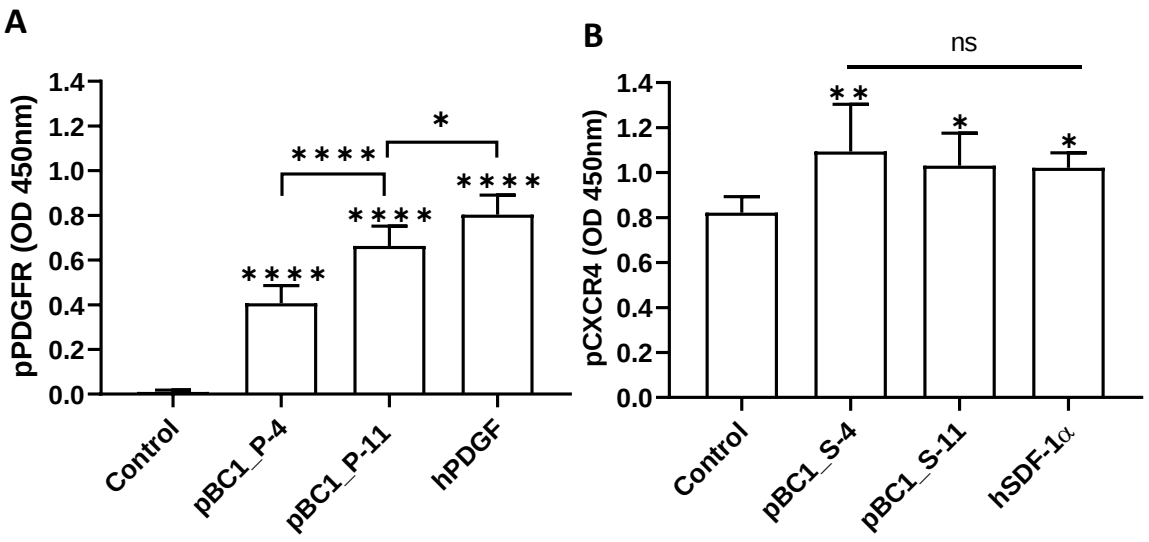

Figure. 17: Biofunctionality of growth factors expressed by *C. reinhardtii*. Biofunctionality of the recombinant growth factors was measured by ELISA by stimulating cells (ASCs for hPDGF-B **(A)**, HUVECs for hSDF-1**(B)**) with equal amounts of *C. reinhardtii* secreted or commercially available recombinant growth factor. *p≤0.05, **p≤0.005, ***p≤0.001, ****p≤0.0001.

According to the ELISA-based semi-quantitative analysis results, both the algae- and bacteria-derived hPDGF-B were able to activate the receptor. Moreover, the highest activation was observed with the protein secreted by pBC1-P-11; it was lower than with the hPDGF-B standard used as a positive control (Fig.17 A). On the other hand, regarding hSDF-1, the recombinant proteins secreted by the UVM4- or UVM-11-derived strains showed similar activity compared to the commercially available hSDF-1, where no statistical differences could be observed (Fig. 17 B).

4.5. Analysis of the angiogenic effect of the recombinant growth factors *in vitro*

An *in-vitro* angiogenesis assay was performed to test the applicability of efficient expressing *C. reinhardtii* transgenic strains and to demonstrate the synergic effect of the three algae-derived growth factors to promote endothelial tube-formation and anastomosis. For this, HUVECs were seeded on an appropriate extracellular-matrix coating material (Matrigel) and stimulated with supernatants obtained from the cultures of transgenic hVEGF-165 *C. reinhardtii* (pBC1_V-4 and pBC1_V-11), alone or in combination with hPDGF-B (pBC1_P-11) and hSDF-1 (pBC1_S-11) secreting algae (Fig. 18). As a control, combinations of commercially available growth factors were used.

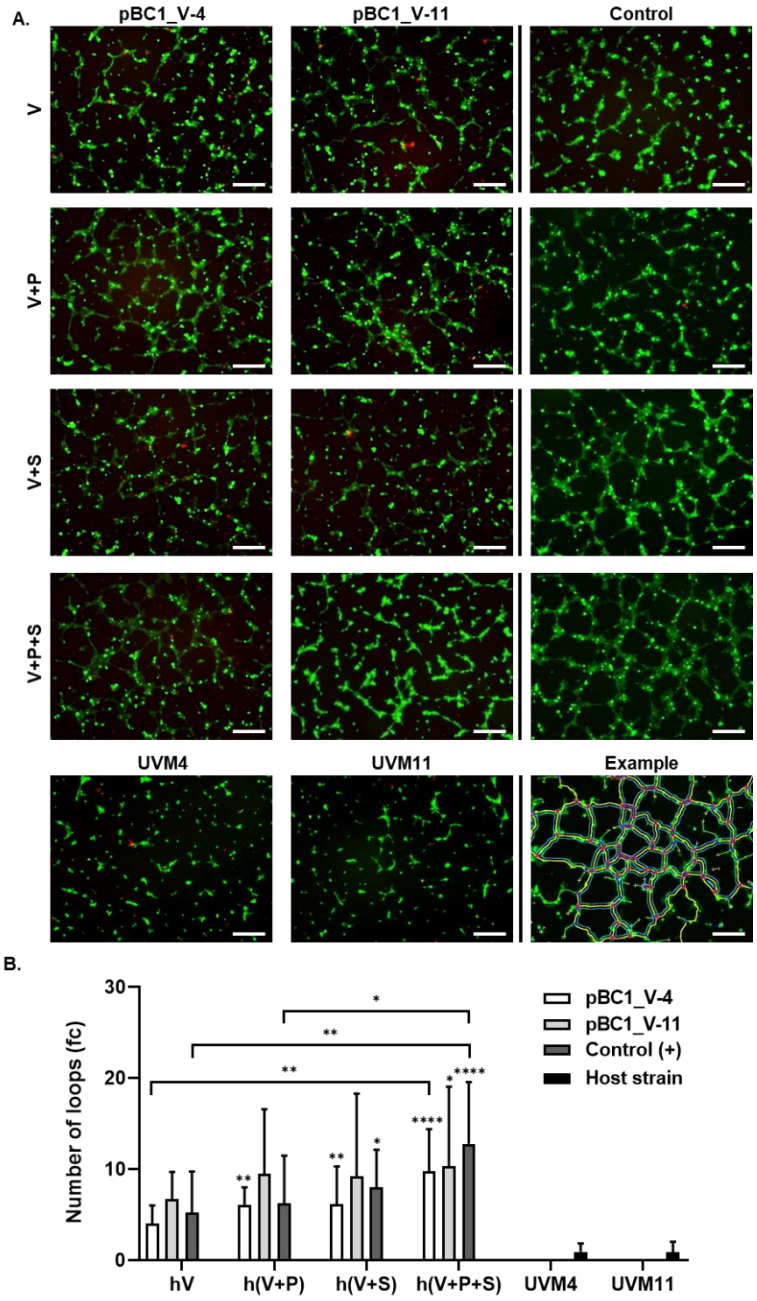

Figure. 18: Angiogenesis assay. The pro-angiogenic effect of conditioned media prepared with concentrated supernatants of hVEGF-165-expressing UVM4 and UVM11 *C. reinhardtii* strains (pBC1_V-4, pBC1_V-11), cultured either alone or in combination with the best-secreting hPDGF-B (pBC1_P-11, V+P) or hSDF-1 (pBC1_S-11, V+S) strains, or with both (V+P+S), was evaluated based on their ability to stimulate vessel-loop formation in human endothelial cells. Conditioned media prepared with the recipient strains (UVM4, UVM11) served as negative control, while conditioned media containing specific concentrations of commercial, bacterially derived recombinant growth factors (hVEGF-165: 30 ng·ml^{-1}, hPDGF-B: 20 ng·ml^{-1}, hSDF-1: 10 ng·ml^{-1}) served as positive controls (Control). The results of three independent experiments were normalized to an internal experimental control using the AIM-V culture media alone and are therefore expressed as fold-change (fc). An example of the results obtained from digital image analysis illustrating the loops quantified for the positive control containing all three growth factors is shown at the bottom right of the panel. Statistical significance with regard to the negative controls (recipient strains) is shown, as are the significant differences observed between the experimental groups and expressed above each set of columns). Only significant differences between groups are specified: *p≤0.05, ** p≤0.01, **** p≤0.0001. The scale bar represents 250 µm.

Upon stimulation with the culture supernatants, the formation of a high number of vessel loops was observed. This loop formation was not observed when using hVEGF-165 alone neither from algae (Fig. 18: pBC1_V-4, pBC1_V-11) or bacterial origin (Fig. 18: Control). This result proofs that this only growth factor does not have the angiogenic effect by its one and needs interaction with the other proteins to stimulates the cells for the new blood vessels formation.

According to this, the synergic angiogenic effect was observed when the three recombinant proteins were stimulating the cells; significant differences were found when the vessel loops formed by the combination of the growth factors were compared to that formed by the recipient-strain controls (Fig. 18: UVM4, UVM11).

Interestingly, significant differences to the negative controls were observed when pBC1_V-4 was combined with pBC1_P-11 or pBC1_S-11 strains, even though no differences were observed between the pBC1-derived clones (pBC1_V-4 and pBC1_V-11) in the VEGFR-2 receptor activation assay (Fig. 9). Surprisingly, the combination of hVEGF-165 with hSDF-1 seemed to be more effective than hVEGF-165 and hPDGF-B, despite the low yields of the recombinant protein expressed by pBC1_S-11 strain (Fig.12 D), it suggests that the hSDF-1 have more effect in the blood vessel formation due to its chemotactic activity.

Therefore, with all these results, it has been demonstrated that by combining optimized transgenic *C. reinhardtii* strains expressing different proteins. It is possible to produce stable recombinant growth factor cocktails with a high biofunctional activity that may help the wound healing process.

5. Discussion

5.1. Genetic engineering of *Chlamydomonas reinhardtii* to express and secrete recombinant human growth factors involved in the wound healing process

As mentioned before, our group has been developing the HULK concept for several years. This approach proposes the *in situ* delivery of oxygen into biomaterials through the incorporation of *C. reinhardtii* microalgae. Moreover, it has been proposed the genetic modification of the algae to make them capable of secreting human recombinant growth factors *in situ* (Centeno-Cerdas et al., 2018; Chavez et al., 2016; Hopfner et al., 2014; Schenck et al., 2015). Our previous results showed that *C. reinhardtii* could express and secrete functional recombinant growth factors. However, the differences between the recombinant protein yields obtained for different growth factors such as hVEGF-165, hPDGF-B, and hSDF-1 were significant. Furthermore, there are other essential proteins with wound healing properties such as TGF-β3, which could be added to the approach to increase the potential of our concept. With this in mind, in this work, we decided to incorporate the findings of three promising studies for high-efficient recombinant protein expression, in the search for the elements required for the development of an efficient *C. reinhardtii* recombinant protein expression platform (Fischer and Rochaix 2001; Lauersen et al., 2015b; Neupert et al., 2009).

5.1.1. Desing of the *C. reinhardtii* expression system

5.1.1.1 Comparing expression vectors pBC1 and pOpt.

First, the efficiency of the pBC1 and pOpt vector systems for nuclear transgene expression created by the groups of Fischer and Rochaix, 2001 and Lauersen et al., 2015, respectively, was compared. These vectors were designed to allow the insertion of transgene coding sequences into expression cassettes, which differ in their nuclear promoters and respective regulatory signals. Both constructs incorporated the *aph*VIII gene under the same hybrid promoter *Hsp70A* and *RBCS2*-i elements, as the paromomycin is a commonly used antibiotic resistance for *Chlamydomonas* transgenic selection, and no differences in the number of clones obtained were observed between the two constructs (Table 8, 9 and 10).

5.1.1.1.1. Transgene integration

The results confirmed that the two vector cassettes pBC1 and pOpt can be used to insert foreign genes into the *C. reinhardtii* genome. However, the integration of the transgene did not occur at similar rates. For instance, the combination pOpt_Vs-4 allowed only 51% of the transformants to

integrate the human transgene, while with pBC1_V-11, 68% of the transformants did (Table 8). The integration percentages obtained for all other recombinant growth factors evaluated were slightly better than for hVEGF-165. For instance, pBC1_T-11 lead to a fraction of 67%, while pOpt_T-11 allowed 85% of the transformants to integrate the transgene (Table 9). Similarly, 72% of pBC1_P-11 clones had integrated hPDGF-B, and 77% of pBC1_S-11 clones had integrated hSDF-1 (Table 10). Thus, in most of the cases, for these new strains expressing human growth factors, the rates for the transgene integration are higher than those reported by Neupert et al. 2009, where the rates for UVM4 and UVM11 strains were 53% and 50% respectively, using pBC1 vector.

The copy number was evaluated only for the hVEGF-165 sequence. The transgenes integration into the genome of *C. reinhardtii* seemed to have some influence on the expression level of the transgenes. In almost all the samples, a single copy of the gene was found, only in pOpt_Vs-11, two copies were observed (Fig. 6B), which is one of the poorest expressing clones (Fig. 8). In this regard, Potvin and Zhang have proposed that multiple gene integration is associated with low levels of transgene expression (Reviewed by Potvin and Zhang 2010a). Additionally, Barahimipour confirmed that the best performing clones for p24 cassette were those who only have a single copy of the transgene (Barahimipour et al., 2016a).

5.1.1.1.2. Transgene design

Significant differences in the transgene transcription rates were observed between the hVEGF-165 generated strains. Even though the heterologous human gene VEGF-165 sequence was optimized for *C. reinhardtii*, to prevent rarely used codons and match the GC-content of the algal-genome (Fuhrmann et al., 1999), and that the same transgene-sequence was inserted into the respective pBC1- and pOpt- expression-cassettes. The results showed that the pBC1_V-11 clone outperformed all other pOpt-derived clones in terms of transcript accumulation (Fig. 7).

Interestingly, both expression vectors incorporated strong constitutive promoters. In the pBC1- vector, the *PsaD* promoter, first reported by Fischer and Rochaix (2001), is included; this promotor regulates an intron-less single open-reading frame gene coding for a 21.3 kDa protein composed of 196 amino acids. Meanwhile, the pOpt- vector include, the fusion promoter *HSP70A-RBCS2*, created by Schroda (2000) to drive nuclear transgene expression in *C. reinhardtii*; this fusion promoter is composed of the *HSP70A* promotor and the *RBCS2* promotor. *HSP70A* is a 70kDa high protein made of 800 amino acids, and *RBCS2*, is a 185 amino acid long 20.6 kDa protein coded in four exons. When the *HSP70A* promoter is located upstream of the *RbcS2*, the *HSP70A* works as a transcriptional activator (Schroda et al., 2000). Nevertheless, according to the results, the pBC1-vector showed better performance no matter which protein (hVEGF-165 or hTGF-B3) was expressed under the *PsaD* promoter.

Some strategies have been suggested to increase transcript maturation and export from the nucleus to potentiate the efficiency of transgene expression. For instance, Lumbreras et al. 1998 postulated the idea of introducing introns from a native gene to improve the expression in *C. reinhardtii*. Since then, researchers have tried to develop strategies to incorporate introns to the expression cassettes or in the coding region (Eichler-Stahlberg et al., 2009; Mussgnug 2015). In this regard, the two expression vectors used in this work had different approaches.

In the *PsaD* promoter used in the pBC1 vector, all the regulatory elements required to the high expression levels of recombinant proteins should lie in the flanking promoter and untranslated region (Fischer and Rochaix 2001). On the other hand, in the second version of the pOpt-vector, used in this thesis, all the reporter transgenes inserted were interrupted by a sequence corresponding to the second intron of *RBCS2* (i2) (Fig. 4) to drive efficient transgene expression (Lauersen et al., 2015b).

Furthermore, it has been described that the differences between the cDNA design and the use of exon-intron structure could contribute to the transgene expression in *Chlamydomonas* (Eichler-Stahlberg et al., 2009; Molino et al., 2018; Ramos-Martinez et al., 2017). In this study, the proteins encoded by endogenous genes from the promoters differ in the exon-intron structure, *RBCS* contains four exons, while *PsaD* is an intron-less gene. Since the hVEGF-165 transgene is derived from a full-length intron-less cDNA, this could explain that the pBC1 system has shown the best performance, as it resembles the architecture of the original gene. However, the results for hTGF-β3 transgene did not show that good performance, compared to hVEGF-165, which suggests other aspects besides the intron-less cDNA sequence will take part in the expression of this recombinant protein, and this will be analyzed in detail further in this thesis.

The results showed that the best transgenic expression yields were obtained with the pBC1-construct, where the intron insertion was not required for hVEGF-165 expression (Fig. 8); this suggests that this particular coding sequence does not need introns to enhance transcription. Nevertheless, for the other angiogenic growth factors (hTGF-β3, hPDGF-B, hSDF-1), low protein yields were obtained compared to hVEGF-165. Then for experiments, it may be interesting to improve the transgene expression, including one intron following the consensus splicing sequence of *C. reinhardtii*, such as Eichler-Stahlberg *et al*. did for erythropoietin expression (Eichler-Stahlberg et al., 2009). Additionally, a recent study developed by Jaeger *et al*. could be implemented with this purpose. They created a new promising tool to improve nuclear transgene expression. The Intronserter is a bioinformatic tool, and it was designed to identify the correct position to insert introns into the target sequence. Hence, the systematic insertion of the first intron of *C. reinhardtii* ribulose-1,5-biphosphate carboxylase/oxygenase small subunit 2 (*RBCS2*i1) through larger transgenes, it has been demonstrated that improves the nuclear transgene expression 5.5 fold over eight other endogenous introns (Jaeger et al., 2019).

5.1.1.1.3. Secretory signals

The secretion of the expressed proteins into the culture medium is a desirable feature for recombinant protein production. *C. reinhardtii* is a eukaryotic organism that can secrete properly glycosylated proteins into the extracellular space when the transgene is nuclear-encoded. This characteristic is essential for the biopharmaceutical production since both O- and N- glycosylations are required for the biological activity and stability of the secreted recombinant protein (Mathieu-Rivet et al., 2017).

For the HULK concept, the secretion of the human angiogenic growth factors is crucial since this would allow the direct delivery of bioactive molecules into the wound. In this work, two different peptide signals for the secretion of the expressed proteins were compared, the signal peptide of the arylsulfatase 2 (*ARS2*) in the pBC1 vector and the carbonyl anhydrase (*cCA1*) in the pOpt vector.

The signal peptide of *ARS2* is a 24 amino acid sequence first reported by Eichler-Stahlberg et al. 2009 that has been shown to enable the efficient secretion of 65% of the total luciferase activity to the culture supernatant. The signal peptide *cCA1* is a 20 amino acid sequence which has been used to test the secretion of different reporter fluorescent proteins (Lauersen et al., 2013a; Lauersen et al., 2015a; Lauersen et al., 2015b).

For hVEGF-165 and hTGF-β3 proteins, both signal peptides led to good secretion results. The pOpt_VEGF-derived clones secreted 71 -81% of the protein and the pOpt_T-11 clone secreted 99.8% of the protein to the culture medium. Similarly, the pBC1_VEGF-derived clones secreted 89 – 91% of the protein, and for pBC1_T-11, almost all the protein was secreted to the culture medium (99.8%). In all cases, the secretion yields achieved were higher than previously described for *ARS2* or *cCA1*. Eichler-Stahlberg *et al*. reported that cell wall deficient algae were able to successfully secrete approximately 65% of the total *Renilla*-luciferase activity and 60% of erythropoietin to the culture supernatant using the *ARS2*-sequence (Eichler-Stahlberg et al., 2009). Moreover, Lauersen *et al*. reported a secretion ratio of around 84% of the Gaussia luciferase (*gLuc*) when the cCA1 peptide was used as a secretory signal (Lauersen et al., 2015b).

Therefore, the present work data suggest that the pBC1-derived clones performed better than the pOpt-derived clones in terms of secretion, especially for the hVEGF-165. These results would imply that the *ARS2* and *cCA1* secretory signals differ in their efficiency, which is contradictory to the results from Baier et al., 2018, where the *cCA1* shows similar results compared to *ARS1* and *ARS2*, but lower compared to the iron assimilatory protein (FEA2) secretory signal analyzed in their study (Baier et al., 2018b). Nevertheless, regarding hTGF-β3 secretion efficiency, there was no difference between pOpt- or pBC1- derived clones, which denotes that protein properties could influence the secretion.

On the other hand, hPDGF-B and hSDF-1, cloned into the pBC1-vector, did not show the same efficient secretion rates, even though the *ARS2* secretory signal was in both cases was evaluated. For hPDGF-B, only 15% of the protein was secreted using from the UVM4-derived clone and 35% from the UVM11-derived clone. Similar results were obtained for hSDF-1, where the secretions rates were 12 % and 15 % for the UVM4-and UVM11-derived clones, respectively. The reason for this low secretion titers is still unclear. However, there are clear differences in the secretion rates between the four recombinant proteins studied in this thesis, which seems to be directly related to each transgene sequence. Regarding this, Molino and co-workers have suggested that the inefficient cleavage of the signal peptide or an early self-cleaving might affect the protein secretion; they also have considered the possibility that some interferences among the amino-acid sequence could inhibit proper protein expression (Molino et al., 2018).

Furthermore, despite several attempts to detect hPDGF-B or hSDF-1, only the secreted hVEGF-165 was detected by immunoblotting. The main reason for this lack of detection could be explained by the low secretion levels of the two proteins. Meanwhile, for hVEGF-165 secretes 448pg and 586.7 pg for each µg of total protein for pBC1_V-4 and pBC1_V-11 respectively (Fig. 8C), the highest secretion for hPDGF-B was achieved by pBC1_P-11 strain (32.9pg/µg Total protein), and for hSDF-1 (5.6 pg/µg Total protein) from the pBC1_S-11 strain (Fig. 16 B, E). For that reason, the hPDGF-B and hSDF-1 were detected by ELISA. García-Cisneros et al. reported a similar situation detecting Herpes simplex virus type 2 (HSV-2). They had reported only 36.3% when the samples were assessed by Western blot, compared to 97.0% of positives when the samples were analyzed using the ELISA test (García-Cisneros et al., 2019).

Two recent studies reported novel strategies to promote a more efficient secretion of microalgae-based recombinant proteins, which could be implemented in the future to optimize the production and secretion of hPDGF-B and hSDF-1, or even hTGF-β3.

In the first one, Ramos-Martinez *et al.* implemented a successful strategy to enhance secretion yields and the stability of recombinant proteins in plant cell cultures. This group showed that linking the metalloprotease gametolysin N-terminal signal sequence to the yellow fluorescent protein Venus, while fusing a synthetic glycosylated serine-proline tandem sequence into its C-terminus, improved its secretion yield by up to 12-fold (Ramos-Martinez et al., 2017).

In the second one, Baier et al. investigated the use of C-terminal fusion proteins to enhance secretion. They first identified the secretion signal of iron assimilatory protein (*FEA2*) as the most effective in targeting the codon-optimized *G. princeps luciferase* (*gLuc*) into the extracellular space, when it was compared to *cCA*, *ARS*1, and *ARS*2. Then, they optimized the *Lolium perenne* ice-binding protein as a fusion protein to increase the reporter protein secretion. Finally, they tested the secretion

efficiency of the newly created expression cassette with the human epidermal growth factor (hEGF) and reported reaching a recombinant protein yield of 40 $mg \cdot L^{-1}$ (Baier et al., 2018a).

The implementation of these two approaches to produce human growth factors from Chlamydomonas might increase the yields of these proteins. However, there might still be some unknown protein-specific effects antagonizing these possible results, which should be carefully analyzed.

5.1.1.1.4. Peptide tags for purification

Peptide tags may be added to the recombinant protein sequence to achieve straightforward isolation and purification of the recombinant proteins. Lauersen *et al.* reported the use of the Strep II tag in the 3'UTR of the gene of interest cassette in the pOpt vector to this end, with this, they achieved the recovery of four different fluorescence protein via Strep-Tactin chromatography. In this work, it was intended to use the Strep-tag (amino acid sequence: WSHPQFEK) as a purification strategy for the algal-derived hVEGF-165. Unfortunately, the transcription rates and the expression yield of pOpt_Vs-derived clones were negatively affected, and even the bioactivity of the recombinant protein could not be detected through Western Blot (Figs. 7, 8, 9). Therefore, the usage of tags appears to reduce the secretion and the growth factor activity, especially in this case, for hVEGF-165. Similar results were observed previously, where the insertion of 6-His- and strep-tags affected the functionality of the fusion proteins (Crozet et al., 2018).

5.1.1.2. Chlamydomonas reinhardtii host strains

The foreign protein expression in *C. reinhardtii* depends on the transgene stability, which is related to a variety of epigenetic mechanisms, including transcriptional or post-transcriptional modifications, and they are involved in the silencing of the transgene expression (Leon-Banares et al., 2004). The UVM strains were generated to solve silencing problems (Neupert et al., 2009). Then, in this thesis, two different mutant strains created and selected by Neupert et al., 2009 were compared as an attempt to find a better performing clone capable of produce higher amounts of recombinant growth factors than the ones our group previously reported.

After comparing the performance of the obtained pBC1_V-4- and pBC1_V11-derived strains, it was concluded that the UVM11 derived strain outperformed the previously reported pBC1_V-4 transgenic strain (Chavez et al., 2016). Then, the next logical step was to explore if this could be reproducible for the hPDGF-B and hSDF-1 expressing UVM4 strains previously created (Centeno-Cerdas et al., 2018).

Since the transformation of UVM4 and UVM11-strains occurred at different times, it is not possible to confirm the statistical significance of the potential differences in transformation efficiency

between the strains. The transformation of the UVM11-strain with the pBC1_P and pBC1_S constructs led to more efficient strains with overall improved yields of recombinant protein (Fig. 16A, D), as well as happened for pBC1_V-11 (Fig. 8). However, remarkable differences were observed in the percentage of growth factor secreting clones obtained for each transgene (Table 10), where only a few clones of each construct (pBC1-P-11 and pBC1_S-11) reach high-expression yields of the proteins (Fig. 14A, B). The same situation has been shown by the clones expressing hVEGF-165 and hTGF-β3 (Fig. 5, 10).

Interestingly, most of the synthesized hPDGF-B and hSDF-1 were retained inside the *Chlamydomonas* cells (Fig. 16 B, C, E, F), which is the opposite of the results from the other two growth factors. This low secretion yields suggest that there might be a specific characteristic of each protein that affects the secretion. Nevertheless, the UVM11 strain always performed better than the UVM4 strain.

Neupert et al. suggested that the alterations of the chromatin structure could be the reason for the enhanced transgene expression in the UVM-strains, but the exact molecular basis for this is unknown (Neupert et al., 2009). This chromatin alteration has been identified as a transcriptional gene silencing effect, which is mediated by DNA methylation (Kong et al., 2015; Leon-Banares et al., 2004). Moreover, Neupert *et al*. pointed out that mRNA instability, as well as inefficient translation, are also important determinants of transgene expression rates.

The variety of the expression yields and the secretion rates shown by the recombinant proteins in this thesis agree with the argument exposed by the authors mentioned above. Meanwhile, the pBC1_V-11 and pBC1_T-11 clones have secreted the majority of the protein that they expressed (91.15% and 99.84%, respectively), regarding pBC1_P-11 and pBC1_S-11 clones secreted significantly less protein (22 % and 24%, respectively). These rates are closer to the numbers reported by Kong et al.; they also reported a low percentage of protein secretion, where only 21.2% and 17.6% of the UVM4 and UVM11 clones, respectively, were able to secrete squalene synthase (Kong et al., 2014). One possible explanation would be that the gene silencing mechanism in the UVM strains does not work uniformly for each clone or construct, even though Neupert et al. reported that all their clones accumulate high protein levels (Neupert et al., 2009). It makes sense to suspect that the transcription repression acts differently for each transgene, or the location of each mRNA in the genomic region interferes in the transcription levels.

As a possible outlook, a recent study attempted to implement Neupert's UV-induced mutagenesis strategy to create expression-efficient strains from DNA methyltransferase deficient *C. reinhardtii*-mutants (Kurniasih et al., 2016). They reported a ratio of almost 74% highly expressing transformants when using one of these mutants, in contrast to the 39% obtained with UVM4, which

suggests the creation of a more robust transgene expressing strain, and another possibility to obtain highly hPDGF-B and hSDF-1 expressing strains.

5.1.2. *C. reinhardtii* expressing hTGF-β3

A particular analysis is required for the new strains expressing hTGF-β3. Since the pBC1_T and pOpt_T constructs have shown remarkable differences in the percentage of secreting clones, only 1.6 and 0.6% respectively of the clones, have secreted hTGF-B3 (Table 9) compared to the other growth factors (Tables 8, 10), and a deficient number of high-expressing clones was obtained (Fig. 10C, D).

Although the secretion yield from recombinant hTGF-β3 was high (around 99% for both expression vectors)(Fig. 12C), the amount of protein in the supernatant was deficient, just 12pg hTGF-β3/µg Total Protein (Fig. 12B). This result suggests that the proper assembly and production of hTGF-β3 from *C. reinhardtii* is still a challenge. This trouble may be related to the fact that a very complex mechanism is needed for a complete functional assembly of the human protein TGF-β-family. The mechanism is a multistage process controlled by several enzymes and proteins to synthesize the mature and functional TGF-β homodimer, which is possible could not be correctly suited by the algae to produce human proteins (Poniatowski et al., 2015).

Lastly, the biological function of recombinant hTGF-β3 could not be demonstrated (Fig. 13). Since, for both algal-derived recombinant proteins, as well as the negative and positive controls, the results showed no different significant values that allowed any conclusion about the phosphorylation activity of the recombinant hTGF-β3. One possible explanation for this observation is the basal activity of the Smad2 receptors in the 3T3 cells, which is quite constant as it has been demonstrated for other receptors such as eukaryotic initiation factor 4E or mitogen-activated protein kinase, and thus, it does not enable to show the protein bio-functionality (Scheper et al., 2001). In order to circumvent this problem, the synergic effect of the Connective-tissue growth factor (CTGF) on the phosphorylation of the Smad2 receptor could be implemented. It has been demonstrated that CTGF enhances the TGF-β receptor (Reviewed by Gressner and Gressner 2008).

5.1.3. *C. reinhardtii* as a platform of pro-angiogenic proteins expression

The results showed that the rates of recombinant protein expression rates differed for each transgene (hVEGF-165, hTGF-β3, hPDGF-B, hSDF-1), transformation construct (pBC1 and pOpt), and strain (UVM4 and UVM11).

5.1.3.1. mRNA accumulation and protein expression

The mRNA accumulation was evaluated for hVEGF-165 by Northern blot (Fig.7). When this protein was transcripted by the pOpt expression vector, the transgenes were controlled by the same promoter and regulatory elements; the only difference was the strep-tag in the 3'UTR. The mRNA accumulation and protein expression of hVEGF-165 in the *C. reinhardtii* was not always the same. However, it was tightly correlated with each other, except for pOpt_Vs-11, this clone has shown a reduced mRNA accumulation, which was consistent with the lowest result for protein expression and secretion observed from this construct. On the other hand, when the pBC1 expression vector was the platform to express hVEGF-165 from *C. reinhardtii*, the pBC1_V-11 had the highest values in both cases, transcript accumulation and protein expression (Fig. 7, 8). Barahimipour et al. observed the same situation. They found a correlation between the protein accumulation and the mRNA abundance, and have observed different mRNA accumulation of *the CrP24* gene in UVM11 and Elow47 strains. They suggested that those differences in mRNA accumulations can be a consequence of the different ribosome coverage of the transcripts (Barahimipour et al., 2016a).

Additionally, the mRNA stability or inefficient translation has been related to codon usage, and due to the high GC content of the *C. reinhardtii* nuclear genome, the codon optimization is crucial in the transgene expression. Since the same codon-optimized hVEGF-165, hTGF-β3, hPDGF-B, and hSDF-1 sequences were cloned into the UVM4 or UVM11 strains, it makes sense to assume that the expression differences observed in this thesis, might be influenced by epigenetic differences in the chromatin status, after the incorporation of the transgenes into the nuclear genome as it was mentioned before regarding these UV mutants (reviewed by Barahimipour et al., 2015).

5.1.3.2 Glycosylation in C. reinhardtii and its influence in the bio-functionality of the proteins

The glycosylation is an essential characteristic for biopharmaceutical products because it is a critical factor to their stability, half-life, and biological activity. Considering that the enzymes involved in the post-translational modification, are localized in the endoplasmic reticulum and the Golgi apparatus, then the expressed proteins in *C. reinhardtii* must travel through these organelles to be glycosylated (Mathieu-Rivet et al., 2017; Ramos-Martinez et al., 2017).

The high secretion of recombinant hVEGF-165 compared to the other angiogenic growth factors produced (hPDGF-B and hSDF-1) in *C. reinhardtii,* might be explained by the post-translational of each protein. Meanwhile, VEGF is an *N*-glycosylated protein (Kang et al., 2013), PDGF-B is mostly *O*-glycosylated (Dai et al., 2015) and SDF-1 can show *N*- or *O*-glycosylation (Drury et al., 2011). In eukaryotic cells, the most common post-translational modification is *N*-glycosylation. However, Mathieu-River *et al.* had identified substantial differences in the endogenous *N*-glycan structures from

C. reinhardtii in comparison with those from humans (Mathieu-Rivet et al., 2013), which can be a problem for the therapeutic protein production in this alga or the functionality of the protein.

Additionally, even though an improvement of recombinant hPDGF-B and hSDF-1 synthesis in UVM11-derived clones was observed compared to the previously reported (Fig. 16 A, D), the secretion rates were not as high as for recombinant hVEGF-165 (Fig. 8D). These differences in secretion yields besides the glycosylation might be explained by the proteolytic activity of the enzymes in *the Chlamydomonas* cytosol. Potvin and Zhang have argued that these proteolytic enzymes may lead to the degradation of foreign proteins after synthesis or interfere in the proper folding and post-translational modification (Potvin and Zhang 2010a).

Furthermore, the glycosylation is directly related to the proper folding and the correct formation of disulfide bonds in the proteins. This characteristic is essential for the biological activity of biopharmaceutical production (Walsh & Jefferis, 2006).

VEGF is a homodimeric glycoprotein, and the covalent dimerization of this protein is required for binding to its receptor and biological activity (Kang et al., 2013). The pBC1_V4 and pBC1_V11 clones had shown no differences with the biological activity from the commercially available hVEGF-165; these results suggest the both UVM4 and UVM11 derived clones can do the proper folding and glycosylation for this protein. The same situation was observed for hSDF-1; the biological activity of both clones was similar to the commercially available (Fig. 17B). In physiological conditions, SDF-1 exists as dimer and monomer in equilibrium (Holmes et al., 2001), the function of mono- and dimeric glycoprotein SDF-1 is related to the cell migration (Drury et al., 2011). Interestingly, in the case of hPDGF-B, a significantly increased bioactivity was observed in the pBC1_P11 clone (Fig 17A). PDGF is a dimeric protein, that can be assembled as homo- and heterodimers of disulfide-bonded A- and B-polypeptide chains, because of that, PDGF can bind two receptors simultaneously and then form a bridge between the receptors, which is required for its biological activity (Heldin & Westermark, 1999).

Therefore, future research must include a detailed analysis of the secreted angiogenic growth factors by mass spectroscopy to understand its structures better and might evaluate which glycan structures should be added to increase the protein accumulation in *C. reinhardtii*.

5.2. Synergic effect of human growth factors in angiogenesis

The angiogenic capacity of the combination of three recombinant growth factors was evaluated based on their potential to induce the formation of a new vascular network from pre-existing blood vessels in an *in vitro* angiogenesis assay. This essay attempts to emulate the effect of the growth factor gradient induced on endothelial cells upon an injury and evaluate their capacity to form vessel tubes. The evaluated parameter was loop formation. These loops are the result of two mechanisms

required for angiogenesis; first, the endothelial cell should elongate itself for tube formation, and second, the tube-vessel anastomosis, which is formed by the fusion of sprouts or when two tip cells or one tip cell and stalk cell get in contact (Bazmara et al., 2015).

By treating HUVECs with different combinations of hVEGF-165, hPDGF-B, and hSDF-1 secreted by C. reinhardtii, a synergic effect of the three recombinant growth factors was observed (Fig. 17). Interestingly, the highest number of vessel loops was observed when the three were used to stimulate the cells. The number of loops had shown an increase of 2 fold when the cells were stimulated with the triplet derived Chlamydomonas growth factors, compared to loops observed after the single stimulation with hVEGF. The same behavior was observed when the HUVECs were stimulated with the commercially available growth factors. These results had demonstrated the feasibility of producing biofunctional human growth factors from *C. reinhardtii*, similar to the commercially available proteins, which can increase blood vessel formation. This effect was partially described before by Bai et al., where tube formation upon dual delivery of commercially available VEGF, fibroblast growth factor (FGF), and PDGF observed an increase of 2 fold in the total tubular length. In contrast, the single delivery of any of these proteins did not show a significant increase in the total tubular length (Bai et al., 2018).

As mentioned before, the HULK concept aims to deliver oxygen and growth factors *in situ* to improve wound healing. According to this idea, the results from the present work are one step toward achieving this goal. This thesis could have a significant impact on translational medicine since it would be possible to combine transgenic *C. reinhardtii* strains to produce growth factors that stimulate specific cellular processes by single delivery or multiple combinations besides oxygen supply. Even more ambitious, prepare a cocktail of growth factors, according to the needs of the patient, once a full-set of transgenic algae strains for every therapeutic peptide in the market is established. Moreover, this could also be implemented in combination with biomaterials, which has been shown to lead to promising results. For instance, Lai et al., designed a scaffold with nanofibers to release first hFGF and endothelial growth factor (EGF) and later VEGF and SDF, to accelerate wound closure and enhance maturation of newly formed wound vasculature (Lai et al., 2014).

5.3. Conclusion and future perspectives

The optimization of foreign gene expression from the nuclear genome in *C. reinhardtii* has been a focus of research for several years. In this regard, parallel efforts have contributed to enhancing heterologous protein synthesis and secretion in this alga by understanding the main drawbacks and developing strategies and tools that are related to them.

Along with this research line, this thesis aimed to find an optimized strategy that would lead to the creation of highly efficient algal strains, which could be used to expand the catalog of available algal-derived pro-angiogenic recombinant growth factors. For this, two different expression vectors, in combination with two different strains, were screened to find a combination that led to the highest protein yields.

The results obtained showed that the vector pBC1 and the strain UVM11 led to the most efficient levels of transgene expression and protein synthesis, yet, this was not equally significant for all GFs. Thus, an understanding of the requirements that guarantee high recombinant protein expression remains to be achieved. However, despite the low yields recovered from hTGF-β3, hPDGF-B, and hSDF-1, the synergic effect of the recombinant proteins expressed by *C. reinhardtii* demonstrated their angiogenic capacity. This finding strongly supports the future implementation of photosynthetic microalgae derived pharmaceuticals to treat chronic-wound healing, once it is possible to maximally exploit the advantages of human protein expression in *C. reinhardtii.*

6. References

Aguirre A, González-Vázquez A, Navarro M, Castano O, Planell JA, Engel E (2012) Control of microenvironmental cues with a smart biomaterial composite promotes endothelial progenitor cell angiogenesis. European cells & materials 24:90-106; discussion 106 doi:10.22203/eCM.v024a07

Ataliotis P, Mercola M (1997) Distribution and functions of platelet-derived growth factors and their receptors during embryogenesis. Int Rev Cytol 172:95-127 doi:10.1016/s0074-7696(08)62359-1

Bai Y, Bai L, Zhou J, Chen H, Zhang L (2018) Sequential delivery of VEGF, FGF-2 and PDGF from the polymeric system enhance HUVECs angiogenesis in vitro and CAM angiogenesis. Cellular Immunology 323:19-32 doi:https://doi.org/10.1016/j.cellimm.2017.10.008

Baier T, Kros D, Feiner RC, Lauersen KJ, Muller KM, Kruse O (2018a) Engineered Fusion Proteins for Efficient Protein Secretion and Purification of a Human Growth Factor from the Green Microalga Chlamydomonas reinhardtii. ACS Synth Biol 7(11):2547-2557 doi:10.1021/acssynbio.8b00226

Baier T, Kros D, Feiner RC, Lauersen KJ, Müller KM, Kruse O (2018b) Engineered Fusion Proteins for Efficient Protein Secretion and Purification of a Human Growth Factor from the Green Microalga Chlamydomonas reinhardtii. ACS Synthetic Biology 7(11):2547-2557 doi:10.1021/acssynbio.8b00226

Bandyopadhyay B, Fan J, Guan S, Li Y, Chen M, Woodley DT, Li W (2006) A "traffic control" role for TGFbeta3: orchestrating dermal and epidermal cell motility during wound healing. J Cell Biol 172(7):1093-105 doi:10.1083/jcb.200507111

Barahimipour R, Neupert J, Bock R (2016a) Efficient expression of nuclear transgenes in the green alga Chlamydomonas: synthesis of an HIV antigen and development of a new selectable marker. Plant Mol Biol 90(4-5):403-18 doi:10.1007/s11103-015-0425-8

Barahimipour R, Neupert J, Bock R (2016b) Efficient expression of nuclear transgenes in the green alga Chlamydomonas: synthesis of an HIV antigen and development of a new selectable marker. Plant Molecular Biology 90(4):403-418 doi:10.1007/s11103-015-0425-8

Barahimipour R, Strenkert D, Neupert J, Schroda M, Merchant SS, Bock R (2015) Dissecting the contributions of GC content and codon usage to gene expression in the model alga Chlamydomonas reinhardtii. Plant J 84(4):704-17 doi:10.1111/tpj.13033

Barrera DJ, Rosenberg JN, Chiu JG, Chang Y-N, Debatis M, Ngoi S-M, Chang JT, Shoemaker CB, Oyler GA, Mayfield SP (2015) Algal chloroplast produced camelid VHH antitoxins are capable of neutralizing botulinum neurotoxin. Plant Biotechnology Journal 13(1):117-124 doi:10.1111/pbi.12244

Barrientos S, Brem H, Stojadinovic O, Tomic-Canic M (2014) Clinical application of growth factors and cytokines in wound healing. Wound repair and regeneration: official publication of the Wound Healing Society [and] the European Tissue Repair Society 22(5):569-578 doi:10.1111/wrr.12205

Barrientos S, Stojadinovic O, Golinko MS, Brem H, Tomic-Canic M (2008) Growth factors and cytokines in wound healing. Wound Repair Regen 16(5):585-601 doi:10.1111/j.1524-475X.2008.00410.x

Bazmara H, Soltani M, Sefidgar M, Bazargan M, Mousavi Naeenian M, Rahmim A (2015) The Vital Role of Blood Flow-Induced Proliferation and Migration in Capillary Network Formation in a Multiscale Model of Angiogenesis. PloS one 10(6):e0128878-e0128878 doi:10.1371/journal.pone.0128878

Berthold P, Schmitt R, Mages W (2002) An Engineered Streptomyces hygroscopicus aph 7" Gene Mediates Dominant Resistance against Hygromycin B in Chlamydomonas reinhardtii. Protist 153(4):401-412 doi:https://doi.org/10.1078/14344610260450136

Blankenship RE (2014) Molecular Mechanisms of Photosynthesis. Wiley

Bohne A-V, Schwarz C, Schottkowski M, Lidschreiber M, Piotrowski M, Zerges W, Nickelsen J (2013) Reciprocal Regulation of Protein Synthesis and Carbon Metabolism for Thylakoid Membrane Biogenesis. PLOS Biology 11(2):e1001482 doi:10.1371/journal.pbio.1001482

Buchanan BB, Gruissem W, Jones RL (2000) Biochemistry & molecular biology of plants. American Society of Plant Physiologists, Rockville, Md.

Castaño O, Pérez-Amodio S, Navarro-Requena C, Mateos-Timoneda MÁ, Engel E (2018) Instructive microenvironments in skin wound healing: Biomaterials as signal releasing platforms. Advanced Drug Delivery Reviews 129:95-117 doi:https://doi.org/10.1016/j.addr.2018.03.012

Centeno-Cerdas C, Jarquín-Cordero M, Chávez MN, Hopfner U, Holmes C, Schmauss D, Machens H-G, Nickelsen J, Egaña JT (2018) Development of photosynthetic sutures for the local delivery of oxygen and recombinant growth factors in wounds. Acta Biomaterialia 81:184-194 doi:https://doi.org/10.1016/j.actbio.2018.09.060

Cerutti H, Johnson AM, Gillham NW, Boynton JE (1997) Epigenetic silencing of a foreign gene in nuclear transformants of Chlamydomonas. The Plant Cell 9(6):925 doi:10.1105/tpc.9.6.925

Chang S, Li Y, Yuan F, Qu M, Song Y, Zhang Z, Yang G-Y, Wang Y (2017) Monomeric CXCL12 outperforms its dimeric and wild type variants in the promotion of human endothelial progenitor cells' function. Biochemical and Biophysical Research Communications 488(2):303-310 doi:https://doi.org/10.1016/j.bbrc.2017.03.172

Chavez MN, Schenck TL, Hopfner U, Centeno-Cerdas C, Somlai-Schweiger I, Schwarz C, Machens HG, Heikenwalder M, Bono MR, Allende ML, Nickelsen J, Egana JT (2016) Towards autotrophic tissue engineering: Photosynthetic gene therapy for regeneration. Biomaterials 75:25-36 doi:10.1016/j.biomaterials.2015.10.014

Cheng JW, Sadeghi Z, Levine AD, Penn MS, von Recum HA, Caplan AI, Hijaz A (2014) The role of CXCL12 and CCL7 chemokines in immune regulation, embryonic development, and tissue regeneration. Cytokine 69(2):277-83 doi:10.1016/j.cyto.2014.06.007

Croft MT, Moulin M, Webb ME, Smith AG (2007) Thiamine biosynthesis in algae is regulated by riboswitches. Proceedings of the National Academy of Sciences 104(52):20770 doi:10.1073/pnas.0705786105

Crozet P, Navarro FJ, Willmund F, Mehrshahi P, Bakowski K, Lauersen KJ, Pérez-Pérez M-E, Auroy P, Gorchs Rovira A, Sauret-Gueto S, Niemeyer J, Spaniol B, Theis J, Trösch R, Westrich L-D, Vavitsas K, Baier T, Hübner W, de Carpentier F, Cassarini M, Danon A, Henri J, Marchand CH, de Mia M, Sarkissian K, Baulcombe DC, Peltier G, Crespo J-L, Kruse O, Jensen P-E, Schroda M, Smith AG, Lemaire SD (2018) Birth of a Photosynthetic Chassis: A MoClo Toolkit Enabling Synthetic Biology in the Microalga Chlamydomonas reinhardtii. ACS Synthetic Biology 7(9):2074-2086 doi:10.1021/acssynbio.8b00251

Czarkowska-Paczek B, Bartlomiejczyk I, Przybylski J (2006) The serum levels of growth factors: PDGF, TGF-beta and VEGF are increased after strenuous physical exercise. Journal of physiology and pharmacology: an official journal of the Polish Physiological Society 57:189-97

Dai M, Yu C, Fang T, Fu L, Wang J, Zhang J, Ren J, Xu J, Zhang X, Chen W (2015) Identification and Functional Characterization of Glycosylation of Recombinant Human Platelet-Derived Growth Factor-BB in Pichia pastoris. PLOS ONE 10(12):e0145419 doi:10.1371/journal.pone.0145419

Dauvillée D, Delhaye S, Gruyer S, Slomianny C, Moretz SE, d'Hulst C, Long CA, Ball SG, Tomavo S (2010) Engineering the Chloroplast Targeted Malarial Vaccine Antigens in Chlamydomonas Starch Granules. PLOS ONE 5(12):e15424 doi:10.1371/journal.pone.0015424

Dekker JP, Boekema EJ (2005) Supramolecular organization of thylakoid membrane proteins in green plants. Biochimica et Biophysica Acta (BBA) - Bioenergetics 1706(1):12-39 doi:https://doi.org/10.1016/j.bbabio.2004.09.009

Demurtas OC, Massa S, Ferrante P, Venuti A, Franconi R, Giuliano G (2013) A Chlamydomonas-Derived Human Papillomavirus 16 E7 Vaccine Induces Specific Tumor Protection. PLOS ONE 8(4):e61473 doi:10.1371/journal.pone.0061473

Dent RM, Haglund CM, Chin BL, Kobayashi MC, Niyogi KK (2005) Functional Genomics of Eukaryotic Photosynthesis Using Insertional Mutagenesis of Chlamydomonas reinhardtii. Plant Physiology 137(2):545-556 doi:10.1104/pp.104.055244

Dent RM, Han M, Niyogi KK (2001) Functional genomics of plant photosynthesis in the fast lane using Chlamydomonas reinhardtii. Trends Plant Sci 6(8):364-71

Ding J, Hori K, Zhang R, Marcoux Y, Honardoust D, Shankowsky HA, Tredget EE (2011) Stromal cell-derived factor 1 (SDF-1) and its receptor CXCR4 in the formation of postburn hypertrophic scar (HTS). Wound Repair Regen 19(5):568-78 doi:10.1111/j.1524-475X.2011.00724.x

Dreesen IAJ, Hamri GC-E, Fussenegger M (2010) Heat-stable oral alga-based vaccine protects mice from Staphylococcus aureus infection. Journal of Biotechnology 145(3):273-280 doi:https://doi.org/10.1016/j.jbiotec.2009.12.006

Dreifke MB, Jayasuriya AA, Jayasuriya AC (2015) Current wound healing procedures and potential care. Materials science & engineering C, Materials for biological applications 48:651-662 doi:10.1016/j.msec.2014.12.068

Drury LJ, Ziarek JJ, Gravel S, Veldkamp CT, Takekoshi T, Hwang ST, Heveker N, Volkman BF, Dwinell MB (2011) Monomeric and dimeric CXCL12 inhibit metastasis through distinct CXCR4 interactions and signaling pathways. Proceedings of the National Academy of Sciences 108(43):17655 doi:10.1073/pnas.1101133108

Duan D, Derynck R (2019) Transforming growth factor–β (TGF-β)–induced up-regulation of TGF-β receptors at the cell surface amplifies the TGF-β response. Journal of Biological Chemistry 294(21):8490-8504 doi:10.1074/jbc.RA118.005763

Dunnill C, Patton T, Brennan J, Barrett J, Dryden M, Cooke J, Leaper D, Georgopoulos NT (2017) Reactive oxygen species (ROS) and wound healing: the functional role of ROS and emerging ROS-modulating technologies for augmentation of the healing process. International Wound Journal 14(1):89-96 doi:10.1111/iwj.12557

Eberhard S, Finazzi G, Wollman FA (2008) The Dynamics of Photosynthesis. Annual Review of Genetics 42:463-515 doi:10.1146/annurev.genet.42.110807.091452

Eichler-Stahlberg A, Weisheit W, Ruecker O, Heitzer M (2009) Strategies to facilitate transgene expression in Chlamydomonas reinhardtii. Planta 229(4):873-883 doi:10.1007/s00425-008-0879-x

Eisenbud DE (2012) Oxygen in Wound Healing: Nutrient, Antibiotic, Signaling Molecule, and Therapeutic Agent. Clinics in Plastic Surgery 39(3):293-310 doi:10.1016/j.cps.2012.05.001

Esland L, Larrea-Alvarez M, Purton S (2018) Selectable Markers and Reporter Genes for Engineering the Chloroplast of Chlamydomonas reinhardtii. Biology (Basel) 7(4):46 doi:10.3390/biology7040046

Ferrara N (2001) Role of vascular endothelial growth factor in regulation of physiological angiogenesis. American Journal of Physiology-Cell Physiology 280(6):C1358-C1366 doi:10.1152/ajpcell.2001.280.6.C1358

Ferrara N, Gerber H-P, LeCouter J (2003) The biology of VEGF and its receptors. Nature Medicine 9(6):669-676 doi:10.1038/nm0603-669

Fischer N, Rochaix JD (2001) The flanking regions of PsaD drive efficient gene expression in the nucleus of the green alga Chlamydomonas reinhardtii. Molecular Genetics and Genomics 265(5):888-894 doi:10.1007/s004380100485

Folestad E, Kunath A, Wagsater D (2018) PDGF-C and PDGF-D signaling in vascular diseases and animal models. Mol Aspects Med 62:1-11 doi:10.1016/j.mam.2018.01.005

G Dunahay T (1993) Transformation of Chlamydomonas reinhardtii with silicon carbide whiskers, vol 15,

G Rodriguez P, N Felix F, Woodley D, Shim E (2008) The Role of Oxygen in Wound Healing: A Review of the Literature, vol 34,

Gallaher SD, Fitz-Gibbon ST, Strenkert D, Purvine SO, Pellegrini M, Merchant SS (2018) High-throughput sequencing of the chloroplast and mitochondrion of Chlamydomonas reinhardtii to generate improved de novo assemblies, analyze expression patterns and transcript speciation, and evaluate diversity among laboratory strains and wild isolates. The Plant Journal 93(3):545-565 doi:10.1111/tpj.13788

García-Cisneros S, Sánchez-Alemán MÁ, Conde-Glez CJ, Lara-Zaragoza SJ, Herrera-Ortiz A, Plett-Torres T, Olamendi-Portugal M (2019) Performance of ELISA and Western blot to detect antibodies against HSV-2 using dried blood spots. Journal of Infection and Public Health 12(2):224-228 doi:https://doi.org/10.1016/j.jiph.2018.10.007

Gong J, Meng HB, Hua J, Song ZS, He ZG, Zhou B, Qian MP (2014) The SDF-1/CXCR4 axis regulates migration of transplanted bone marrow mesenchymal stem cells towards the pancreas in rats with acute pancreatitis. Mol Med Rep 9(5):1575-82 doi:10.3892/mmr.2014.2053

Gordillo GM, Sen CK (2003) Revisiting the essential role of oxygen in wound healing. The American Journal of Surgery 186(3):259-263 doi:10.1016/s0002-9610(03)00211-3

Greaves NS, Ashcroft KJ, Baguneid M, Bayat A (2013) Current understanding of molecular and cellular mechanisms in fibroplasia and angiogenesis during acute wound healing. J Dermatol Sci 72(3):206-17 doi:10.1016/j.jdermsci.2013.07.008

Gregory JA, Li F, Tomosada LM, Cox CJ, Topol AB, Vinetz JM, Mayfield S (2012) Algae-Produced Pfs25 Elicits Antibodies That Inhibit Malaria Transmission. PLOS ONE 7(5):e37179 doi:10.1371/journal.pone.0037179

Gregory JA, Topol AB, Doerner DZ, Mayfield S (2013) Alga-Produced Cholera Toxin-Pfs25 Fusion Proteins as Oral Vaccines. Applied and Environmental Microbiology 79(13):3917 doi:10.1128/AEM.00714-13

Gressner OA, Gressner AM (2008) Connective tissue growth factor: a fibrogenic master switch in fibrotic liver diseases. Liver International 28(8):1065-1079 doi:10.1111/j.1478-3231.2008.01826.x

Guerra A, Belinha J, Jorge RN (2018) Modelling skin wound healing angiogenesis: A review. Journal of Theoretical Biology 459:1-17 doi:https://doi.org/10.1016/j.jtbi.2018.09.020

Guest JF, Vowden K, Vowden P (2017) The health economic burden that acute and chronic wounds impose on an average clinical commissioning group/health board in the UK. Journal of Wound Care 26(6):292-303 doi:10.12968/jowc.2017.26.6.292

Guo R, Chai L, Chen L, Chen W, Ge L, Li X, Li H, Li S, Cao C (2015) Stromal cell-derived factor 1 (SDF-1) accelerated skin wound healing by promoting the migration and proliferation of epidermal stem cells. In Vitro Cellular & Developmental Biology - Animal 51(6):578-585 doi:10.1007/s11626-014-9862-y

Gupta R, Tongers J, Losordo DW (2009) Human studies of angiogenic gene therapy. Circ Res 105(8):724-736 doi:10.1161/CIRCRESAHA.109.200386

Han S, Hu Z, Lei A (2008) Expression and function analysis of the metallothionein-like (MT-like) gene from Festuca rubra in Chlamydomonas reinhardtii chloroplast. Science in China Series C: Life Sciences 51(12):1076-1081 doi:10.1007/s11427-008-0136-3

Harris EH (2001) CHLAMYDOMONAS AS A MODEL ORGANISM. Annual Review of Plant Physiology and Plant Molecular Biology 52(1):363-406 doi:10.1146/annurev.arplant.52.1.363

Harris EH, Stern DB, Witman G (2009) The Chlamydomonas sourcebook, 2nd edn. Elsevier/Academic Press, Amsterdam ; Boston

He D-M, Qian K-X, Shen G-F, Zhang Z-F, Li Y-N, Su Z-L, Shao H-B (2007) Recombination and expression of classical swine fever virus (CSFV) structural protein E2 gene in Chlamydomonas reinhardtii chroloplasts. Colloids and Surfaces B: Biointerfaces 55(1):26-30 doi:https://doi.org/10.1016/j.colsurfb.2006.10.042

Heitzer M, Eckert A, Fuhrmann M, Griesbeck C (2007) Influence of Codon Bias on the Expression of Foreign Genes in Microalgae. In: León R, Galván A, Fernández E (eds) Transgenic Microalgae as Green Cell Factories. Springer New York, New York, NY, pp 46-53

Heldin C-H, Westermark B (1999) Mechanism of Action and In Vivo Role of Platelet-Derived Growth Factor. Physiological Reviews 79(4):1283-1316 doi:10.1152/physrev.1999.79.4.1283

Hempel F, Maier UG (2016) Microalgae as Solar-Powered Protein Factories. In: Vega MC (ed) Advanced Technologies for Protein Complex Production and Characterization. Springer International Publishing, Cham, pp 241-262

Hippler M (2017) Chlamydomonas. Biotechnology and biomedicine. Springer, Cham, Switzerland

Holmes WD, Consler TG, Dallas WS, Rocque WJ, Willard DH (2001) Solution Studies of Recombinant Human Stromal-Cell-Derived Factor-1. Protein Expression and Purification 21(3):367-377 doi:https://doi.org/10.1006/prep.2001.1402

Hopf HW, Rollins MD (2007) Wounds: An Overview of the Role of Oxygen. Antioxidants & Redox Signaling 9(8):1183-1192 doi:10.1089/ars.2007.1641

Hopfner U, Schenck T-L, Chavez M-N, Machens H-G, Bohne A-V, Nickelsen J, Giunta R-E, Egaña J-T (2014) Development of photosynthetic biomaterials for in vitro tissue engineering. Acta Biomaterialia 10(6):2712-2717 doi:

Hou Q, Qiu S, Liu Q, Tian J, Hu Z, Ni J (2013) Selenoprotein-Transgenic Chlamydomonas reinhardtii. Nutrients 5(3) doi:10.3390/nu5030624

Howard MA, Asmis R, Evans KK, Mustoe TA (2013) Oxygen and wound care: A review of current therapeutic modalities and future direction. Wound Repair and Regeneration 21(4):503-511 doi:10.1111/wrr.12069

Hughes GC, Biswas SS, Yin B, Coleman RE, DeGrado TR, Landolfo CK, Lowe JE, Annex BH, Landolfo KP (2004) Therapeutic angiogenesis in chronically ischemic porcine myocardium: comparative effects of bFGF and VEGF. The Annals of Thoracic Surgery 77(3):812-818 doi:10.1016/j.athoracsur.2003.09.060

Jaeger D, Baier T, Lauersen KJ (2019) Intronserter, an advanced online tool for design of intron containing transgenes. Algal Research 42:101588 doi:https://doi.org/10.1016/j.algal.2019.101588

Janssen M, Janssen M, de Winter M, Tramper J, Mur LR, Snel J, Wijffels RH (2000) Efficiency of light utilization of Chlamydomonas reinhardtii under medium-duration light/dark cycles. Journal of Biotechnology 78(2):123-137 doi:https://doi.org/10.1016/S0168-1656(99)00233-3

Jiang B, Zhang G, Brey EM (2013) Dual delivery of chlorhexidine and platelet-derived growth factor-BB for enhanced wound healing and infection control. Acta Biomaterialia 9(2):4976-4984 doi:https://doi.org/10.1016/j.actbio.2012.10.005

Jinkerson RE, Jonikas MC (2015) Molecular techniques to interrogate and edit the Chlamydomonas nuclear genome. The Plant Journal 82(3):393-412 doi:10.1111/tpj.12801

Johnson KE, Wilgus TA (2014) Vascular Endothelial Growth Factor and Angiogenesis in the Regulation of Cutaneous Wound Repair. Advances in wound care 3(10):647-661 doi:10.1089/wound.2013.0517

Jones CS, Luong T, Hannon M, Tran M, Gregory JA, Shen Z, Briggs SP, Mayfield SP (2013) Heterologous expression of the C-terminal antigenic domain of the malaria vaccine candidate Pfs48/45 in the green algae Chlamydomonas reinhardtii. Applied Microbiology and Biotechnology 97(5):1987-1995 doi:10.1007/s00253-012-4071-7

Kang WK, Lee MH, Kim YH, Kim MY, Kim J-Y (2013) Enhanced secretion of biologically active, non-glycosylated VEGF from Saccharomyces cerevisiae. Journal of Biotechnology 164(4):441-448 doi:https://doi.org/10.1016/j.jbiotec.2013.02.004

Kindle KL, Schnell RA, Fernández E, Lefebvre PA (1989) Stable nuclear transformation of Chlamydomonas using the Chlamydomonas gene for nitrate reductase. The Journal of Cell Biology 109(6):2589 doi:10.1083/jcb.109.6.2589

Knighton DR, Hunt TK, Scheuenstuhl H, Halliday BJ, Werb Z, Banda MJ (1983) Oxygen tension regulates the expression of angiogenesis factor by macrophages. Science 221(4617):1283 doi:10.1126/science.6612342

Kong F, Yamasaki T, Kurniasih SD, Hou L, Li X, Ivanova N, Okada S, Ohama T (2015) Robust expression of heterologous genes by selection marker fusion system in improved Chlamydomonas strains. Journal of Bioscience and Bioengineering 120(3):239-245 doi:https://doi.org/10.1016/j.jbiosc.2015.01.005

Kong F, Yamasaki T, Ohama T (2014) Expression levels of domestic cDNA cassettes integrated in the nuclear genomes of various Chlamydomonas reinhardtii strains. Journal of Bioscience and Bioengineering 117(5):613-616 doi:https://doi.org/10.1016/j.jbiosc.2013.10.025

Kurniasih S, Yamasaki T, Kong F, Okada S, Widyaningrum D, Ohama T (2016) UV-mediated Chlamydomonas mutants with enhanced nuclear transgene expression by disruption of DNA methylation-dependent and independent silencing systems. Plant Molecular Biology 92 doi:10.1007/s11103-016-0529-9

Lai H-J, Kuan C-H, Wu H-C, Tsai J-C, Chen T-M, Hsieh D-J, Wang T-W (2014) Tailored design of electrospun composite nanofibers with staged release of multiple angiogenic growth factors for chronic wound healing. Acta Biomaterialia 10(10):4156-4166 doi:https://doi.org/10.1016/j.actbio.2014.05.001

Lauersen KJ, Berger H, Mussgnug JH, Kruse O (2013a) Efficient recombinant protein production and secretion from nuclear transgenes in Chlamydomonas reinhardtii. J Biotechnol 167(2):101-10 doi:10.1016/j.jbiotec.2012.10.010

Lauersen KJ, Berger H, Mussgnug JH, Kruse O (2013b) Efficient recombinant protein production and secretion from nuclear transgenes in Chlamydomonas reinhardtii. Journal of Biotechnology 167(2):101-110 doi:https://doi.org/10.1016/j.jbiotec.2012.10.010

Lauersen KJ, Huber I, Wichmann J, Baier T, Leiter A, Gaukel V, Kartushin V, Rattenholl A, Steinweg C, von Riesen L, Posten C, Gudermann F, Lutkemeyer D, Mussgnug JH, Kruse O (2015a) Investigating the dynamics of recombinant protein secretion from a microalgal host. J Biotechnol 215:62-71 doi:10.1016/j.jbiotec.2015.05.001

Lauersen KJ, Kruse O, Mussgnug JH (2015b) Targeted expression of nuclear transgenes in Chlamydomonas reinhardtii with a versatile, modular vector toolkit. Applied Microbiology and Biotechnology 99(8):3491-3503 doi:10.1007/s00253-014-6354-7

Leduc C, Sobilo L, Toumi H, Mondon P, Lespessailles E, Ossant F, Kurfurst R, Pichon C (2016) TGF-beta-induced early gene-1 overexpression promotes oxidative stress protection and actin cytoskeleton rearrangement in human skin fibroblasts. Biochimica et Biophysica Acta (BBA) - General Subjects 1860(6):1071-1078 doi:https://doi.org/10.1016/j.bbagen.2016.02.009

Leon-Banares R, Gonzalez-Ballester D, Galvan A, Fernandez E (2004) Transgenic microalgae as green cell-factories. Trends Biotechnol 22(1):45-52 doi:10.1016/j.tibtech.2003.11.003

León R, Fernández E (2007) Nuclear Transformation of Eukaryotic Microalgae. In: León R, Galván A, Fernández E (eds) Transgenic Microalgae as Green Cell Factories. Springer New York, New York, NY, pp 1-11

Lumbreras V, Stevens DR, Purton S (1998) Efficient foreign gene expression in Chlamydomonas reinhardtii mediated by an endogenous intron. The Plant Journal 14(4):441-447 doi:10.1046/j.1365-313X.1998.00145.x

Maes C, Carmeliet P, Moermans K, Stockmans I, Smets N, Collen D, Bouillon R, Carmeliet G (2002) Impaired angiogenesis and endochondral bone formation in mice lacking the vascular endothelial growth factor isoforms VEGF164 and VEGF188. Mechanisms of Development 111(1):61-73 doi:https://doi.org/10.1016/S0925-4773(01)00601-3

Manuell AL, Beligni MV, Elder JH, Siefker DT, Tran M, Weber A, McDonald TL, Mayfield SP (2007) Robust expression of a bioactive mammalian protein in Chlamydomonas chloroplast. Plant Biotechnol J 5(3):402-12 doi:10.1111/j.1467-7652.2007.00249.x

Mathieu-Rivet E, Lerouge P, Bardor M (2017) Chlamydomonas reinhardtii: Protein Glycosylation and Production of Biopharmaceuticals. pp 45-72

Mathieu-Rivet E, Scholz M, Arias C, Dardelle F, Schulze S, Le Mauff F, Teo G, Hochmal AK, Blanco-Rivero A, Loutelier-Bourhis C, Kiefer-Meyer M-C, Fufezan C, Burel C, Lerouge P, Martinez F, Bardor M, Hippler M (2013) Exploring the N-glycosylation Pathway in Chlamydomonas reinhardtii Unravels Novel Complex Structures. Molecular & Cellular Proteomics 12(11):3160 doi:10.1074/mcp.M113.028191

Mayfield SP, Franklin SE, Lerner RA (2003) Expression and assembly of a fully active antibody in algae. Proceedings of the National Academy of Sciences 100(2):438 doi:10.1073/pnas.0237108100

Menon SN, Flegg JA, McCue SW, Schugart RC, Dawson RA, McElwain DLS (2012) Modelling the interaction of keratinocytes and fibroblasts during normal and abnormal wound healing processes. Proc Biol Sci 279(1741):3329-3338 doi:10.1098/rspb.2012.0319

Merchant SS, Prochnik SE, Vallon O, Harris EH, Karpowicz SJ, Witman GB, Terry A, Salamov A, Fritz-Laylin LK, Marechal-Drouard L, Marshall WF, Qu LH, Nelson DR, Sanderfoot AA, Spalding MH, Kapitonov VV, Ren Q, Ferris P, Lindquist E, Shapiro H, Lucas SM, Grimwood J, Schmutz J, Cardol P, Cerutti H, Chanfreau G, Chen CL, Cognat V, Croft MT, Dent R, Dutcher S, Fernandez E,

Fukuzawa H, Gonzalez-Ballester D, Gonzalez-Halphen D, Hallmann A, Hanikenne M, Hippler M, Inwood W, Jabbari K, Kalanon M, Kuras R, Lefebvre PA, Lemaire SD, Lobanov AV, Lohr M, Manuell A, Meier I, Mets L, Mittag M, Mittelmeier T, Moroney JV, Moseley J, Napoli C, Nedelcu AM, Niyogi K, Novoselov SV, Paulsen IT, Pazour G, Purton S, Ral JP, Riano-Pachon DM, Riekhof W, Rymarquis L, Schroda M, Stern D, Umen J, Willows R, Wilson N, Zimmer SL, Allmer J, Balk J, Bisova K, Chen CJ, Elias M, Gendler K, Hauser C, Lamb MR, Ledford H, Long JC, Minagawa J, Page MD, Pan J, Pootakham W, Roje S, Rose A, Stahlberg E, Terauchi AM, Yang P, Ball S, Bowler C, Dieckmann CL, Gladyshev VN, Green P, Jorgensen R, Mayfield S, Mueller-Roeber B, Rajamani S, Sayre RT, Brokstein P, Dubchak I, Goodstein D, Hornick L, Huang YW, Jhaveri J, Luo Y, Martinez D, Ngau WC, Otillar B, Poliakov A, Porter A, Szajkowski L, Werner G, Zhou K, Grigoriev IV, Rokhsar DS, Grossman AR (2007) The Chlamydomonas genome reveals the evolution of key animal and plant functions. Science 318(5848):245-50 doi:10.1126/science.1143609

Minagawa J, Takahashi Y (2004) Structure, function and assembly of Photosystem II and its light-harvesting proteins. Photosynthesis Research 82(3):241-263 doi:10.1007/s11120-004-2079-2

Mizuno K, Matsuyama W, Mitsuyama H, Watanabe M, Higashimoto I, Osame M, Arimura K (2005) Clinical investigation: increased serum stromal derived factor 1 alpha levels in pulmonary tuberculosis. Clin Exp Immunol 139(3):490-497 doi:10.1111/j.1365-2249.2005.02721.x

Molino JVD, de Carvalho JCM, Mayfield SP (2018) Comparison of secretory signal peptides for heterologous protein expression in microalgae: Expanding the secretion portfolio for Chlamydomonas reinhardtii. PLoS One 13(2):e0192433 doi:10.1371/journal.pone.0192433

Moulin M, Nguyen GTDT, Scaife MA, Smith AG, Fitzpatrick TB (2013) Analysis of Chlamydomonas thiamin metabolism in vivo reveals riboswitch plasticity. Proceedings of the National Academy of Sciences of the United States of America 110(36):14622-14627 doi:10.1073/pnas.1307741110

Mussgnug JH (2015) Genetic tools and techniques for Chlamydomonas reinhardtii. Applied Microbiology and Biotechnology 99(13):5407-5418 doi:10.1007/s00253-015-6698-7

Nelson N, Yocum CF (2006) Structure and function of photosystems I and II. Annu Rev Plant Biol 57:521-65 doi:10.1146/annurev.arplant.57.032905.105350

Neupert J, Karcher D, Bock R (2009) Generation of Chlamydomonas strains that efficiently express nuclear transgenes. Plant J 57(6):1140-50 doi:10.1111/j.1365-313X.2008.03746.x

Nissen N, Polverini P, Koch A, V Volin M, L Gamelli R, A DiPietro L (1998) Nissen NN, Polverini PJ, Koch AE, Volin MV, Gamelli RL, DiPietro LAVEGF mediates angiogenic activity during the proliferative phase of wound healing. Am J Pathol 152:1445-1452. The American journal of pathology 152:1445-52

Occleston NL, O'Kane S, Laverty HG, Cooper M, Fairlamb D, Mason T, Bush JA, Ferguson MW (2011) Discovery and development of avotermin (recombinant human transforming growth factor beta

3): a new class of prophylactic therapeutic for the improvement of scarring. Wound Repair Regen 19 Suppl 1:s38-48 doi:10.1111/j.1524-475X.2011.00711.x

Ong HT, Dilley RJ (2018) Novel non-angiogenic role for mesenchymal stem cell-derived vascular endothelial growth factor on keratinocytes during wound healing. Cytokine & Growth Factor Reviews 44:69-79 doi:https://doi.org/10.1016/j.cytogfr.2018.11.002

Pan Q, Chathery Y, Wu Y, Rathore N, Tong RK, Peale F, Bagri A, Tessier-Lavigne M, Koch AW, Watts RJ (2007) Neuropilin-1 binds to VEGF121 and regulates endothelial cell migration and sprouting. J Biol Chem 282(33):24049-56 doi:10.1074/jbc.M703554200

Penn JW, Grobbelaar AO, Rolfe KJ (2012) The role of the TGF-β family in wound healing, burns and scarring: a review. Int J Burns Trauma 2(1):18-28

Poniatowski ŁA, Wojdasiewicz P, Gasik R, Szukiewicz D (2015) Transforming growth factor Beta family: insight into the role of growth factors in regulation of fracture healing biology and potential clinical applications. Mediators of inflammation 2015:137823-137823 doi:10.1155/2015/137823

Potvin G, Zhang Z (2010a) Strategies for high-level recombinant protein expression in transgenic microalgae: a review. Biotechnol Adv 28(6):910-8 doi:10.1016/j.biotechadv.2010.08.006

Potvin G, Zhang Z (2010b) Strategies for high-level recombinant protein expression in transgenic microalgae: A review. Biotechnology Advances 28(6):910-918 doi:https://doi.org/10.1016/j.biotechadv.2010.08.006

Ramos-Martinez EM, Fimognari L, Sakuragi Y (2017) High-yield secretion of recombinant proteins from the microalga Chlamydomonas reinhardtii. Plant Biotechnology Journal 15(9):1214-1224 doi:10.1111/pbi.12710

Rasala BA, Barrera DJ, Ng J, Plucinak TM, Rosenberg JN, Weeks DP, Oyler GA, Peterson TC, Haerizadeh F, Mayfield SP (2013) Expanding the spectral palette of fluorescent proteins for the green microalga Chlamydomonas reinhardtii. The Plant Journal 74(4):545-556 doi:10.1111/tpj.12165

Rasala BA, Lee PA, Shen Z, Briggs SP, Mendez M, Mayfield SP (2012) Robust Expression and Secretion of Xylanase1 in Chlamydomonas reinhardtii by Fusion to a Selection Gene and Processing with the FMDV 2A Peptide. PLOS ONE 7(8):e43349 doi:10.1371/journal.pone.0043349

Rasala BA, Mayfield SP (2015) Photosynthetic biomanufacturing in green algae; production of recombinant proteins for industrial, nutritional, and medical uses. Photosynthesis Research 123(3):227-239 doi:10.1007/s11120-014-9994-7

Rasala BA, Muto M, Lee PA, Jager M, Cardoso RMF, Behnke CA, Kirk P, Hokanson CA, Crea R, Mendez M, Mayfield SP (2010) Production of therapeutic proteins in algae, analysis of expression of seven human proteins in the chloroplast of Chlamydomonas reinhardtii. Plant Biotechnology Journal 8(6):719-733 doi:10.1111/j.1467-7652.2010.00503.x

Roy S, Khanna S, Nallu K, Hunt TK, Sen CK (2006) Dermal wound healing is subject to redox control. Molecular therapy : the journal of the American Society of Gene Therapy 13(1):211-220 doi:10.1016/j.ymthe.2005.07.684

Rumpho ME, Pelletreau KN, Moustafa A, Bhattacharya D (2011) The making of a photosynthetic animal. The Journal of experimental biology 214(Pt 2):303-311 doi:10.1242/jeb.046540

Rybska M, Knap S, Stefańska K, Jankowski M, Chamier-Gliszczyńska A, Popis M, Jeseta M, Bukowska D, Antosik P, Kempisty B, M. Jaśkowski J (2018) Transforming growth factor (TGF) – Is it a key protein in mammalian reproductive biology? , vol 6,

Salcedo R, Oppenheim JJ (2003) Role of chemokines in angiogenesis: CXCL12/SDF-1 and CXCR4 interaction, a key regulator of endothelial cell responses. Microcirculation 10(3-4):359-70 doi:10.1038/sj.mn.7800200

Sanon S, Hart DA, Tredget EE (2016) Chapter 2 - Molecular and Cellular Biology of Wound Healing and Skin Regeneration. In: Albanna MZ, Holmes Iv JH (eds) Skin Tissue Engineering and Regenerative Medicine. Academic Press, Boston, pp 19-47

Sasso S, Stibor H, Mittag M, Grossman AR (2018) From molecular manipulation of domesticated Chlamydomonas reinhardtii to survival in nature. eLife 7:e39233 doi:10.7554/eLife.39233

Scaife MA, Nguyen GTDT, Rico J, Lambert D, Helliwell KE, Smith AG (2015) Establishing Chlamydomonas reinhardtii as an industrial biotechnology host. The Plant Journal 82(3):532-546 doi:10.1111/tpj.12781

Schenck TL, Hopfner U, Chavez MN, Machens HG, Somlai-Schweiger I, Giunta RE, Bohne AV, Nickelsen J, Allende ML, Egana JT (2015) Photosynthetic biomaterials: a pathway towards autotrophic tissue engineering. Acta Biomater 15:39-47 doi:10.1016/j.actbio.2014.12.012

Scheper GC, Morrice NA, Kleijn M, Proud CG (2001) The mitogen-activated protein kinase signal-integrating kinase Mnk2 is a eukaryotic initiation factor 4E kinase with high levels of basal activity in mammalian cells. Mol Cell Biol 21(3):743-754 doi:10.1128/MCB.21.3.743-754.2001

Schneider CA, Rasband WS, Eliceiri KW (2012) NIH Image to ImageJ: 25 years of image analysis. Nature methods 9(7):671-675 doi:10.1038/nmeth.2089

Schroda M, Beck CF, Vallon O (2002) Sequence elements within an HSP70 promoter counteract transcriptional transgene silencing in Chlamydomonas. The Plant Journal 31(4):445-455 doi:10.1046/j.1365-313X.2002.01371.x

Schroda M, Blöcker D, Beck CF (2000) The HSP70A promoter as a tool for the improved expression of transgenes in Chlamydomonas. The Plant Journal 21(2):121-131 doi:10.1046/j.1365-313x.2000.00652.x

Sen CK (2009) Wound healing essentials: let there be oxygen. Wound Repair Regen 17(1):1-18 doi:10.1111/j.1524-475X.2008.00436.x

Sen CK, Gordillo GM, Roy S, Kirsner R, Lambert L, Hunt TK, Gottrup F, Gurtner GC, Longaker MT (2009) Human skin wounds: A major and snowballing threat to public health and the economy. Wound Repair and Regeneration 17(6):763-771 doi:10.1111/j.1524-475X.2009.00543.x

Shibuya M (2011) Vascular Endothelial Growth Factor (VEGF) and Its Receptor (VEGFR) Signaling in Angiogenesis: A Crucial Target for Anti- and Pro-Angiogenic Therapies. Genes & cancer 2(12):1097-1105 doi:10.1177/1947601911423031

Shimogawara K, Fujiwara S, Grossman A, Usuda H (1998) High-efficiency transformation of Chlamydomonas reinhardtii by electroporation. Genetics 148(4):1821-1828

Siddiqui A, Galiano RD, Connors D, Gruskin E, Wu L, Mustoe TA (1996) Differential effects of oxygen on human dermal fibroblasts: acute versus chronic hypoxia. Wound Repair and Regeneration 4(2):211-218 doi:10.1046/j.1524-475X.1996.40207.x

Singer AJ, Clark RA (1999) Cutaneous wound healing. N Engl J Med 341(10):738-746 doi:10.1056/nejm199909023411006

Singh S, Young A, McNaught C-E (2017) The physiology of wound healing. Surgery (Oxford) 35(9):473-477 doi:https://doi.org/10.1016/j.mpsur.2017.06.004

Soria-Guerra R, Ramírez Alonso J, Ibañez Salazar A, Govea-Alonso D, Paz T, Bañuelos-Hernandez B, S. Korban S, Rosales-Mendoza S (2014) Expression of an HBcAg-based antigen carrying angiotensin II in Chlamydomonas reinhardtii as a candidate hypertension vaccine, vol 116,

Su Z-L, Qian K-X, Tan C-P, Meng C-X, Qin S (2005) Recombination and Heterologous Expression of Allophycocyanin Gene in the Chloroplast of Chlamydomonas reinhardtii. Acta Biochimica et Biophysica Sinica 37(10):709-712 doi:10.1111/j.1745-7270.2005.00092.x

Sun M, Qian K, Su N, Chang H, Liu J, Shen G (2003) Foot-and-mouth disease virus VP1 protein fused with cholera toxin B subunit expressed in Chlamydomonas reinhardtii chloroplast. Biotechnology Letters 25(13):1087-1092 doi:10.1023/A:1024140114505

Surzycki R, Greenham K, Kitayama K, Dibal F, Wagner R, Rochaix J-D, Ajam T, Surzycki S (2009) Factors effecting expression of vaccines in microalgae. Biologicals 37(3):133-138 doi:https://doi.org/10.1016/j.biologicals.2009.02.005

Tandara AA, Mustoe TA (2004) Oxygen in wound healing--more than a nutrient. World J Surg 28(3):294-300 doi:10.1007/s00268-003-7400-2

Taunt HN, Stoffels L, Purton S (2018) Green biologics: The algal chloroplast as a platform for making biopharmaceuticals. Bioengineered 9(1):48-54 doi:10.1080/21655979.2017.1377867

Tran M, Henry RE, Siefker D, Van C, Newkirk G, Kim J, Bui J, Mayfield SP (2013a) Production of anti-cancer immunotoxins in algae: Ribosome inactivating proteins as fusion partners. Biotechnology and Bioengineering 110(11):2826-2835 doi:10.1002/bit.24966

Tran M, Van C, Barrera DJ, Pettersson PL, Peinado CD, Bui J, Mayfield SP (2013b) Production of unique immunotoxin cancer therapeutics in algal chloroplasts. Proceedings of the National Academy of Sciences 110(1):E15 doi:10.1073/pnas.1214638110

Tran M, Zhou B, Pettersson PL, Gonzalez MJ, Mayfield SP (2009) Synthesis and assembly of a full-length human monoclonal antibody in algal chloroplasts. Biotechnology and Bioengineering 104(4):663-673 doi:10.1002/bit.22446

Vecchi V, Barera S, Bassi R, Dall'Osto (2020) Potential and Challenges of Improving Photosynthesis in Algae. Plants 9:67 doi:10.3390/plants9010067

Velazquez OC (2007) Angiogenesis and vasculogenesis: Inducing the growth of new blood vessels and wound healing by stimulation of bone marrow–derived progenitor cell mobilization and homing. Journal of Vascular Surgery 45(6, Supplement):A39-A47 doi:https://doi.org/10.1016/j.jvs.2007.02.068

Walsh G, Jefferis R (2006) Post-translational modifications in the context of therapeutic proteins. Nature Biotechnology 24(10):1241-1252 doi:10.1038/nbt1252

Wang X, Brandsma M, Tremblay R, Maxwell D, Jevnikar AM, Huner N, Ma S (2008) A novel expression platform for the production of diabetes-associated autoantigen human glutamic acid decarboxylase (hGAD65). BMC Biotechnology 8(1):87 doi:10.1186/1472-6750-8-87

Werner S, Grose R (2003) Regulation of Wound Healing by Growth Factors and Cytokines. Physiological Reviews 83(3):835-870 doi:10.1152/physrev.2003.83.3.835

West JB (2013) Joseph Priestley, oxygen, and the Enlightenment. American Journal of Physiology-Lung Cellular and Molecular Physiology 306(2):L111-L119 doi:10.1152/ajplung.00310.2013

Yamakawa S, Hayashida K (2019) Advances in surgical applications of growth factors for wound healing. Burns & Trauma 7(1):10 doi:10.1186/s41038-019-0148-1

Yan N, Fan C, Chen Y, Hu Z (2016) The Potential for Microalgae as Bioreactors to Produce Pharmaceuticals. International Journal of Molecular Sciences 17(6) doi:10.3390/ijms17060962

Yang Z, Li y, Chen F, Li D, Zhang Z, Liu Y, Zheng D, Wang Y, Shen G (2006) Expression of human soluble TRAIL in Chlamydomonas reinhardtii chloroplast. Chinese Science Bulletin 51(14):1703-1709 doi:10.1007/s11434-006-2041-0

Yeboah A, Maguire T, Schloss R, Berthiaume F, Yarmush ML (2017) Stromal Cell-Derived Growth Factor-1 Alpha-Elastin Like Peptide Fusion Protein Promotes Cell Migration and Revascularization of Experimental Wounds in Diabetic Mice. Advances in wound care 6(1):10-22 doi:10.1089/wound.2016.0694

Yoon S-M, Kim SY, Li KF, Yoon BH, Choe S, Kuo MM-C (2011) Transgenic microalgae expressing Escherichia coli AppA phytase as feed additive to reduce phytate excretion in the manure of

young broiler chicks. Applied Microbiology and Biotechnology 91(3):553-563 doi:10.1007/s00253-011-3279-2

Zhang M, Qiu L, Zhang Y, Xu D, Zheng JC, Jiang L (2017) CXCL12 enhances angiogenesis through CXCR7 activation in human umbilical vein endothelial cells. Sci Rep 7(1):8289 doi:10.1038/s41598-017-08840-y

Zhang R, Patena W, Armbruster U, Gang SS, Blum SR, Jonikas MC (2014) High-Throughput Genotyping of Green Algal Mutants Reveals Random Distribution of Mutagenic Insertion Sites and Endonucleolytic Cleavage of Transforming DNA. The Plant Cell 26(4):1398 doi:10.1105/tpc.114.124099

Zhang Y-K, Shen G-F, Ru B-G, Gong Z-X (2006) Survival of Human Metallothionein-2 Transplastomic Chlamydomonas reinhardtii to Ultraviolet B Exposure. Acta Biochimica et Biophysica Sinica 38(3):187-193 doi:10.1111/j.1745-7270.2006.00148.x

Zhao W, Jin K, Li J, Qiu X, Li S (2017) Delivery of stromal cell-derived factor 1α for in situ tissue regeneration. J Biol Eng 11:22-22 doi:10.1186/s13036-017-0058-3

Ziegler ME, Hatch MM, Wu N, Muawad SA, Hughes CC (2016) mTORC2 mediates CXCL12-induced angiogenesis. Angiogenesis 19(3):359-71 doi:10.1007/s10456-016-9509-6

7. Appendix

7.1. Transgene DNA-sequence of hVEGF-165

7.1.1. Transgene DNA-sequence cloned for pBC1_VEGF

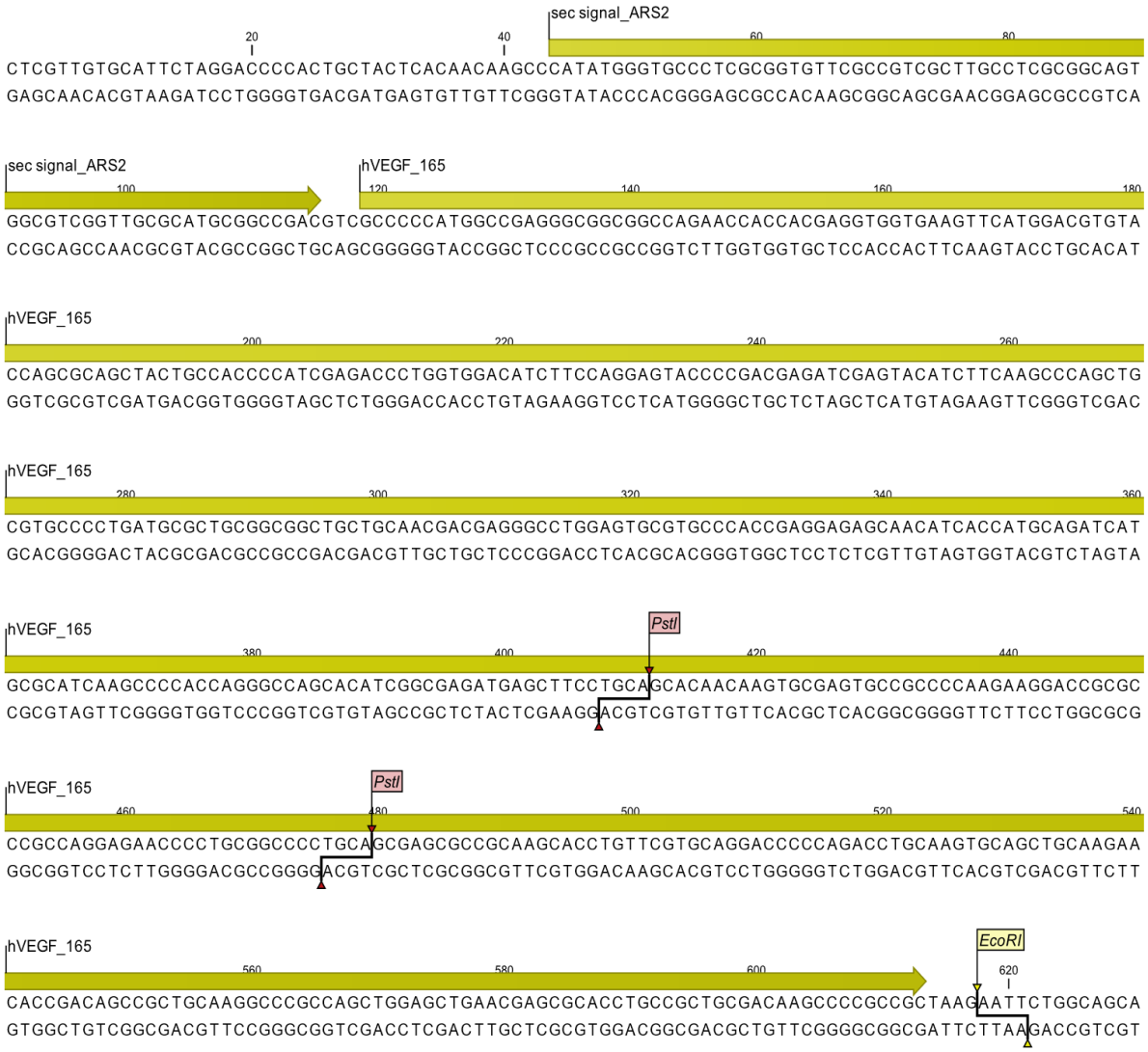

7.1.2. Transgene DNA-sequence cloned for pOpt_VEGF

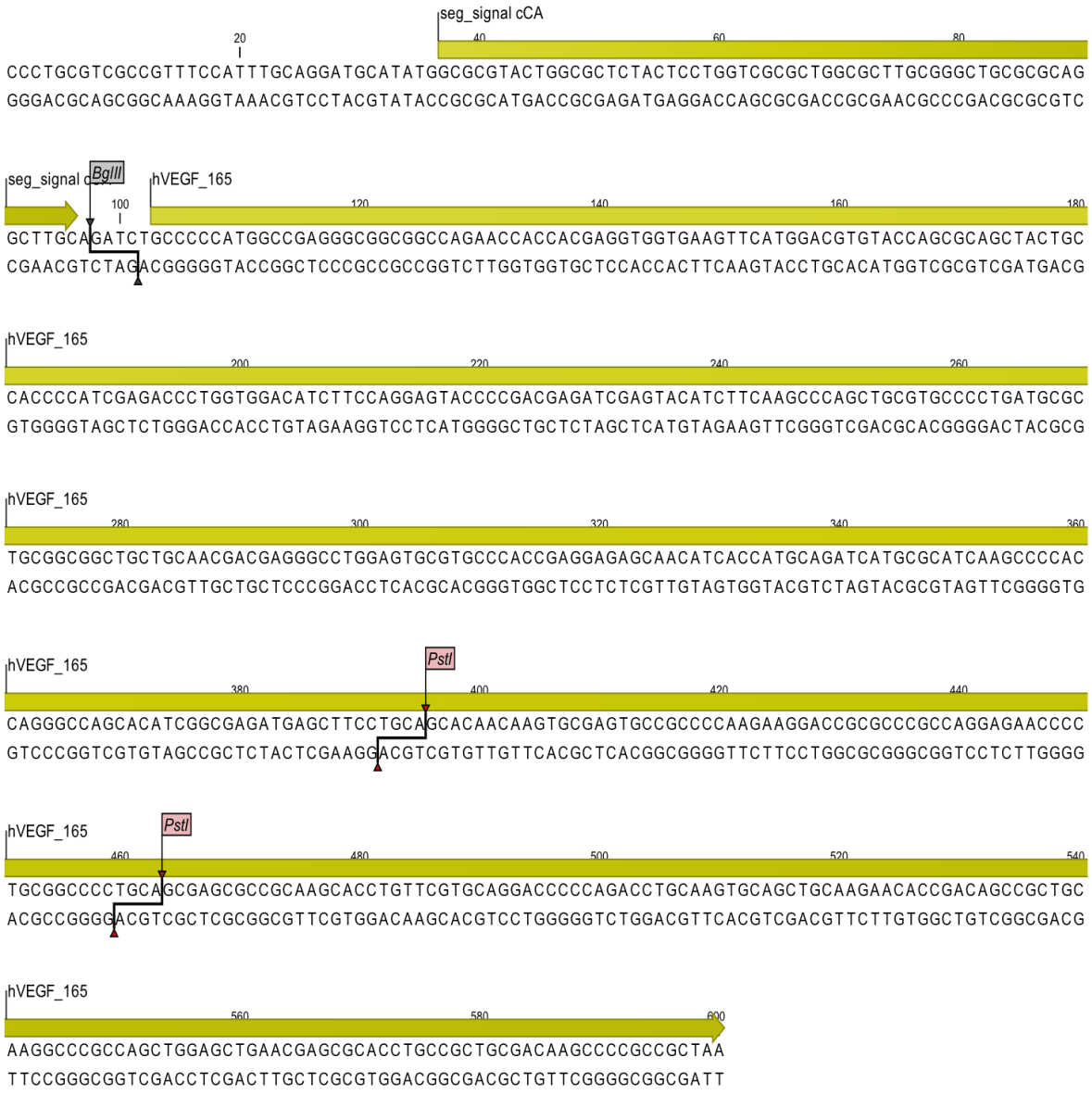

7.1.3. Transgene DNA-sequence cloned for pOpt_VEGF_strep-tag

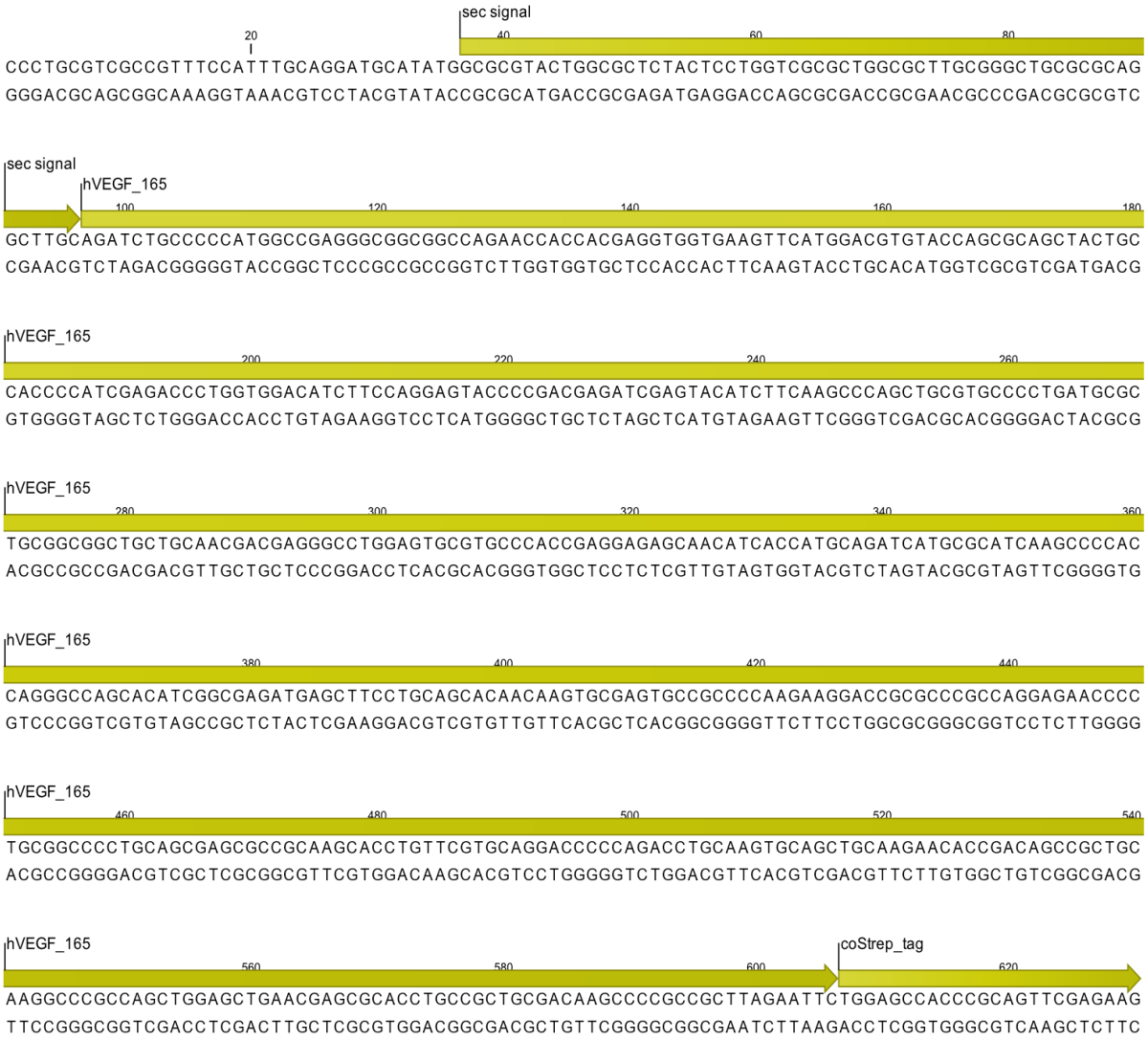

7.2. Transgene DNA-sequence of hTGF-β3

7.2.1. Transgene DNA-sequence cloned for pBC1_TGF

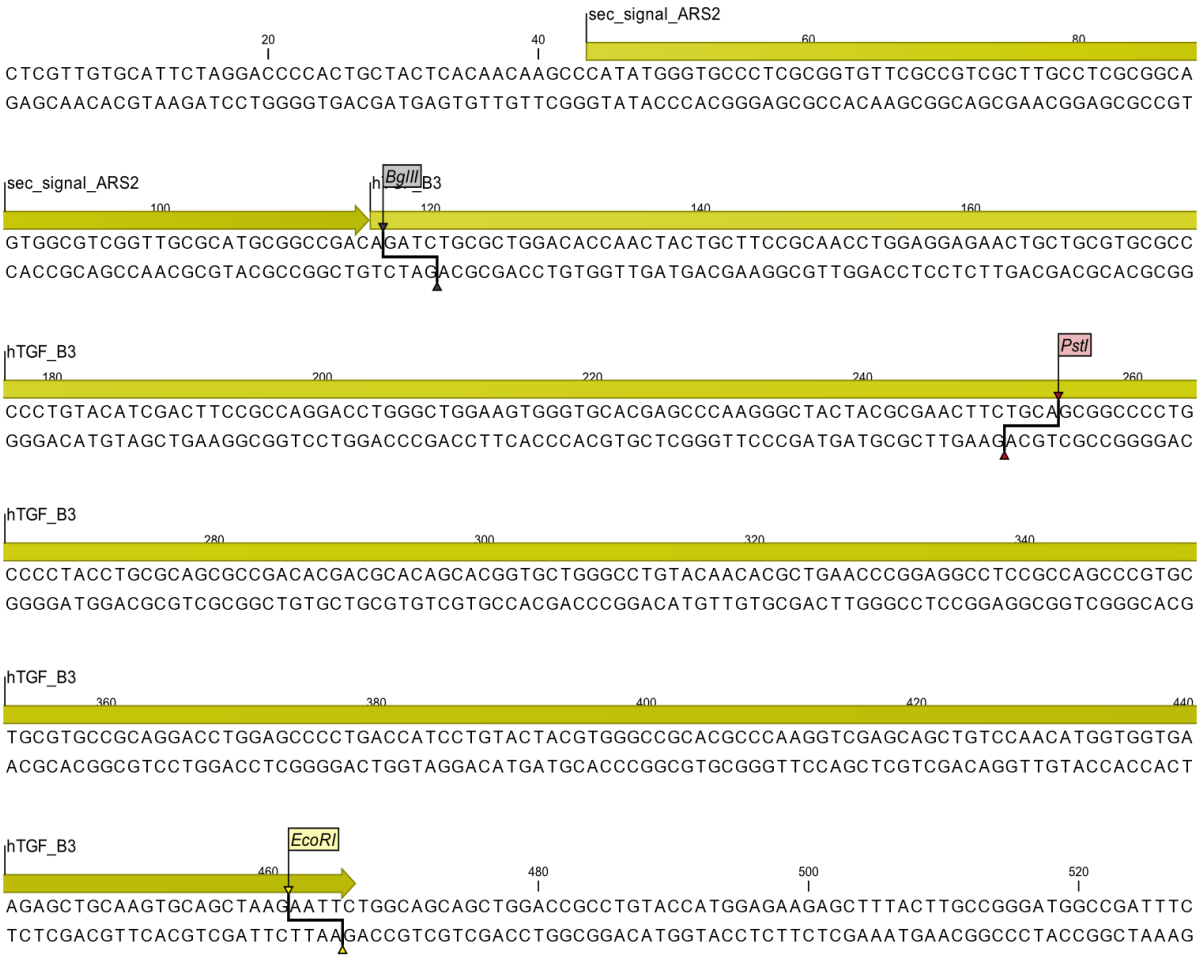

7.2.2. Transgene DNA-sequence of pOpt_TGF

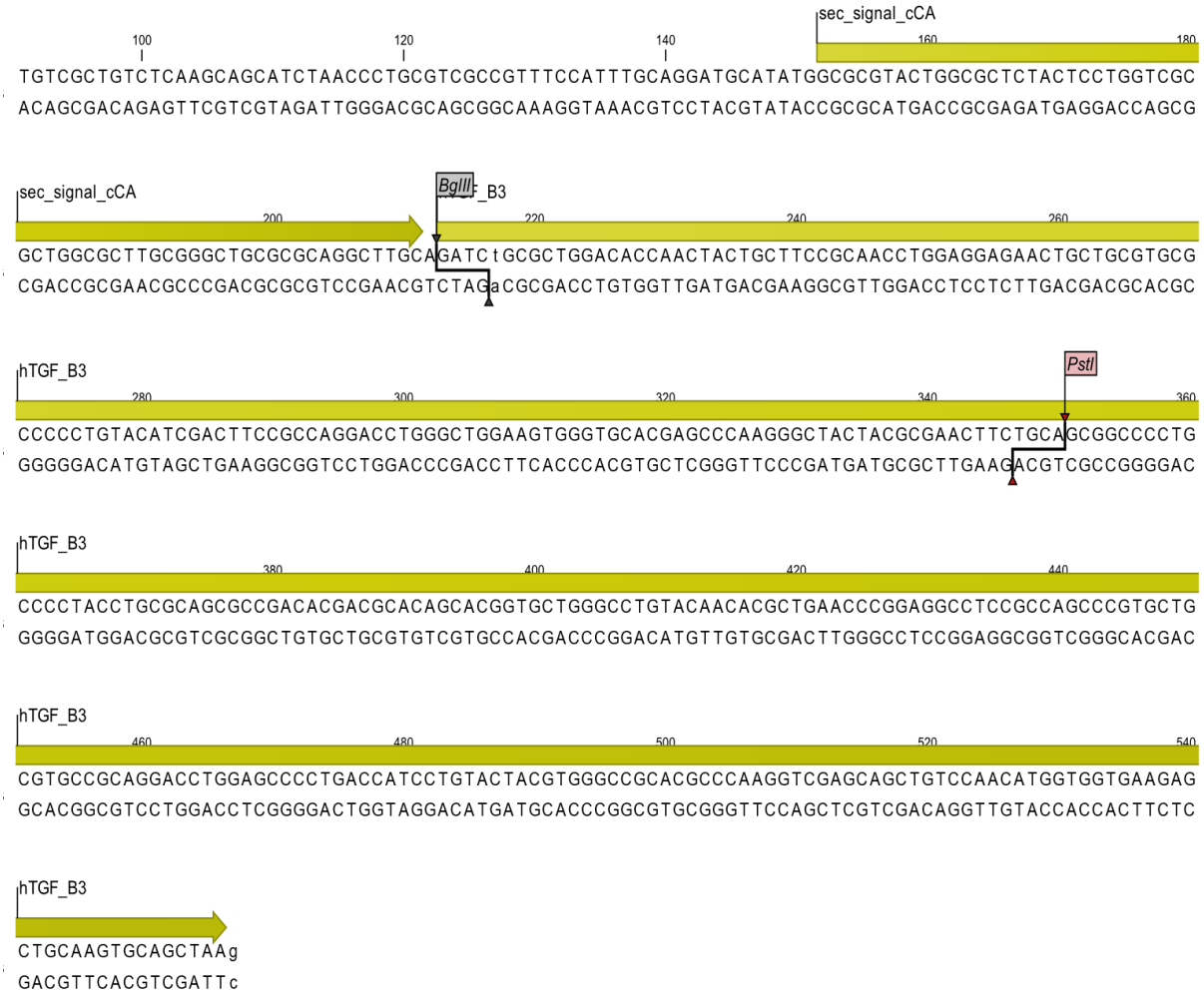

7.3. Transgene DNA-sequence of hPDGF-B

7.3.1. Transgene DNA-sequence cloned for pBC1_PDGF

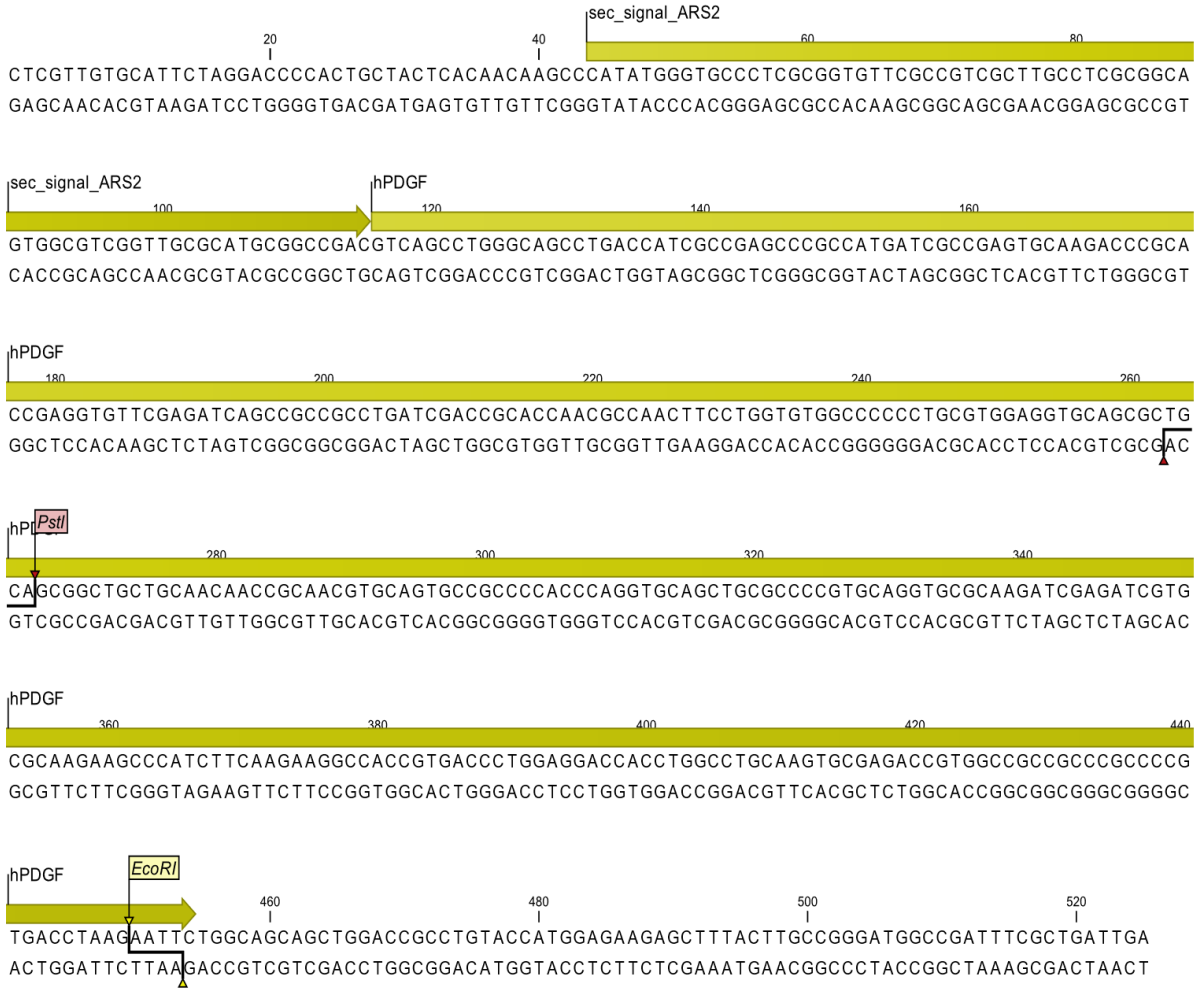

7.4. Transgene DNA-sequence of hSDF-1

Publications

Centeno-Cerdas, C., **Jarquín-Cordero, M.**, Chávez, M. N., Hopfner, U., Holmes, C., Schmauss, D., Machens, H. G., Nickelsen, J., Egaña, J. T. (2018). Development of photosynthetic sutures for the local delivery of oxygen and recombinant growth factors in wounds. Acta Biomaterialia, 81, 184-194. doi:https://doi.org/10.1016/j.actbio.2018.09.060

Montserrat Jarquín-Cordero, Myra Noemi Chávez, Carolina Centeno-Cerdas, Alexandra-Viola Bohne, Ursula Hopfner, Hans-Günter Machens, José Tomas Egaña, Jörg Nickelsen. (2019). Towards a biotechnological platform for the production of human pro-angiogenic growth factors in the green alga Chlamydomonas reinhardtii. Applied Microbiology and Biotechnology 104:725–739 https://doi.org/10.1007/s00253-019-10267-6

Acknowledgment

I want to express my profound thanks to my supervisor Prof. Dr. Jörg Nickelsen, for receiving me in his research group, providing me the opportunity to work in this extraordinary project and for all his valuable suggestions during the development of this thesis.

I would also like to thank Prof. Dr. José Tomás Egaña for his encouragement and valuable feedback and interest in this research work.

I want to thank the Instituto Tecnológico de Costa Rica (Costa Rica Institute of Technology) for providing me with the financial support to carry out my doctoral studies in Munich, Germany.

Heartiest thanks to my husband Pablo Caballero Polancos, no tengo palabras para expresarte toda mi gratitud, has puesto mucho esfuerzo, compañía e interés en esta tesis, me has acompañado y soportado todo el tiempo en este trayecto.

I am genuinely grateful to Dr. Myra-Noemi Chávez for her patience, guidance, and interest during these years; even we were so far away from each other, you were always there to help me.

I thank Dr. Alexandra-Viola Bohne for all your support and knowledge that you share with me.

My special thanks to all the former and current lab group members of my two labs, Anne, Anna, Laura, Steffen, Daniel, Julia, Tsong, Matthias, and Korbi from LMU lab and Carolina, Sarah, Philipp, Matthias, Eliza, Matthias and Chris from TUM lab. Thank you, guys, for all the time, support, encourage and laughs during this Ph.D. time.

I wish to acknowledge the help provided by Mrs. Karin Findeisen and Mrs. Simone Boos, as well as Mrs. Ursula Hopfner and Mrs. Manuela Kirsch, without you girls, working in the labs can be madness.

Finally, I also thank my family and friends, who through despite different time zones and internet connection problems, always encouraged and support me through the whole process.

EIDESSTATTLICHE VERSICHERUNG UND ERKLÄRUNG

Eidesstattliche Versicherung

Ich versichere hiermit an Eides statt, dass die vorgelegte Dissertation von mir selbständig und ohne unerlaubte Hilfe angefertigt ist.

München, den 24.07. 2020

Montserrat Jarquín-Cordero

Erklärung

Hiermit erkläre ich, dass die Dissertation nicht ganz oder in wesentlichen Teilen einer anderen Prüfungskommission vorgelegt worden ist. Des Weitern habe ich mich nicht anderweitig einer Doktorprüfung ohne Erfolg unterzogen.

München, den 24.07. 2020

Montserrat Jarquín-Cordero